INVESTIGATION OF THE PROTEINS OF *Leishmania tropica* CAUSING VISCEROTROPISM IN HUMANS USING MASS SPECTROMETRY

A Thesis Submitted to
the Graduate School of
İzmir Institute of Technology
in Partial Fulfillment of the Requirements for the Degree of

MASTER OF SCIENCE

in Chemistry

by
Merve BEYAZ

July 2022
İZMİR

ACKNOWLEDGEMENTS

I would like to thank several people who accompanied and supported me during my thesis studies.

First of all, I would like to express my sincere gratitude to my supervisor Prof. Dr. Talat YALÇIN, for his guidance, support, and endless knowledge. He encouraged me in every step of this study and gave me moral support even in the most challenging moments by sharing his life experiences whenever it is needed. I always consider myself lucky to be a part of the Biological Mass Spectrometry and Proteomics Laboratory, and I am very grateful to him for giving me the chance.

I would like to thank my committee members Prof. Dr. Ahmet ÖZBİLGİN and Prof. Dr. Çağlar KARAKAYA, for their suggestions and contributions.

I would also like to thank The Scientific and Technological Research Council of Turkey (TÜBİTAK) for the financial support for the research project (Project No:119S469). The State Planning Organization, DPT (Project No: 2008K120730) is also gratefully acknowledged for its financial assistance in the foundation of the IZTECH Biological Mass Spectrometry and Proteomics Laboratory. And I wish to acknowledge the Parasites Bank of the Manisa Celal Bayar University for the isolation and extraction of L. tropica proteins.

Furthermore, I am deeply grateful to my friends from National Mass Spectrometry Application and Research Center Dr. Melike DİNÇ and Dr. Çağdaş TAŞOĞLU, for their guidance, sharing of their experiences and knowledge, contributions, and kind helps to this work.

Moreover, I am also deeply grateful to my dear friends Sema SARISÖZEN, Deniz PERÇİN, Jülide ÇINDIRLAR, and Şeyda BÜKÜLMEZ for their companionship, understanding, and moral support.

Most importantly, I owe my eternal gratitude to my mother Aylin BEYAZ, my father Vural BEYAZ, and my lovely sister Sena BEYAZ. The love, kindness, inspiration, and great patience they have shown me throughout my entire life make me feel like the luckiest person in the world.

ABSTRACT

INVESTIGATION OF THE PROTEINS OF *Leishmania tropica* CAUSING VISCEROTROPISM IN HUMANS USING MASS SPECTROMETRY

Leishmaniasis is a neglected tropical disease in 98 countries and five continents worldwide. The most prevalent forms of this parasitic disease are Cutaneous, Mucocutaneous, and Visceral Leishmaniasis. While Cutaneous Leishmaniasis causes disfiguring skin conditions and lesions, Mucocutaneous Leishmaniasis damages the mucosal tissues of the mouth, nose, and throat. The visceral form of Leishmaniasis causes weight loss, fever, diarrhea, lymph nodes, and spleen or liver enlargement. Today, Leishmania *tropica*, one of the strains of the Leishmania parasite, no longer causes only Cutaneous Leishmaniasis (CL) but also Visceral Leishmaniasis (VL). The reason for this visceralism in *L. tropica* is not fully understood.

Mass spectrometry has a vital place in proteomic analyses; it provides information about expression levels and the identification of proteins. In this study, the proteins of *L. tropica* causing CL and CL are analyzed using the mass spectrometric shotgun method. Off-line HPLC separation followed by LC-MS/MS analyses are performed, and differential proteins between CL and VL isolates of *L. tropica* are determined.

Results indicate that among the differentially abundant proteins between two sample groups, paraflagellar rod proteins, elongation factor 1-alpha protein, and surface antigen proteins might play a role in avoiding immune recognition. Also, proteins with peroxidoxin function, cytochrome b5, and endoribonuclease might help parasite survival in macrophages. And finally, thiol-specific antioxidant protein may have a role in viscerotropism in *L. tropica*.

ÖZET

İNSANLARDA *Leishmania tropica*'nın İÇ ORGANLARA YÖNELMESİNE SEBEP OLAN PROTEİNLERİN KÜTLE SPEKTROMETRE KULLANILARAK ARAŞTIRILMASI

Leşmanyöz, dünya çapında 98 ülkede ve beş kıtada ihmal edilen bir tropikal hastalıktır. Bu paraziter hastalığın en yaygın biçimleri Kutanöz, Mukokutanöz ve Viseral Leşmanyözdür. Kutanöz Leşmanyöz ciltte şekil bozukluğuna ve lezyonlara neden olurken, Mukokutanöz Leşmanyöz ağız, burun ve boğazdaki mukozal dokulara zarar verir. Leşmanyözün viseral formu kilo kaybına, ateşe, ishale, lenf düğümlerine ve dalak veya karaciğer büyümesine neden olur. Günümüzde leşmanya parazitinin suşlarından biri olan L. tropica, artık sadece Kutanöz Leşmanyöze (CL) değil, aynı zamanda Viseral Leşmanyöze (VL) de neden olmaktadır. L. tropica'daki bu visseralizmin nedeni tam olarak anlaşılamamıştır.

Kütle spektrometresi, proteomik analizlerde hayati bir yere sahiptir; ekspresyon seviyeleri ve proteinlerin tanımlanması hakkında bilgi sağlar. Bu çalışmada, CL ve CL'ye neden olan L. tropica proteinleri kütle spektrometresi kullanılarak analiz edilmiştir. Off-line HPLC ayrımı, ardından LC-MS/MS analizleri gerçekleştirilmiş ve L. tropica'nın CL ve VL izolatları arasındaki farklı proteinler belirlenmiştir.

Sonuçlar, iki numune grubu arasındaki diferansiyel olarak bol proteinler arasında, kamçı proteinleri, EF-1alfa ve yüzey antijen proteinlerinin, bağışıklık tanımadan kaçınmada rol oynayabileceğini göstermektedir. Ayrıca peroksidoksin fonksiyonlu proteinler, sitokrom b5 ve endoribonükleaz makrofajlarda parazitin hayatta kalmasına yardımcı olabilir. Ve son olarak, tiyol-spesifik antioksidan protein, L. tropica'da visserotropizmde rol oynayabilir.

TABLE OF CONTENTS

LIST OF FIGURES

Figure **Page**

LIST OF TABLES

Table **Page**

CHAPTER 1

Leishmania PARASITE AND LEISHMANIASIS

1.1. *Leishmania* Parasite

A parasite is an organism that exists inside or on a host that is another organism. The parasite uses the host's resources to survive and maintain its life cycle. Parasites vary widely, from one-celled protozoa to worms visible to the naked eye. Several parasites cause different parasitic infections and severe diseases in humans and animals [1]. Leishmania spp. is a kind of parasite which causes a disease called Leishmaniasis. Pathogenic Leishmania species are transmitted to humans by the bite of infected sandflies [2,3]. These flagellated protozoa parasites are involved in a class of kinetoplastida which have a special organelle called kinetoplast in their mitochondrion. Kinetoplastids are flagellated protists belonging to the phylum Euglenzoa. Their only distinguishing feature is the presence of kinetoplast, which contains a large mass of DNA. A number of parasites that cause serious diseases in humans and other animals belong to this class. Furthermore, depending on the number of flagella, kinetoplastids are classified into two monophyletic groups: the biflagellate bodonoids and uniflagellate trypanosomatids. Kinetoplastids change their morphologies in order to adapt to the new environment in the mammalian host [4].

1.2. Morphology and Life Cycle of *Leishmania*

There are two morphological forms of Leishmania, promastigote and amastigote (Figure 1.1.). The stage of promastigote is extracellular and motile with a flagellum in the midgut of the sandfly. Promastigotes have an elongated cell shape with a width of 1.5-5 μm and a length of 15-20 μm, and they multiply by dividing longitudinally at 27 °C inside the midgut of the vector.

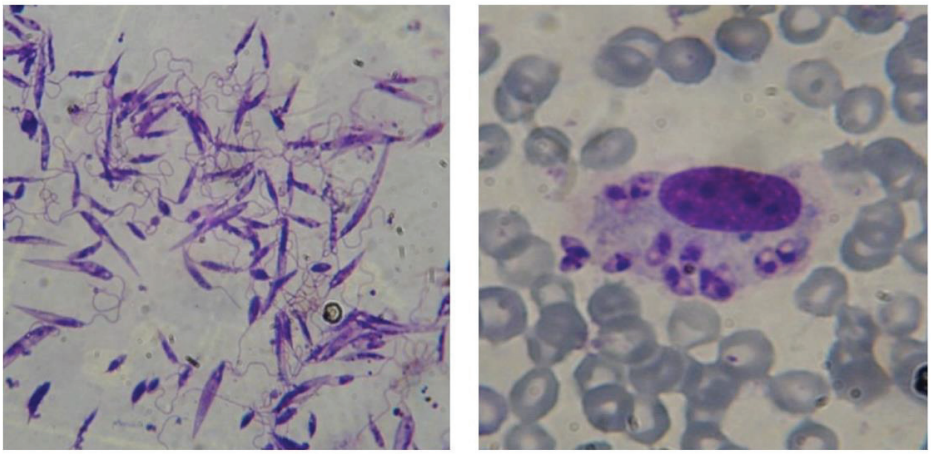

Promastigotes Amastigotes

Figure 1.1. Morphological Forms of Leishmaniasis [5]

The stage of amastigote is intracellular and non-motile in the macrophages of the mammalian host without a flagellum. Amastigotes have a width of 1-3 µm and a length of 2-5 µm and can be circular or oval. They multiply by dividing longitudinally at 37 °C inside the macrophages of the mammalian host [6]. These dimorphic organisms are able to infect macrophages and dendritic cells in both forms.

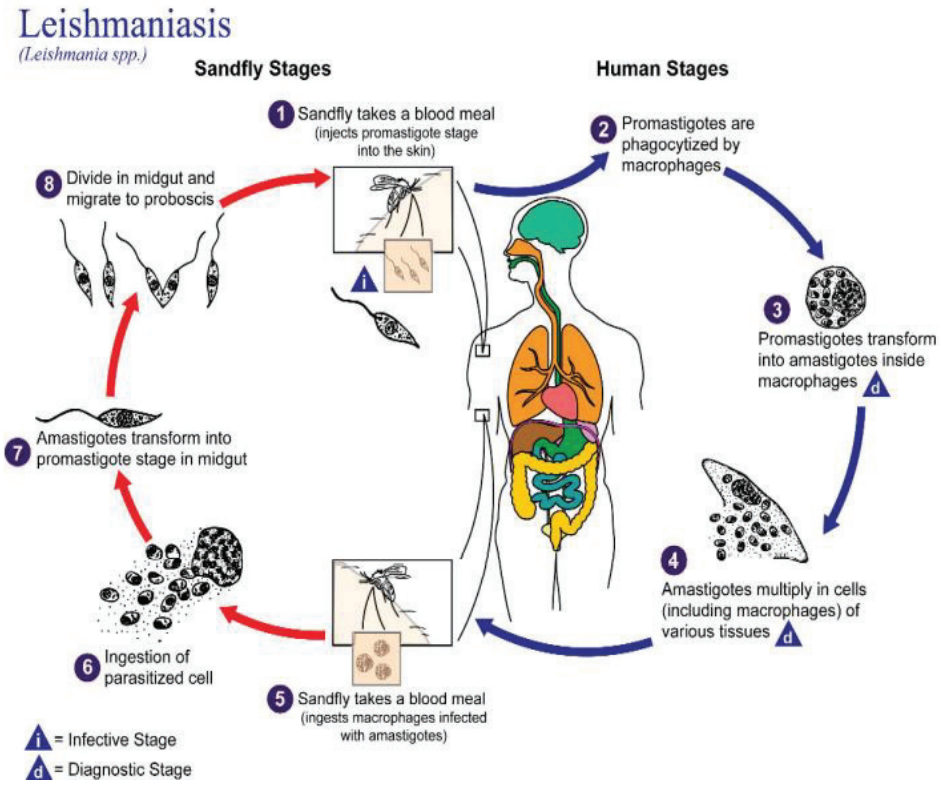

Figure 1.2. Life Cycle of Leishmania spp.

A schematic representation of the life cycle of Leishmania is shown in Figure 1.2. The cycle begins with the bite of the infected sandfly. During the blood meal of sandflies, the parasite is transmitted to the host body in promastigote form and invades macrophages during phagocytosis. Then, amastigotes multiply by simple division and leave the infected cells to spread out and infect new macrophages, different tissues, and related organs depending on the subgenus of Leishmania. While the amastigotes are in the bloodstream in the host body, another sandfly that bites the host is infected. The amastigote form of the parasite transforms into the promastigote stage in the midgut. This way can complete the dimorphic life cycle of Leishmania [1,7].

1.3. Clinical Forms of Leishmaniasis

Leishmaniasis has a wide range of clinical features depending on the Leishmania subgenus. The most prevalent forms of the disease are Cutaneous, Mucocutaneous, and Visceral Leishmaniasis. *L. major, L. tropica,* and *L. mexicana* cause Cutaneous Leishmaniasis. This form of Leishmaniasis causes disfiguring skin conditions. It starts as a nodule at the site of the sandfly bite and grows to localized cutaneous skin lesions. Mostly the lesions are seen on the ears, nose, upper lip, cheeks, legs, hands and forearms, and ankles. The incubation period is 1 to 4 weeks after the first bite and generally self-heal with indelible scars in 3 to 18 months [2].

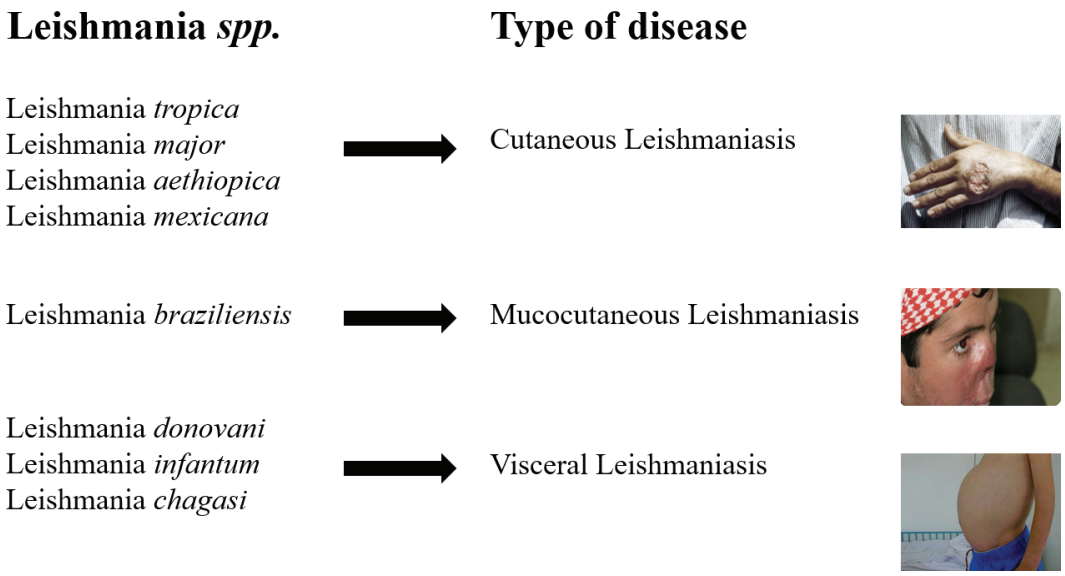

Figure 1.3. Clinical Forms of Leishmaniasis and Relating Leishmania Subgenus

In the Mucocutaneous form of Leishmaniasis, lesions can cause to destruction of the mucosal tissues of the mouth, nose, and throat. The causative agent for Mucocutaneous Leishmaniasis is *L. braziliensis*. Other reasons for this disease include multiple or large primary lesions or delayed healing of the primary Cutaneous Leishmaniasis. Mostly undernourished young adult male migrants are at risk for this form of disease. Mucocutaneous Leishmaniasis may appear months, years, or decades after a cutaneous lesion. Therefore, it is hard to diagnose [2].

L. donovani, *L. infantum*, and *L. chagasi* cause Visceral Leishmaniasis. It is the most dangerous form of Leishmaniasis, and it can be lethal in untreated cases. The parasites spread out from the bite of the sandfly to visceral organs. The incubation period is 3 to 8 months. Preschool children, undernourished individuals, and people with HIV/AIDS are among the at-risk group [8,9]. The symptoms of Visceral Leishmaniasis are weight loss, fever, diarrhea, lymph nodes, and spleen or liver enlargement [2].

1.4. Endemicity of Leishmaniasis

Although Leishmaniasis is the second most common tropical disease that causes morbidity and mortality, it is still accepted as a "neglected tropical disease". This neglected tropical disease is a public health problem in 98 countries in Asia, Africa, Europe, North America, and South America. According to World Health Organization (WHO) reports (2010), over 350 million people are at risk in endemic areas, 2 million new cases observed, and 50 000 deaths from the disease are recorded each year [10].

Different clinical forms of Leishmaniasis are endemic in different territories. According to WHO reports (2012), 70% of the Cutaneous Leishmaniasis cases emerge in Afghanistan, Algeria, Brazil, Colombia, Costa Rica, Ethiopia, Iran, Sudan, and the Syrian Arab Republic; and yet 90% of the Visceral Leishmaniasis cases occur in Bangladesh, Brazil, Ethiopia, India, South Sudan, and Sudan [11].

With the development of technology, the diversification of transportation ways allows the frequency of human relations to increase by providing accessible and fast travel opportunities, compared to the previous years, and has accelerated the spread of Leishmaniasis. Environmental factors including global warming and climate change also affect the prevalence of the disease by providing an expansion in areas suitable for the living conditions of sandflies [3].

Distribution of VL cases among geographical regions between 1997 and 2000 (data from Ministry of Health)

	1997	1998	1999	2000	Total (%)
Mediterranean	51	13	5	9	78 (48.5%)
Aegean	8	8	4	10	30 (18.6%)
Central Anatolia	8	10	9	3	30 (18.6%)
Marmara	1	1	1	9	12 (7.5%)
Southeastern Anatolia	1	1	1	2	5 (3.1%)
Black Sea	2	1	1	1	5 (3.1%)
Eastern Anatolia	0	0	1	0	1 (0.6%)
Total	71	34	22	34	161 (100.0%)

Distribution of CL cases among geographical regions between 1994 and 2000 (data from Ministry of Health)

	1994	1995	1996	1997	1998	1999	2000	Total (%)
Southeastern Anatolia	4,185	2,810	2,410	482	802	275	272	11,236 (61.7%)
Mediterranean	1,494	1,036	1,447	714	606	708	818	6,823 (37.5%)
Central Anatolia	13	4	0	6	10	17	22	72 (0.4%)
Aegean	0	0	0	30	22	6	12	70 (0.4%)
Black Sea	0	0	0	0	0	2	9	11 (0.1%)
Eastern Anatolia	0	0	0	0	0	2	2	4 (0.0%)
Marmara	0	0	0	0	0	0	0	0 (0.0%)
Total	5,692	3,850	3,857	1,232	1,440	1,010	1,135	18,216 (100.0%)

Figure 1.4. Distribution of CL and VL cases [12]

Recently, Leishmaniasis has become a severe health problem in Turkey as well. Cutaneous Leishmaniasis cases become widespread in Turkey after over 2 million refugees from Syria [13]. Another reason is the rising average temperatures in Turkey, which could increase the survival time [14,15].

L. infantum and *L. tropica* are the causative agents of Visceral Leishmaniasis and Cutaneous Leishmaniasis [12,16]. Visceral Leishmaniasis is prevalent mainly in Aegean, Mediterranean, and Central Anatolia, whereas Cutaneous Leishmaniasis cases occur primarily in the Mediterranean, and Southeastern Anatolia regions, seen in Aegean and Central Anatolia regions [12]. According to the Ministry of Health reports, 46.003 new Cutaneous Leishmaniasis cases were recorded in Turkey between 1990 and 2000, 96% of them were from the Southeastern Anatolia region [17].

CHAPTER 2

MASS SPECTROMETRY AND PROTEOMICS

2.1. Introduction to Mass Spectrometry

Mass spectrometry is an analytical technique that measures the mass-to-charge ratio (m/z) of the gas-phase ions. The neutral analyte is ionized by different ionization techniques, and those ions are separated and detected by mass analyzers based on their m/z ratio. Mass spectrometer outputs a spectrum that indicates m/z - relative abundance. This mass spectrum data provides information about molecular mass, structure, abundance, purity, and composition of the analyte.

Mass spectrometry was discovered by J. J. Thomson at the end of the 1880s. Thomson and his laboratory assistant E. Everett were working on cathode rays, and they built an instrument that measures *e/m* (charge-to-mass ratio) and *e* by using an electric field inside a cathode ray tube. In other words, this instrument measured the mass of the electron. After these discoveries, Thomson and Francis Aston developed an instrument that generated ions by using gas discharge tubes. These ions passed through the parallel electric and magnetic field, deflected into parabolic trajectories, and detected by a photographic plate. This instrument is accepted as the first mass spectrometer. The first commercial mass spectrometers were used in the petrochemical field in the 1940s. It was used to diagnose organic substances and observe the molecular structure of amino acids and peptides in the 1950s. In the 1980s, as the ionization techniques were improved, large proteins, nucleic acids, complex carbohydrates, and other macromolecules were analyzed, thus applications of mass spectrometry became more and more important [18].

At present, mass spectrometry can be used in a wide range of areas, such as archaeology, biotechnology, chemistry, environmental analysis, forensics, geology, petroleum and pharmaceutical industries, and proteomics. Drug testing, the analysis of large biomolecules, identification of impurities, diagnosis of certain diseases, and determination of isotopic abundance are achievable with the help of mass spectrometry.

2.1.1. Instrumentation

A mass spectrometer includes three essential parts which are the ion source, the mass analyzer, and the detector (Figure 2.1.). Firstly, the sample is entered into the system through the sample inlet. It can be HPLC (high-performance liquid chromatography), GC (gas chromatography), a syringe, or a probe. The ion source generates gas-phase ions from the neutral analyte. Next, generated charged particles are accelerated and focused by the electric or magnetic field and separated according to the m/z ratio in the mass analyzer. Finally, the ion energy is detected and recorded by the detector and transmitted into an electrical signal to create a mass spectrum. With the aim of preventing collision among ions and other gas molecules, the main three parts of the system are under vacuum conditions (10^{-5} - 10^{-7} Torr). Thereby, a mean free path is provided for ions, and they can reach the detector without colliding with each other.

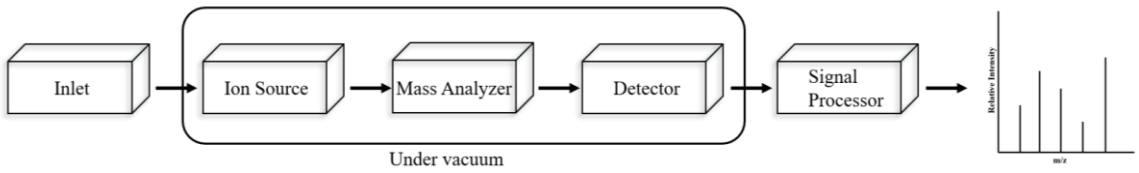

Figure 2.1. The Basic Components of a Mass Spectrometer

2.2. Ionization Methods

The ion source creates gas-phase ions from neutral analytes to allow analysis, fragmentation, and detection. The ionization methods are classified as soft and hard ionization. Hard ionization methods provide a high degree of fragmentation, and it yields structural information. However, the molecular signal can be weak due to excessive fragmentation. Soft ionization methods perform ionization with minimum fragmentation, so they provide molecular weight information. Also, they can create gas-phase ions from large biomolecules with high efficiency. The most common soft ionization techniques are electrospray ionization (ESI) and matrix-assisted laser desorption/ionization (MALDI) [19].

2.2.1. Electrospray Ionization (ESI)

The invention of electrospray ionization dates back to the late 1960s with the work of Dole and his coworkers. They formed charged gas-phase particles from a polystyrene polymer by dissolving the sample in a buffer or a solvent and introducing it into the mass spectrometer in the spray form. In the early 1980s, this technique is greatly optimized by coupling it to a quadrupole mass analyzer. These days, ESI-MS is used for both qualitative and quantitative analysis in a wide range of studies, from non-volatile and thermally labile simple inorganic chemicals to complex biochemical structures [20].

In principle, the analyte solution can be injected into the capillary through a syringe pump or an HPLC system. A high voltage is applied at the capillary tip to produce a spray. Meanwhile, the electric field separates the positive and negative charges in the analyte solution. When the operation is in the positive ion mode, the positive ions migrate towards the counter electrode, and they accumulate on the surface of the liquid in the capillary tip. The electric potential applied at the tip causes the formation of highly charged droplets.

The droplets collide with a neutral gas (usually N_2) to dry off the buffer. As the solvent vaporizes, the droplets become smaller, charges repel each other, and the surface tension increases. Eventually, the repulsive and coulombic forces exceed the Rayleigh limit, and the droplet explodes into smaller droplets. This process continues until they contain one or two analyte ions and a small amount of solvent. Finally, the pure gas-phase ions are obtained, and the sample ions are sprayed into the mass analyzer [19,20].

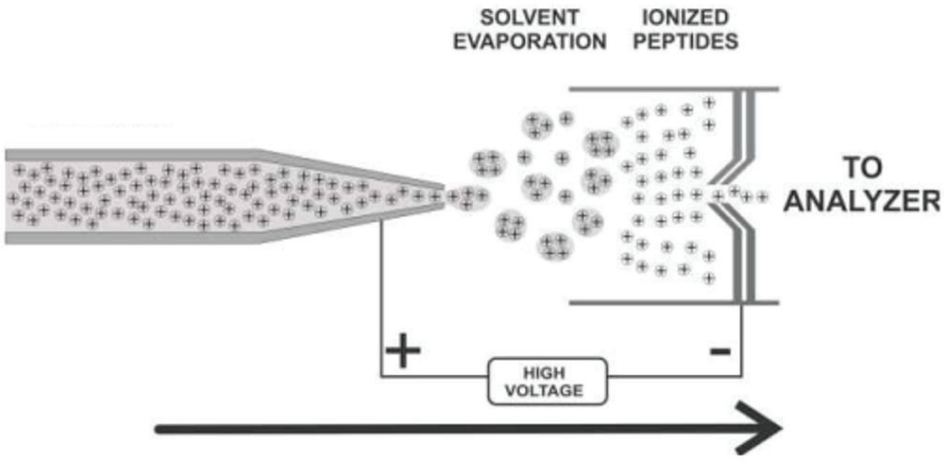

Figure 2.2. Schematic Representation of an ESI [19]

ESI can produce multiply charged ions of high molecular weight compounds with the increasing number of charges as the molecular weight increases. Thus, larger molecules can be observed at lower m/z. Furthermore, ESI has excellent detection limits thanks to its very low chemical background. It is also compatible with tandem mass spectrometry, with quadrupole, ion trap, and time-of-flight mass analyzers.

2.2.2. Matrix-Assisted Laser Desorption/Ionization (MALDI)

Matrix-assisted laser desorption ionization (MALDI) was firstly introduced in 1988 by Karas and Hillenkamp. It is a soft ionization technique for large, non-volatile, and thermally labile compounds, such as proteins, oligonucleotides, synthetic polymers, and large inorganic compounds [21].

In MALDI analyses, first, the sample is dissolved in a volatile solvent and mixed with a suitable matrix in a ratio of 1:1000. The matrix is a weak organic acid that has an absorption at the laser wavelength. It should isolate the analyte molecules and prevent their aggregation. The analyte-matrix mixture is spotted onto a MALDI target. As the solvent evaporates, the analyte molecules cocrystallize with the matrix.

The MALDI target is placed into the mass spectrometer and ionization occurs under vacuum conditions. The matrix-analyte crystal is exposed with a pulsed UV-laser beam, generally nitrogen laser at 337 nm or neodymium-doped yttrium aluminum garnet (Nd: YAG) at 355 nm. When the matrix is excited, it transfers its energy to the analyte and provides ionization without fragmentation. And lastly, the gas-phase analyte ions are accelerated and directed into the mass analyzer using an electric field.

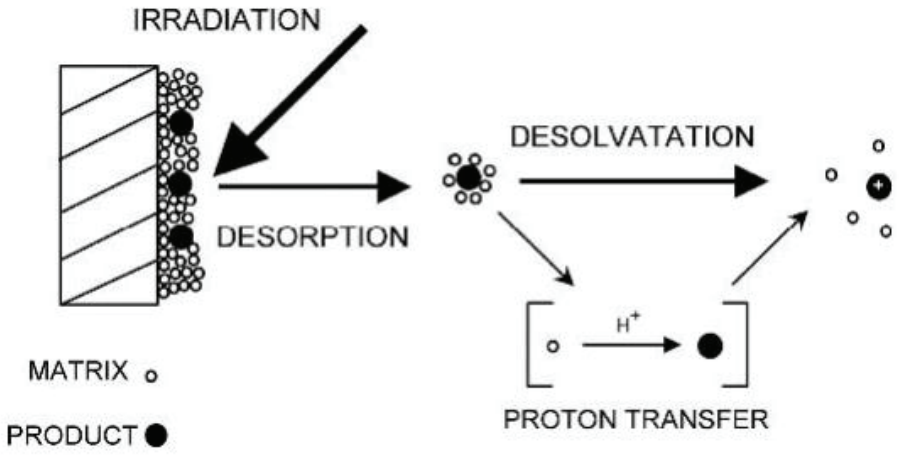

Figure 2.3. Schematic Representation of the MALDI Process [21]

The matrix selection is a critical factor for MALDI analyses. The most common matrixes are 3,5-dimethoxy-4-hydroxycinnamic acid (sinapinic acid), α-cyano-4-hydroxycinnamic acid (CHCA), and 2,5-dihydroxybenzoic acid (DHB). SA and CHCA are mostly used for biological samples; SA is for large proteins, CHCA is for peptides. DHB is generally preferred for hydrophobic, glyco- and phosphopeptides. In some situations, the mixture of these matrixes can be useful. Additionally, in the MALDI system, the matrix acts as a proton donor in positive ionization mode or a proton acceptor in negative ionization mode. The matrix also reduces the sample damage caused by the laser beam by absorbing the majority of incident energy.

Among the soft ionization methods, MALDI is one of the most tolerant techniques of contaminants such as buffers, salts, and surfactants. It can also be used to ionize large biomolecules with very high molecular masses of more than 100 kDa. In addition to all of these advantages, MALDI is a very fast technique that can obtain results in a very short amount of time [19–21].

2.3. Mass Analyzers

A mass analyzer is the part of the mass spectrometer where the gas-phase ions of the analyte are separated according to their m/z ratios by using electric or magnetic fields. Following the separation, the ions are transmitted and focused on a detector.

The three main characteristics of the mass analyzers are the upper mass limit, the transmission, and the resolution. The upper mass limit is the highest m/z ratio that can be measured. The transmission is defined as the ratio of the number of ions reaching the detector to the number of ions produced by the ion source. Finally, the resolution means the ability to separate two distinct mass signals.

There are several mass analyzers for mass spectrometry, but the most common ones for biomolecules and proteomic studies are Quadrupole (Q), Ion trap (IT), Time-of-flight (TOF), Orbitrap, and Fourier transform-ion cyclotron resonance (FT-ICR). Two or more analyzers can be used together in a mass spectrometer which increases the resolution and performance of the instrument. The quadrupole-quadrupole, magnetic sector-quadrupole, and quadrupole-time-of-flight are some of the common hybrid tandem systems.

Mostly the mass analyzers are coupled with the particular ion sources, such as TOF is used with MALDI, Quadrupole and Ion trap are connected to ESI source for

proteomic studies. MALDI-TOF MS allows the identification of proteins depending on the peptide masses with peptide mass fingerprint (PMF), whereas ESI MS/MS indicates peptide fragmentation [21].

2.3.1. Quadrupole (Q)

Quadrupole mass analyzer was firstly described by Paul Wolfgang in the 1950s. It includes four parallel, cylindrical electrical rods as shown in Figure 2.4. The opposite rods are linked to direct current (DC) and alternating radio frequency (RF) voltages. Two reciprocal rods are positively charged, while the other two are negatively charged.

Fundamentally, the ions are focused among the quadrupole rods by an electric field, and DC and RF voltages create a magnetic field. Ions oscillate in a particular trajectory; the ones that have an m/z ratio are specific to the voltages applied goes toward the detector, whereas the remaining ions hit the rods and cannot reach the detector.

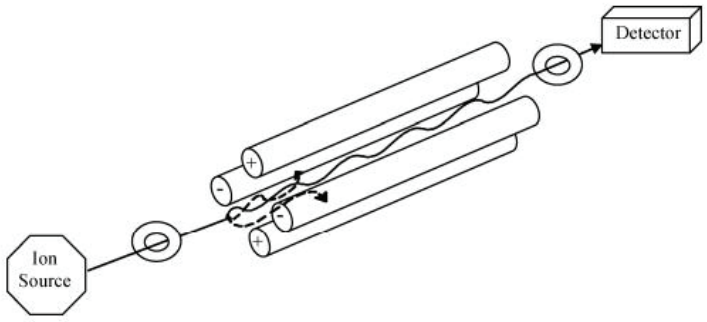

Figure 2.4. Representation of a Quadrupole Mass Analyzer [20]

Quadrupole analyzers are easy to use, robust, low cost, and relatively small in size. Another advantage is that they can be coupled to other analyzers or additional quadrupoles, such as triple quadrupole (QqQ) or quadrupole linked to a TOF (Q-TOF), and this way increases the mass range and resolving power of quadrupole analyzers [19–21].

2.3.2. Ion Trap (IT)

An ion trap is a mass analyzer that traps and stores the ions in two or three dimensions by using both electric and magnetic fields. Therefore, ion traps can be divided into two groups; the 2D ion traps, also known as linear ion traps (LIT), and the 3D ion

traps which are also called quadrupole ion traps (QIT). The first ion trap in history is a QIT which is invented by W. Paul and W. Steinwedel in 1980.

The QIT includes two electrodes and one ring electrode which provides to trap the ions. When all the ions are together in the analyzer, RF voltage of constant amplitude and frequency is applied to the ring electrode so that ions oscillate in the x-y direction based on their m/z values. Helium gas is used to prevent the expansion of the trajectories and to keep the ions in the middle of the trap. The end-cap electrodes are either earthed or DC voltage applied to trap the ions in the z-direction. Some of the ions are expelled according to their m/z ratio. When they are to be detected, the voltage is changed such that ions come out of the ion trap through the little slits, and they are sent to the detector.

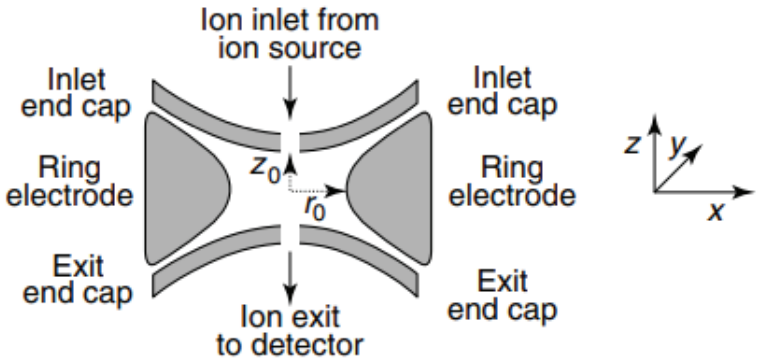

Figure 2.5. Diagram of 3D Ion Trap [21]

Quadrupole ion traps are commonly used due to their high sensitivity, high selectivity, and mechanical simplicity. Besides, they can be combined with other mass analyzers, and they can perform tandem mass spectrometry experiments owing to their ability to "store" the selected ions [22].

2.3.3. Time-of-Flight (TOF)

The principle of a time-of-flight mass analyzer was firstly described by Stephens in 1946. However, the first commercial instrument was built by Wiley and McLaren in 1955. Time-of-flight analyzers separate the ions according to their velocities. The relation between the flight time and the m/z ratio of ions is the main distinctive property among the ions.

First, the electrical potential is applied to accelerate the ions and to give them the same amount of kinetic energy. After this, the ions enter the field-free region where ions move through without any factor causing acceleration, and they fly in the tube toward the detector according to their kinetic energies. Since the velocity is inversely proportional to the mass of the ions, the lighter ions reach the detector faster than the heavier ones. Finally, the time required to pass through the flight tube is recorded. Because it is characteristic of different m/z values, the ions are quantified according to the duration of flight time.

TOF analyzer is generally coupled with MALDI that generates ions in short pulses as TOF requires. In addition, since MALDI produces singly charged ions, m/z can be accepted as equal to the mass of the ion. MALDI-TOF is a very sensitive instrument that can detect low quantities of an analyte with high accuracy [21].

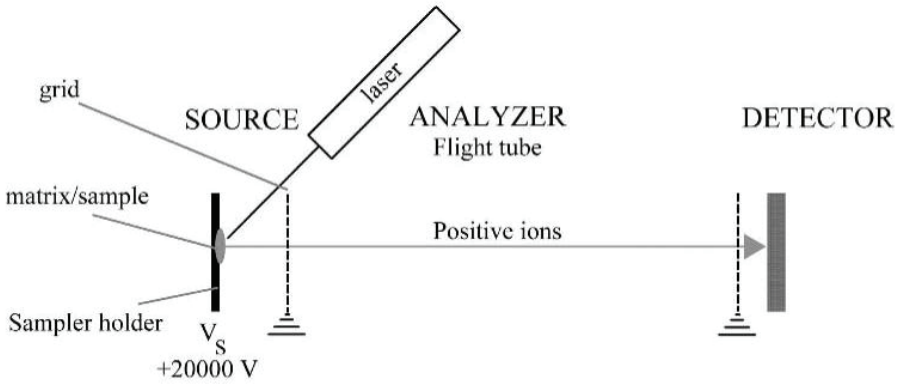

Figure 2.6. Principle of a MALDI-TOF Instrument [21]

2.4. Ion Detectors

The last component of a mass spectrometer is an ion detector. Electrical signals coming from the analyzer are detected and transformed into a usable signal by a detector. Desirable properties for a detector include low noise, fast response, wide dynamic range, long-term stability, low cost, and high amplitude. There are various types of detectors, but the most common ones are electron multiplier (EM) and multichannel plate (MCP).

2.4.1. Electron Multiplier (EM)

Electron multiplier (EM) is a type of detector which has multiple dynodes inside. Ions arrive at the detector and strike on a metal surface of a cathode. This strike causes the emission of several secondary electrons. These electrons are accelerated and strike on another dynode. This process repeats many times. Finally, all electrons are collected and detected by a metal anode [21].

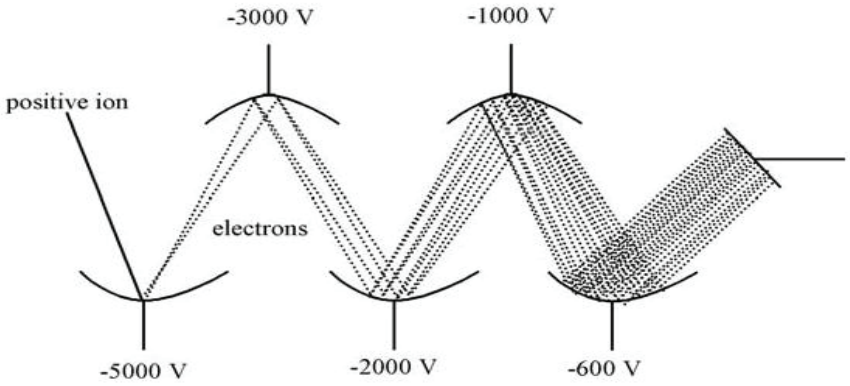

Figure 2.7. Schematic Diagram of EM [21]

2.4.2. Multichannel Plate (MCP)

A multichannel plate includes multiple independent glass channels which act as individual electron multipliers. As the ions strike on the surface of the channels, secondary electrons are created and detected [21].

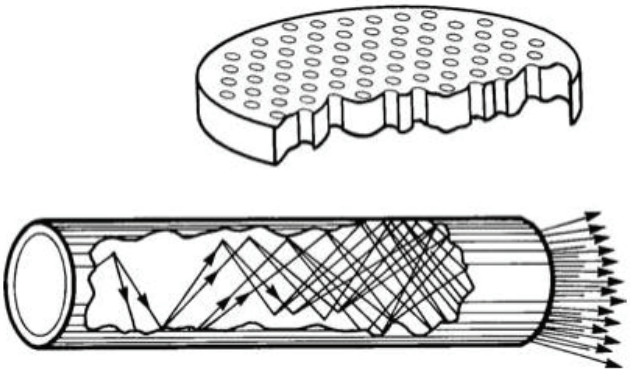

Figure 2.8. Diagram of a MCP and Electron Multiplication Within a Channel [21]

2.5. Proteomics

2.5.1. Introduction to Proteomics

Proteome is defined as the total proteins expressed in a genome, cell, tissue, or organism. The term “proteome” is derived from the words “protein” and “genome”. It was first suggested by Marc Wilkins as the “PROTEin complement expressed by a genOME” at the Conference on Genome and Plant Maps (Siena, Italy) in 1994.

The Human Genome Project was the first attempt to investigate the relationship between genes and proteins. The primary objectives for the project were to identify, characterize, and sequence the entire human genome, and determine the complete sequence of DNA bases in the human genome. It was discovered that although genomic studies provided information about the genes and their possible protein products in organisms, understanding biological activity could not be possible only through genes. Since the resulting DNA sequence does not include information of the time and the rate at which a gene is used, proteins become the focal point. It is estimated that human genome includes approximately 30,000 genes whereas encoded protein numbers range from 200,000 to 2 million owing to alternative splicing, post-translational modifications (PTMs), and protein degradation [23]. Since gene expression analysis cannot be used to understand the diversity of proteins, proteomic analysis is essential to determine cell function at the protein level. This situation shows that proteins are more dynamic, and they interact with other proteins by moving through the body, unlike genes. Furthermore, proteins provide information about PTMs, cell type, cell interactions, the immune system, and the environmental conditions which cannot be obtained by genomic studies.

Proteomics is a scientific discipline of molecular biology which investigates the composition, structure, function, and interaction of proteins. It is aimed to study the entire proteome in a single or series of experiments. Proteomics focuses on the active genes in cells. Thus, proteomics and genomics operate together. The primary goal of proteomics is to understand the functional relationship among proteins by characterizing the information flow within the organisms through protein pathways and networks. Proteomics plays an important role in catching biomarkers and identifying the progression of diseases such as cancer tumors, Alzheimer’s disease, and Down syndrome [24–26].

2.5.1.1. Types of Proteomics

Proteomics is classified into three main groups which are expression proteomics, structural proteomics, and functional proteomics.

Expression proteomics basically aims to identify the proteins in an organism at a certain time. For the purpose of gaining information about the physiology and pathogenic mechanism of a disease, the changes in the entire proteome of diseased and healthy cells are analyzed. Also, protein expression levels of organisms in different conditions are compared in order to provide knowledge on the responses to any physical and biochemical stresses. Stress-related proteins are specified and determined by two-dimensional gel electrophoresis (2D-GE) or mass spectrometry.

In structural proteomics, the purpose is to identify the molecular structure and complexity of proteins and to provide information about the function of protein complexes and protein-protein interactions. X-ray crystallography and NMR spectroscopy methods are used to determine the three-dimensional structure of proteins.

Finally, functional proteomics characterizes the functional groups to obtain information about the functions and activities of all the proteins in the proteome. Protein-protein interactions, protein-drug interactions, and PTMs are analyzed to detect the disease mechanism [27].

2.5.1.2. Mass Spectrometry-Based Proteomics

Mass spectrometry has an important role in proteomic analyses for the investigation and identification of analytes. Proteomic studies have accelerated with the development of soft ionization methods such as MALDI and ESI. Mass spectrometry provides information about protein expression and helps the identification of global proteins.

The workflow of mass spectrometry-based proteomic studies consists of 5 steps. The proteins are first extracted and purified from the mixture of DNA, RNA, and other complex components. Next, the proteins are separated by two-dimensional polyacrylamide gel electrophoresis (2D-PAGE) or chromatographic techniques. Then, isolated and separated proteins are exposed to enzymatic digestion, generally trypsin is used as protease. And finally, the peptides are analyzed by mass spectrometer and

searched in protein database to identify the protein, and to gain information about amino acid sequence and modifications.

2.5.2. Separation Techniques Before Mass Analysis

A successful MS-based proteomic study requires proper sample preparation. High concentration and sample purity are essential for sensitive and accurate mass measurement. The proteins should be isolated from the contaminants such as lipids, carbohydrates, salts, detergents, and nucleic acids which reduce the quality of MS signals and hamper the correct identification of proteins. Some physicochemical properties of proteins such as size, charge, shape, isoelectric point, hydrophobicity, solubility, metal affinity, and structure can be used for the separation of the proteins in the mixture. That is why it is important to choose the correct techniques for separation and purification before the MS analysis. Although there are several methods for the separation and purification of proteins, they can be classified into two main groups: gel-based methods and gel-free methods.

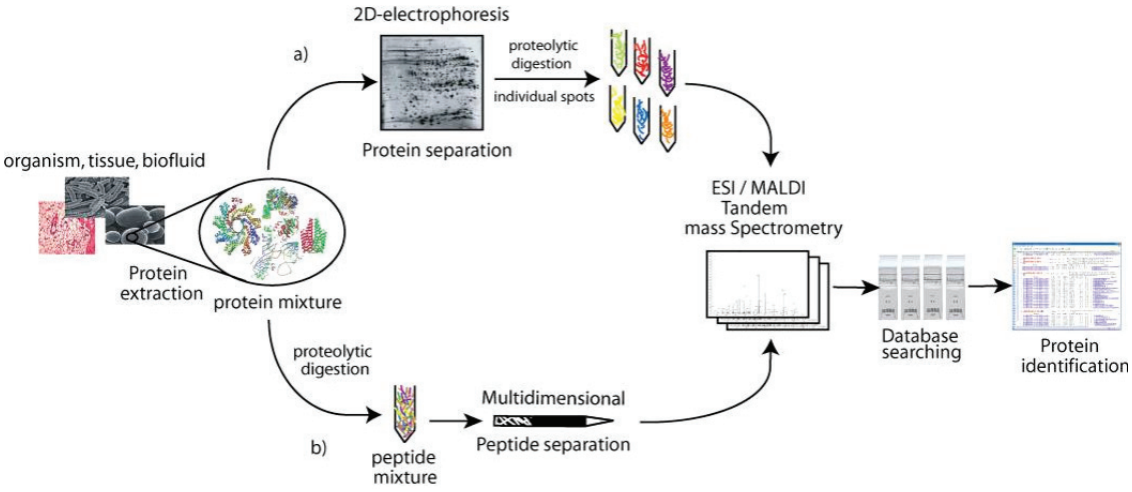

Figure 2.9. Proteomic Analysis by Gel-Based (a) and Gel-Free (b) Methods [28]

2.5.2.1. Gel-Based Methods

The most common gel-based method in MS-based proteomic studies is two-dimensional gel electrophoresis (2D-GE) which is based on the migration of charged particles with the help of an electric field. 2D-GE provides the separation of complex

protein mixtures extracted from cells, tissues, or other biological samples as individual proteins. This powerful method was first introduced by P. H. O'Farrell in 1975. Originally, the first-dimension separation was carried out in narrow tubes containing carrier ampholyte polyacrylamide gels [29].

In the first dimension, purified proteins are separated according to their isoelectric points (pI) in a pH gradient with isoelectric focusing (IEF). The isoelectric point is where the net charge of the protein is zero. Proteins are positively charged when pH value is below their pI and they are negatively charged when pH value is under their pI. Proteins migrate along the pH gradient under the electric field until they find the spot where their net charge is zero. Thus, IEF is a charge-dependent separation technique.

On the other hand, in the second dimension, focused proteins are separated based on their molecular masses by sodium dodecyl sulfate-polyacrylamide gel electrophoresis (SDS-PAGE). SDS is an anionic detergent. It forms micelles around each protein, masks the charge of the proteins, and forms anionic complexes which are all negatively charged per unit mass. This way, each protein has a unique place on the SDS-PAGE. At the end of the separation, proteins can be seen as a spot or a thin band on the gel.

To be able to observe the separated proteins on the gel, different staining procedures are applied such as Coomassie staining, silver staining, Sypro Ruby staining. After the staining, the gels are analyzed, and proteins of interest are determined. The proteins are excised from the gel and digested by a protease, generally trypsin. Finally, they are analyzed by mass spectrometry, usually MALDI-TOF, to identify and characterize the proteins.

The 2D-GE method allows the visualization of hundreds to thousands of proteins. Differential proteins between two different conditions can be determined, such as stress impacts, disease state differences, or toxic influences. With the developments, 2D-GE has gained more reproducibility, especially when immobilized pH gradients (IPG) took the place of carrier ampholytes. Despite these advantages, the reproducibility of gel electrophoresis is still poor, and it has a small dynamic range of staining. Since there are many protein spots, the excising and destaining procedures of each spot are very time-consuming. Moreover, low soluble proteins and membrane proteins are not apparent on the gel. In order to overcome these challenges, new proteomic approaches are being investigated [30].

2.5.2.2. Gel-Free Methods

All chromatographic techniques are based on the principle which is related to the interaction between the sample components and stationary and mobile phases. The sample is loaded the column and they attach to the stationary phase according to their affinities. While the flow of the mobile phase drags the analyte along the stationary phase, the components in the analyte are separated from each other. Thus, the separation in a typical liquid chromatography depends on the retarding time of the compounds in the column.

High performance liquid chromatography (HPLC) coupled with ESI is a very preferable method in MS based-proteomic analysis with its high recovery, reproducibility, speed, and high resolution. The deficiencies in gel-based method are eliminated with this on-line procedure, such as ion suppression effect is reduced, the intensity of low abundance peptides is increased, sample preparation is minimalized, and the impurities in analyte are removed. With all the developments, HPLC-ESI has become the main method for biological applications. Besides, HPLC has several separation modes which are reverse phase, normal phase, hydrophilic interaction, ion-exchange, gel filtration, and affinity. Reverse phase (RP) among them is the most frequently used one in proteomic studies due to its mobile phase content [31,32]. In RP mode, the mobile phase is a polar mixture of water and an organic solvent. This organic solvent is most commonly acetonitrile or methanol. The stationary phase, in other words the column type, is a non-polar material consists of long-chain hydrocarbons which is generally C18. The separation is based on the hydrophobic interactions between the sample and stationary phase. Elution is performed by increasing the organic solvent concentration in mobile phase gradually. As the organic solvent content is increased, the peptides are eluted in order according to their polarities. The most polar peptides have the least retention time, which means they are eluted first.

2.5.2.3. Multi-Dimensional Separation

Although one-dimensional liquid chromatography has many advantages over gel-based methods, it still appears to be insufficient considering the complexity of proteomes. Thus, multi-dimensional and orthogonal chromatographic techniques are developed to provide separation with higher resolution, increased dynamic range, and proteome

coverage [28]. The principle of multi-dimensional separation is connecting more than one separation techniques to increase the resolution. Different separation methods based on different molecular properties of molecules are applied one after another, in this way orthogonality is provided. Since RP-LC is always the one prior to the mass analyzer, the former separation is generally performed by ion-exchange chromatography. Strong cation exchange (SCX) liquid chromatography has been the most extensively used the first dimension for 2D-LC separations in proteomic analyses as it utilizes a different peptide separation mechanism than RP [28].

2.5.3. Protein Identification by Mass Spectrometry

Currently, there are two proteomic approaches to identify proteins by using mass spectrometry: top-down proteomics and bottom-up proteomics.

In the top-down proteomic approach, intact proteins are converted to gas-phase by ESI and fragmented by high-resolution mass spectrometry without any enzymatic digestion procedure, yielding the masses of both protein and its fragmented ions. Besides, PTMs on proteins and protein isoforms can be characterized depending on the quality of the spectrum [33]. However, this approach has significant challenges including expensive instrumentation, the need for a large amount of sample, and the restricted number of bioinformatic tools [34].

On the other hand, bottom-up proteomics deals with peptides instead of proteins. Proteins are digested into smaller peptides with a protease, commonly trypsin, and then separated by LC before the analysis. ESI is used to convert separated peptides into the gas phase.

The ions are first profiled to determine the masses of the intact tryptic peptides, in other words, the mass of the precursor ion (MS). These peptide ions are then fragmented in the gas phase to obtain the mass of fragmentation (MS/MS) which produces information on the amino acid sequence and modifications. Because of the solubility and mass range suitability of the peptides, bottom-up proteomics is widely used. The reason trypsin is mostly used for cleavage is its high activity and stability. It breaks down proteins specifically on the carboxy-terminal side of arginine and lysine residues [35] generating peptides in the effective mass range (500-2000 Da). Additionally, arginine and lysine are the most abundant amino acids in the human proteome and are widely dispersed throughout protein [36].

Both approaches have their own set of benefits and drawbacks. For example, top-down proteomics can allow for the acquisition of the entire sequence coverage because peptides might be lost during chromatography. Peptides are frequently assigned to more than one protein resulting a new challenge in protein identification. Moreover, peptides that are too large or too small may have to be ignored during mass analyses. On the other hand, peptide analysis has various advantages over protein analysis including lower molecular mass, effective LC separation, higher sensitivity, and lesser charge states.

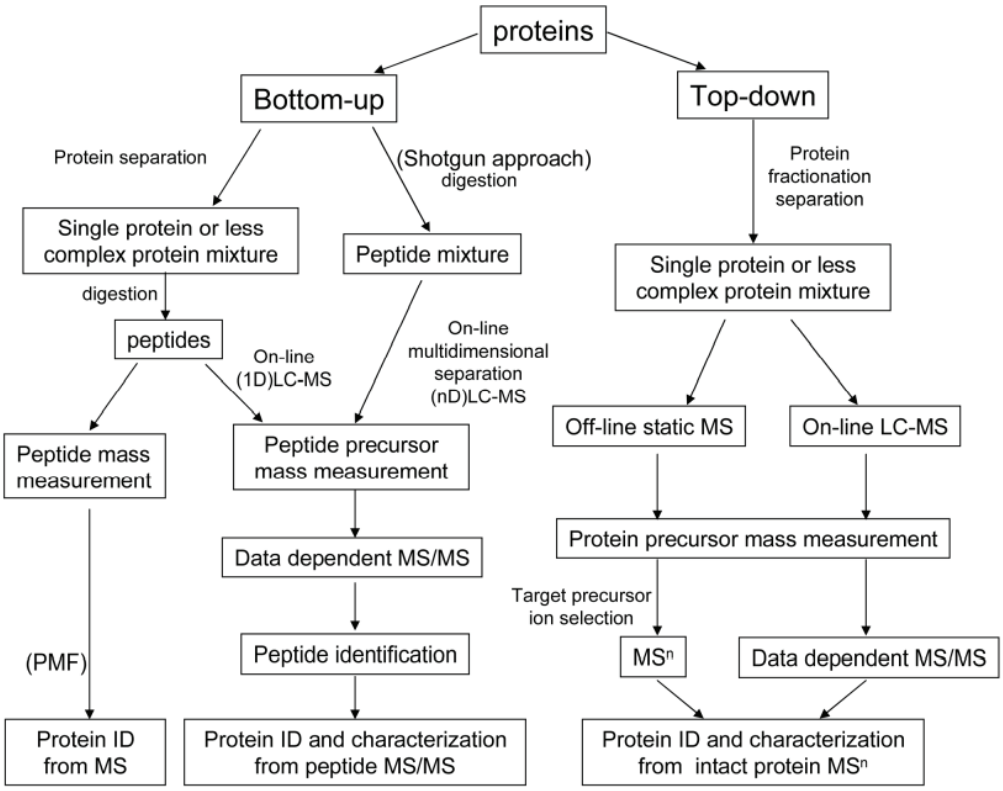

Figure 2.10. Strategies for MS-Based Protein Identification and Characterization [37]

Additionally, there is a new method called shotgun approach in which the sample of protein mixture is digested before the separation [38].

2.5.3.1. Shotgun Proteomic Approach

Multidimensional chromatography coupled with MS is commonly used for gel-free proteomic studies. The main principle of this method is the orthogonality of the dimensions, for this reason each separation is based on different properties. The on-line and off-line methods are the two kinds of multidimensional separation.

In on-line separation method, two different chromatographic methods are coupled. Principally, two LC columns are connected to each other with different stationary phases. Multidimensional protein identification technology (MudPIT) is a gel-free technique that is used to separate and identify the components of complex protein and peptide mixtures. MudPIT is firstly introduced by John Yates and his colleagues [28]. In this method, peptides are separated by 2D liquid chromatography instead of 2D gel electrophoresis. The fused-silica microcapillary column is packed with both strong cation exchange (SCX) and reversed-phase (RP) stationary phases, and this system is combined with ESI MS [28]. SCX liquid chromatography has been the most often used the first dimension for 2D-LC separations in proteomic studies since it uses a distinct peptide separation mechanism than RP. This way the peptides are first separated based on their charge, then hydrophobicity. The compatibility of the two separations, separation efficiency in both dimensions, and separation orthogonality determine the effectiveness of a 2D-LC separation.

The challenges in 2D-PAGE separation such as low-abundance proteins, membrane proteins, proteins with extreme physicochemical properties including molecular weight and isoelectric point can be overcome by MudPIT [39]. Since the peptides can be directly interfaced with the ion source of the mass spectrometer, it enables higher separation. Also, MudPIT eliminates the band broadening that several chromatographic stages cause, which can increase the resolution. First stage LC separation provides better compatibility with subsequent RPLC-MS analysis, as well as the integration of high-throughput methodologies, and ease of automation [28,39].

Digested peptide mixture is directly loaded into the first column without any additional sample handling. The eluent from the SCX column is directly eluted onto the RP column without any extra procedure such as fraction collection. This connection between SCX and RP columns ensures that salts and contaminations are removed from the RP column while the peptide mixture is held in the SCX column, and then the peptides are passed through the RP column. However, SCX has several drawbacks including reduced sample recovery, low capability for resolving peptides, and sample losses due to sample desalting, all of which might affect analytical sensitivity negatively. On the other hand, RP resolves peptides better than SCX, and salt-free buffers produce cleaner samples to use in LC-MS/MS analyses [39].

Although RP separation is better in various ways, two sequential RP separations do not provide orthogonality. The way of obtaining the orthogonality of SCX-RP

separation with 2D RPLC-RPLC is to operate the separations at widely different pH values such as 10 and 3. The charge distribution within peptide chains changes when the pH of the eluent changes, resulting in a difference in separation selectivity between low and high pH RPLC. The 2D-RPLC method is widely used in proteomic studies [39].

In off-line separation, digested peptide mixture is first separated in the first column, generally high pH RPLC column, and then collected and fractioned by using a 96 well plate. At the end of the elution, peptides in the well plate are collected with the concatenation strategy to balance the peptide level in every fraction. The advantage of concatenation is that it improves the proteome coverage in MS/MS analysis. These fractions are loaded to low pH RPLC column and then analyzed in ESI-MS/MS system. This technique is developed by Feng Yang and his colleagues [39].

2.5.4. Protein Quantification by Mass Spectrometry

Since it has been clear that protein identification only provides a limited amount of information, mass spectrometry-based proteomics become quantitative soon after its beginning. Two main approaches exist in quantitative mass spectrometry which are stable isotope labeling and label-free quantification. Stable isotope labeling is based on the mass difference between the labeled and unlabeled ions. The intensity ratio between the isotope variations represents the fold-difference between their abundances. One of the disadvantages is that any variation in sample preparation steps will affect the results. Samples that have been prepared and analyzed separately can be compared by label-free quantification. As mentioned before, variations in sample preparation may cause inaccurate results. Shotgun proteomics is suitable for label-free quantification due to the minimum sample preparation procedure. Protein quantification can be achieved in two ways; peak intensity of LC-MS and spectral counting.

Relative quantification with peak intensity is based on the changes in peptide peak area or peak height in chromatography. It has been observed that calculated and normalized peak areas correlate linearly to protein concentration. However, it has some disadvantages as well. One of them is that the peak intensity of the peptides can be different from run to run, even with the same sample. Also, multiple sample injections onto the same reverse-phase LC column can cause chromatographic shifts which can also affect the accuracy of the results [40].

In spectral counting-based protein quantification, the number of identified MS/MS spectra for the same protein is compared in each of the multiple LC-MS/MS datasets. Because an increase in the protein abundance usually leads to an increase in the number of proteolytic peptides produced by the protein, this results in an increase in the protein sequence coverage. Depending on these, the number of identified unique peptides and also the number of identified total MS/MS spectra for each protein are increased. Spectral counting-based quantification has been shown to have a larger dynamic range than the quantification with peak intensity, and also it is more reproducible. Owing to its simplicity of application, no specific methods have been developed for spectral counting. Yet, for accurate and reliable results for protein changes in complex mixtures, spectral counting datasets should be normalized and statistically analyzed [40].

Some spectral counting methods are protein abundance index (PAI), exponentially modified protein abundance index (emPAI), normalized spectral abundance factor (NSAF), absolute protein expression (APEX), normalized spectral index (SIN). In the emPAI method, the number of experimentally observed peptides and the calculated number of observable peptides are compared. The emPAI values are simply determined since it is implemented into the Mascot server, and it does not require any additional experimental steps. It is useful for determining approximate absolute protein abundance in large-scale analyses [41].

2.5.5. Peptide Sequencing

There are several techniques for protein identification and sequencing. The conventional one is Edman degradation which includes a series of chemical reactions. Phenyl isothiocyanate (PITC) forms a phenylthiocarbamyl derivative of the terminal amino acid residue by reacting with the α-amino group at the N-terminus. Then, the terminal amino acid residue is identified by HPLC, and this process is repeated for the next residue in the sequence. In this way, Edman degradation provides information about the amino acid sequence of the polypeptide. Although Edman degradation is widely used for the determination of extended sequences of peptides, it has some disadvantages. If the amino group has been modified and becomes unable to react with PITC, or the peptide is naturally cyclic and does not have an N-terminus, Edman degradation will not work.

PTMs can be identified and sequenced by MS/MS analysis. For this purpose, multiple mass analyzers can be coupled such as TOF/TOF, QqQ, Q/TOF, and collision-

induced dissociation (CID) technique is used. In principle, an ion with a particular m/z is selected with the first analyzer. The ion is focused and exposed to an inert gas in the collision cell. The kinetic energy of the precursor ion is converted to vibrational energy during the collision, resulting in ion fragmentation. Finally, the second mass analyzer determines the m/z value of the fragment ion. In this process, different ion types can be observed, and there is a specific nomenclature for these ion types based on where the fragmentation occurs [42].

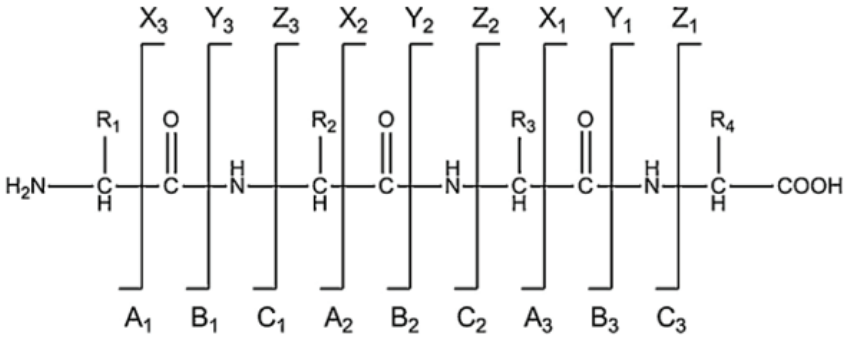

Figure 2.11. Nomenclature System for Peptide Fragment Ions [42]

As seen in the Figure 2.11., the N-terminus cleavages of the fragment ions are symbolized by the letters a-, b-, and c-; while the C-terminus cleavages are named as x-, y-, and z-. While fragmentation, if the positive charge stays in the amino-terminal, backbone cleavage occurs at the peptide amide bond, and b ions are generated. Likewise, if the charge is in the carboxy-terminal, y ions are produced.

2.5.6. Database Search

Tandem mass spectrometers have progressed with each day in shotgun proteomics, getting ever closer to the identification of the entire proteome. Search engines are one of the significant components to identify a proteome. They compare the acquired spectral data from tandem MS to theoretical data generated from a sequence database. Sequest, Mascot, and X! Tandem are some of the widely used search engines. Mascot employs probability-based matching; a protein list with score numbers is obtained as an outcome. As the score increases, the reliability of the identification matches increases.

Some parameters should be arranged before the database search. First, the proper database for searching is selected such as the National Center for Biotechnology

Information (NCBI) and Universal Protein Resource (UniProt). Another parameter is the enzyme used in proteolytic digestion, so the theoretical peptides in the database can be selected. The number of allowed miscleavages, fixed and variable modifications, peptide and MS/MS tolerances, peptide charges, data format, and instrument type are also the parameters that should be privatized for a proper search. One other important parameter is the decoy search which shows sequenced from databases that have been reversed or shuffled. It also estimates the false discovery rate (FDR) which is a measure of data quality. FDR values below 5% should be chosen for proteomic studies. Also, the percolator is an optional filtration that helps to distinguish between positive and negative peptide matches in order to reduce the false recovery rate. As a result, softwares like Mascot use various parameters to identify correct matches for the correct peptides. In this way, a single measurement can reveal thousands of peptides.

2.6. Aim of the Study

Today, Leishmaniasis has become a public health problem in all old-world countries due to transmission of the parasite with female sandflies, increased human relations, changing climate, and global warming. Many studies may be found by looking at this enlargement of the Leishmaniasis infection region. For example, in the study of Alborzi et al., patients with positive spleen punctures and positive bone marrow aspirates were examined to discover dominant Leishmania strains causing Visceral Leishmaniasis in Southern Iran. The findings suggest that Leishmania infantum is the most common causative agent for Visceral Leishmaniasis in Iran. A total of 64 samples were tested. According to the findings, 63 had *L. infantum* and only one had *L. tropica*. Thereby, this demonstrates that *L. tropica* can be a causative agent for Visceral Leishmaniasis [43].

In addition, many Visceral Leishmaniasis suspects from the Aegean and Mediterranean regions have lately been hospitalized with symptoms such as fever, liver and spleen enlargement, and weight loss. The study of Özbilgin et al. showed that it is caused by *L. tropica*, which means that *L. tropica* isolates from Turkey may visceralize in patients, resulting in more severe clinical symptoms. In the light of changing patterns of infectious agents, this could be considered a threat to Turkey. The aim of this study is to unveil the virulence factors of *L. tropica* isolates in the laboratory using *L. tropica* isolates from VL and CL patients by using mass spectrometric shotgun method.

CHAPTER 3

MATERIALS AND METHODS

3.1. Total Protein Extraction of *Leishmania tropica* and the Parasite Growth

Protein samples used in this study were obtained from patients with Cutaneous and Visceral Leishmaniasis caused by Leishmania *tropica*. There were two groups as Cutaneous and Visceral, both had 7 protein samples coded as C1-7 and V1-7, and there was one reference sample from strain. All *L. tropica* samples were cultivated, isolated, and extracted by Prof. Dr. Ahmet Özbilgin's group in Celal Bayar University, Faculty of Medicine, Department of Parasitology.

Frozen *L. tropica* promastigote cells preserved in liquid nitrogen were first dissolved in a 37 °C water bath and cultivated in NNN (Novy-MCNeal-Nicolle) medium at 25 °C. Then, transferred to RPMI-1640 medium containing 10% FCS, 200 U of penicillin/mL, and 0.2 mg of streptomycin/mL. When the promastigote population reached the logarithmic phase which is approximately 108 cell/mL concentration, the growth medium was centrifuged at 4400 rpm for 10 minutes at 4 °C in a clean 15 mL tube. After the centrifugation, pellets were allowed to incubate in RPMI 1640 medium without FCS overnight. Lastly, promastigotes were centrifuged at 4400 rpm to harvest the cells. The medium was removed by washing with PBS (Phosphate-buffered saline) buffer three times. 1 mL of Mammalian Cell Lysis Reagent (Fermentas Life Sciences) was added for cell lysis and the cells were incubated at room temperature on a shaker at 900 rpm. The total protein was extracted by centrifuging at 14500 rpm for 15 minutes at 4 °C. The supernatant was preserved at -20 °C for future proteomic analysis.

3.2. Total Protein Quantification and Purification

Protein samples were first purified by acetone precipitation process. The aim of this process is to exchange the cell lysis reagent with a proper buffer containing 8M urea dissolved in 0.1M Tris-HCl solution at pH 8.3.

In acetone precipitation, 4 volumes of -20 °C acetone was added to 1 volume of protein sample and incubated at -20 °C for 2.5-3 hours. Next, this mixture was centrifuged at 14000 rpm at 4 °C for 15 minutes. After the centrifugation, the supernatant was removed without damaging the protein pellet on the bottom of the tube and the protein was left for air-drying of the remaining acetone. Then, the protein was dissolved in the buffer solution. One of the possible problems that might observed in this process is the denaturation of the proteins which makes the pellet difficult to resolubilize. Also, all of the contaminants may not be removed by a single precipitation. However, several precipitations can cause sample loss [44].

Bradford method was used to determine the total protein concentration. In this method, the presence of the basic amino acid residues is measured which forms protein-dye complex and results in a color change from brown to blue in acidic conditions.

BSA standards were prepared with a range of 0 to 1500 µg protein. 200 µL of Bradford reagent, 5 µL of BSA standards, and 795 µL of ultrapure water were mixed in a 96 well-plate in order to draw the calibration curve. For unknown protein samples, 200 µL of Bradford reagent, 5 µL of protein solution, and 795 µL of ultrapure water were mixed. After the quantification of protein samples with a spectrophotometer, the protein concentration was set to 150-200 µg for each sample.

3.3. In-Solution Digestion of Proteins

In order to digest the complex protein mixture to peptides, in-solution digestion procedure was applied. Filter-aided sample preparation (FASP) method was used to remove excess urea, salts, and other possible contaminants. FASP procedure was applied as described below.

1- Each sample was placed in 30K molecular weight cut-off (MWCO) filters and their volumes were made up to 200 µL with 8M urea solution.
2- 8 µL of 0.2M dithiothreitol (DTT) solution was added as reducing agent and incubated for 20 minutes.
3- The filters were centrifuged at 14000 g for 15 minutes.
4- 100 µL of 50 mM iodoacetamide (IAA) solution was added as alkylating agent and incubated in the dark for 20 minutes.
5- Samples were centrifuged for 15 minutes.

6- Samples were washed with 100 µL of 8M urea solution.
7- Samples were centrifuged for 10 minutes.
8- Samples were washed with 100 µL of 8M urea solution.
9- Samples were centrifuged for 10 minutes.
10- 100 µL of 50 mM ammonium bicarbonate (ABC) solution was added to balance the pH.
11- Samples were centrifuged for 10 minutes.
12- 100 µL of 50 mM ammonium bicarbonate (ABC) solution was added.
13- Samples were centrifuged for 10 minutes.
14- For digestion, 4 µg trypsin (enzyme to protein ratio is 1:50) solution prepared in 50 mM ABC solution was added in every sample and incubated at 37 °C overnight.

Following the incubation, the peptides were washed with 40 µL of ABC solution 3 times into clean tubes and after every ABC solution addition, they were centrifuged for 10 minutes. To decrease the volume for the subsequent HPLC separation, samples were evaporated by a speed-vac concentrator to approximately 20 µL.

3.4. High pH RP Chromatography with Fraction Concatenation and LC-MS/MS Analysis

As a result of the digestion, a very complex mixture of peptides was obtained. The complexity should be reduced in order to improve the proteome coverage in MS/MS analysis. Reducing the complexity was provided by fractionation, which +means pre-separation by off-line HPLC. The HPLC system used for fractionation was SHIMADZU Prominence UFLC and the software was LC Solution Version 1.25 SP3. The column was Reverse Phase C18-Teknokroma Mediterraneasea18 with the dimensions 25 cm x 0,46 cm, 5µm and it was coupled with Sunchrom Micro Fraction Collector. The details about the method are given in Table 3.1. The separation was based on the change in charge distribution in peptide chains as the pH of the eluent changes. In this way, an efficient salt-free separation was provided compared to low pH columns.

Table 3.1. Off-line HPLC Conditions and Parameters

LC Conditions		LC Program	
Column Temperature	40 ˚C	*Time (min)*	*Mobile Phase B*
Mobile Phase A	10 mM Ammonium formate-Water pH 10	0,1	2.0%
Mobile Phase B	10 mM Ammonium formate-Acetonitrile pH 10	2	2.0%
Injection Volume	75 µL	3	8.0%
Flow Rate	0.1 mL/min	33	35.0%
Fraction Duration	30 second/well (loaded to 96 well plate)	43	65.0%
		46	85.0%
		52	85.0%
		54	2.0%
		60	2.0%

First, fractions were collected on a 96 well plate. To decrease the number of fractions, they were assembled. The fractions in the same column were collected in 2 mL clean tubes as shown in Figure 3.1. As a result, all Leishmania protein digests had 12 fractions each.

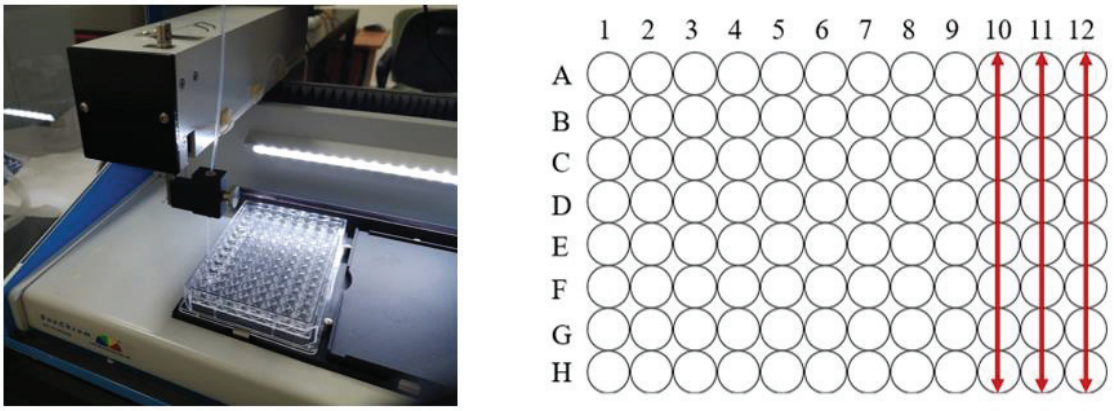

Figure 3.1. Fraction Collection and Assembling Processes

For LC-MS/MS analysis, all 12 fractions were evaporated completely and then dissolved in a suitable amount of mobile phase A. The system used for the analysis was DIONEX UltiMate 3000 with the software Chromeleon Version 6.80 and the column was Zorbax 300SB-C18 with the dimensions 0.3 x 250 mm, 5µm. The data-dependent settings were input as shown in Table 3.2., while the rest of the parameters were kept at their default values. 12 fractions of each sample were again separated by HPLC prior to MS/MS analysis. This second separation was based on the hydrophobicity of the peptides and a low pH reversed-phase column is used. Outlet tubing at the end of the column was

linked to the electrospray inlet. 12 fractions of each sample were analyzed, and data were merged in a single file for each sample. Using the tools in Proteome Discoverer 1.4, data collected in Thermo's raw format was transformed to Mascot Generic File format (mgf).

Table 3.2. LC-MS/MS Conditions and Parameters

MS Data-Dependent Setting Parameters		LC Conditions	
Acquire Time (min)	60	*LC Principle*	Reversed Phase
Scan Events (SE)	11	*Column Oven*	40 ˚C
MS Scan Ranges (m/z)	400-1800	*Mobile Phase A*	0,1% Formic acid-Water
Polarity	Positive	*Mobile Phase B*	0,1% Formic acid-Acetonitrile
Data Type	Centroid	*Injection Volume*	2.5 µL
Activation Type	CID	*Flow*	5 µL/min
Default Charge State	2	LC Program	
Isolation Width (m/z)	2.0	*Time (min)*	*Mobile Phase B*
Activation Time (ms)	30.0	0.00	5.0%
Dynamic Exclusion	Enabled	4.00	5.0%
Repeat Count	1	44.00	5.0%
Repeat Duration (s)	30	48.00	25.0%
Exclusion List	500	52.00	35.0%
Exclusion Duration (s)	20	54.00	60.0%
Exclusion Mass Width	± 1.5	56.00	95.0%
Reject Charge States	1, 4&up	58.00	5.0%
Signal Treshold (counts)	5000	62.00	5.0%
Normalized Collision Energy (V)	35		
ESI			
Spray Voltage (kV)	4,5		
Capillary Temperature (˚C)	220		
Capillary Voltage (V)	7		

3.5. Database Search and Mascot Parameters

Data obtained from LC-MS/MS analysis was merged for every sample and searched in the database by the Mascot server (version 2.3.02). The database used was installed from the Uniprot website (www.uniprot.org) in FASTA format. *L. major* database which has 33,208 entries was combined with *L. tropica* proteins. Search parameters were set as shown in Table 3.3. Besides these parameters, the decoy database was selected for all searches. It is a method of reversing or shuffling the current databases

to verify the accuracy of the results. Hence, actual matches should be expected from decoy searches.

Table 3.3. Mascot Server Search Parameters

Mascot Search Parameters	
Database	*L. major* and *L. tropica*
Enzyme	Trypsin
Missed Cleavages	2
Taxonomy	All Entries
Fixed Modifications	Carbamidomethyl (C)
Variable Modifications	Oxidation (M)
Peptide Tolerance	± 1.2 Da
MS/MS Tolerance	± 0.6 Da
Peptide Charge	2+ and 3+
Data Format	Mascot Generic Format (mgf)
Instrument	ESI-TRAP

Lastly, common and differential proteins between Cutaneous and Visceral Leishmania samples were determined and classified by entering the data into an excel sheet in order to determine if there were any significant differences or correlations between them.

CHAPTER 4

RESULTS AND DISCUSSION

In this study, shotgun proteomic approach was used to compare different clinical forms in Leishmaniasis disease. LC-MS/MS system worked with Mascot Server to obtain reliable results. Since the search parameters are essential, the methods and parameters were optimized before the analyses with another set of samples which was treated as same as the main samples.

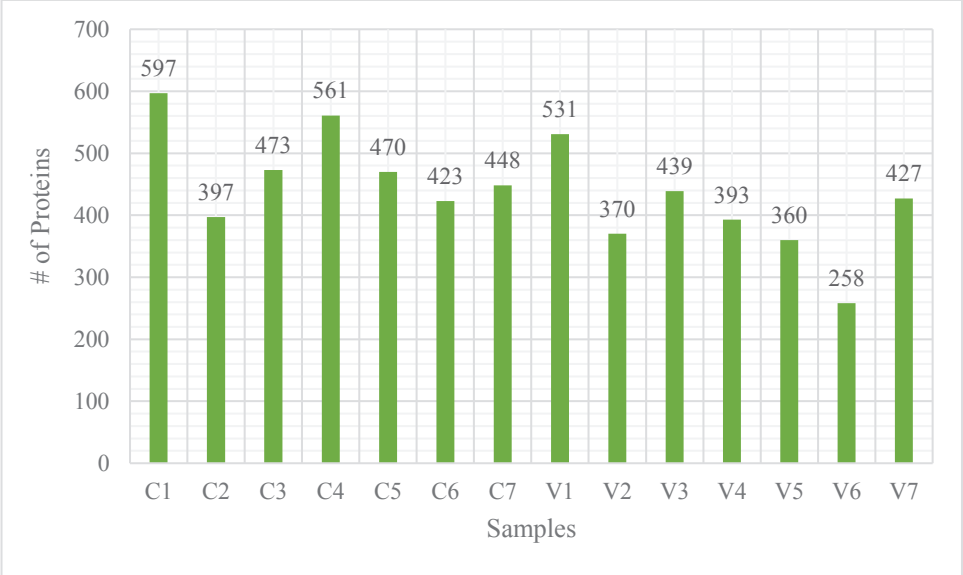

Figure 4.1. The Number of Identified Proteins for Each Sample

The Mascot search for all 7 CL, 7 VL, and one reference *L. tropica* sample resulted in 2111 total proteins, 2102 of which are Leishmania proteins, and the others are contaminants. Identified total protein numbers for each sample are shown in Figure 4.1. as the number of proteins versus samples. The spectral counting data that Mascot calculated by label-free quantification shows the protein abundance in each sample. Since the analysis conditions might not be ideal, the emPAI [45] data were normalized to total for each sample. Since the full protein table occupies too much place, a table containing 541 Leishmania proteins found in at least four samples are listed on the Appendix A, and the Table 4.1. demonstrates a small part of the table.

Table 4.1. emPAI Data of Proteins for All Samples

A0A173DUZ9	A0A145YEQ2	A0A142C7A7	A0A142C7A6	A0A0R6YB19	A0A0R6Y3Z1	A0A0R6XZU5	A0A089GSF5	A0A089FQZ7	**Entry Name**
1,348	0,000	0,000	0,959	0,000	0,000	0,000	0,432	0,432	**C1**
1,792	0,151	0,000	0,979	0,226	0,000	0,226	0,000	1,461	**C2**
1,109	0,000	0,000	1,415	0,089	0,000	0,000	0,000	0,637	**C3**
0,856	0,000	0,787	0,639	0,148	0,561	0,000	0,000	0,708	**C4**
0,000	0,000	0,000	1,413	0,000	0,000	0,000	0,637	0,000	**C5**
2,873	0,000	0,000	1,275	0,000	0,000	0,172	0,000	0,172	**C6**
1,917	0,000	0,418	0,799	0,086	0,307	0,184	0,614	0,000	**C7**
0,000	0,326	0,000	1,639	0,000	0,000	0,144	0,000	0,297	**Ref.**
0,000	0,000	0,000	1,129	0,071	0,580	0,000	0,508	0,508	**V1**
0,000	0,172	1,377	1,119	0,120	0,000	0,000	0,861	0,000	**V2**
0,000	0,148	0,502	1,639	0,000	0,000	0,000	0,000	0,738	**V3**
0,000	0,000	1,346	1,868	0,252	0,000	0,000	0,522	0,000	**V4**
0,000	0,000	0,000	1,576	0,099	0,000	0,000	1,022	0,000	**V5**
0,000	0,000	0,000	2,784	0,000	0,000	0,000	0,778	0,000	**V6**
0,000	0,000	0,000	0,887	0,096	0,341	0,000	0,000	0,205	**V7**

The 14 samples were categorized as C and V and the reference sample was not included in the statistical tests. The tests were done by Perseus [46] software in order to determine the statistically significant proteins among all of them, which means proteins showing significant differences between the two identified groups based on abundance. Student's t-test (p=0.05) determined that 91 of the 2102 proteins showed statistically significant changes between the cutaneous isolates and visceral isolates, which are listed by the decreasing -log(p-value) on Table 4.2. and Table 4.3. The darkest colored cells indicate p<0.01, moderate cells mean p<0.03, and the lightest colored ones are p<0.05. Moreover, Figure 4.2. demonstrates the number of proteins in different significance levels. As shown in the figure, 33 differentially abundant proteins are present at the p<0.01 level in the cutaneous group, while there are 10 proteins at the same level in the visceral group.

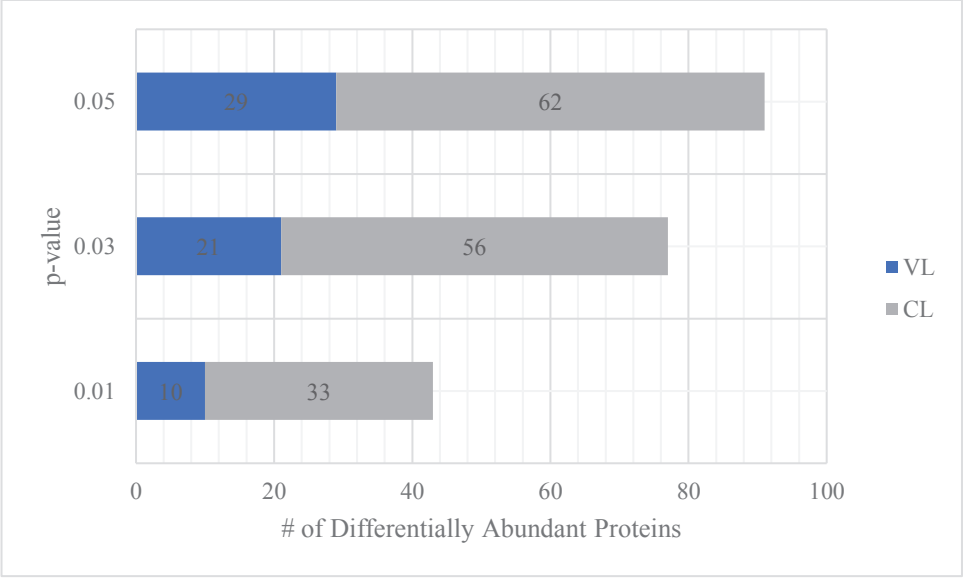

Figure 4.2. The Number of Differentially Abundant Proteins of VL and CL Isolates in Different Significance Levels

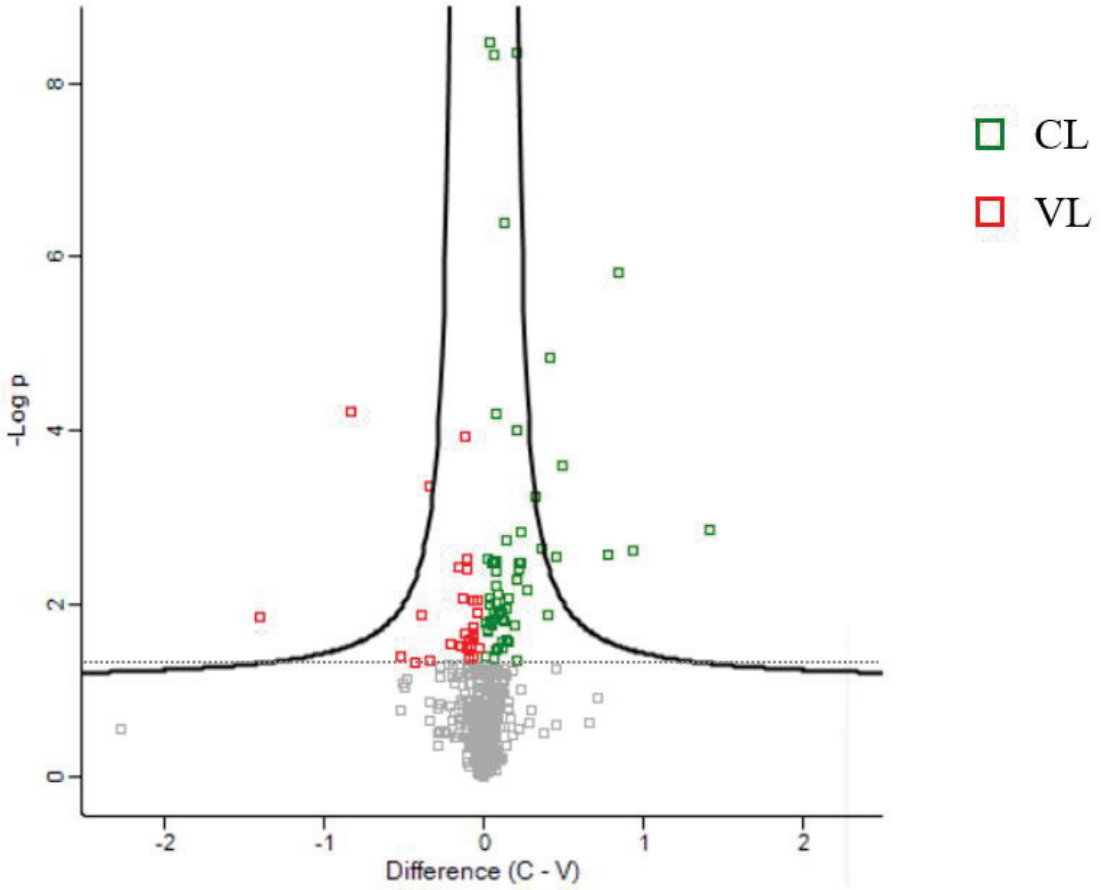

Figure 4.3. Volcano Plot Showing Statistically Significant Proteins Between CL and VL

The 91 proteins are visualized on the Volcano Plot (Figure 4.3.) among all 2102 proteins, above the dashed line. The Volcano Plot is plotted as the difference (fold change) versus p-value. The p-value represents the statistical significance between the two specified groups. The y-axis of the plot is -log(p-value), which results in the highly significant data points appearing on the top of the diagram. Fold change, or difference on the x-axis, is a measure of change in the protein expression levels: The significance of the data increases as the distance from zero-point increases. Red colored 29 proteins are up-regulated in VL compared to CL, while the 62 proteins shown in green down-regulated. The number of those 91 proteins found in also the reference sample is 55, which are listed on the Appending B by the p-value.

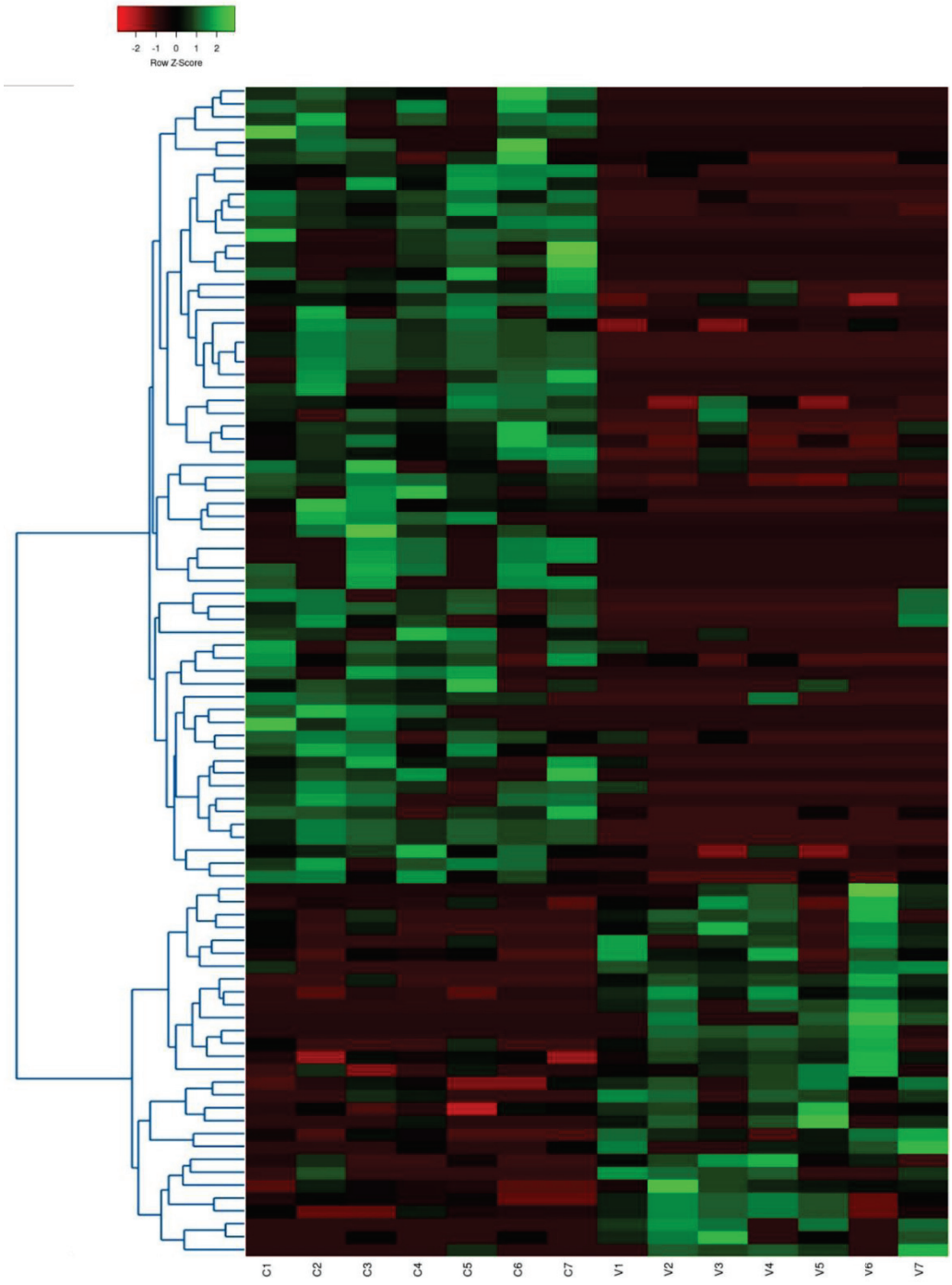

Figure 4.4. Heat Map for Differentially Abundant Proteins

Of the 91 proteins, only 24 proteins increased in abundance, whereas 29 proteins down-regulated in VL. 5 proteins were found in only VL samples and absent in all 7 CL samples, and 33 proteins were only observed in CL samples. In order to focus on the determined 91 protein, clustered heat map presenting differentially expressed proteins between CL and VL is plotted as an alternative illustration (Figure 4.4.). The protein

expression levels are displayed as color gradients in the map, and a dendrogram is present by the heat map, showing hierarchical clustering. The clustering of the data is done by Minitab software in order to group similar data sets.

Table 4.2. Differentially Abundant Proteins in CL

Entry Name	p-value	Difference	Protein Name
Q4Q9P4	8,481303292	0,035428572	Putative kinesin
Q4Q8Q9	8,365930214	0,201000001	Proteasome subunit beta
Q4QG98	8,365930214	0,201000001	60S ribosomal protein L18
Q9XZX9	8,334434401	0,059000001	Surface antigen-like protein
Q4Q7A2	6,403654517	0,125	Succinyl-CoA:3-ketoacid-coenzyme A transferase
Q4Q350	5,818598152	0,838285714	Uncharacterized protein
Q4QEM2	4,837533864	0,419714286	Paraflagellar rod protein 2C
E9AD27	4,204428951	0,074714288	Putative calpain-like cysteine peptidase
Q4Q9Y8	3,996866433	0,201285716	Ferroxidase
A0A1Z1LZQ6	3,600977077	0,492428567	Superoxide dismutase
Q4FX73	3,24112394	0,32914286	40S ribosomal protein S3a (LmS3a-related protein)
A0A173DUZ9	2,851209966	1,413571434	Thiol-specific antioxidant
Q4Q159	2,826551114	0,23842858	Cysteine synthase
E9ADA3	2,740592587	0,138285716	Uncharacterized protein
E9ADX3	2,633132657	0,365285718	Tryparedoxin
Q4Q9D0	2,614448742	0,933571411	Putative 10 kDa heat shock protein
Q4Q156	2,56777442	0,773428559	EF-hand domain-containing protein
Q4QG97	2,553688272	0,453142864	40S ribosomal protein S12
Q4QCD3	2,508738028	0,024	Uncharacterized protein
Q4Q5P6	2,505636398	0,07757143	Putative 26S proteasome regulatory subunit
Q4QEB3	2,504857599	0,06	GMP reductase
Q4Q8I6	2,47992919	0,222714284	Putative RNA binding protein rbp16
Q4QC87	2,474725586	0,049428572	T-complex protein 1 subunit delta
E9AE33	2,473171449	0,229285715	Histone H2A
Q4QIQ0	2,397014758	0,214000002	Putative 3-hydroxyacyl-ACP dehydratase
Q4Q5J8	2,383505524	0,079000003	RRM_8 domain-containing protein
Q4QEI9	2,277601854	0,209142855	Elongation factor 1-alpha
E9AFL0	2,213811416	0,073714286	CCT-eta
Q4Q1C4	2,150588338	0,27385714	Succinate--CoA ligase [ADP-forming] subunit beta, mitochondrial
Q4Q0X8	2,107772619	0,095428571	Proteasome regulatory ATPase subunit
Q4Q0Q0	2,07430654	0,159571429	40S ribosomal protein SA
Q4Q4N5	2,056565487	0,042999999	Myosin XXI
E3VNP2	2,018199367	0,078428569	Phosphoglucomutase (Fragment)
Q4Q3I5	1,995735509	0,041142858	IFT81_CH domain-containing protein
Q4Q1B2	1,939797298	0,146000002	Fibrillarin
Q4QB32	1,92847029	0,099000001	T-complex protein 1 subunit gamma
Q4QFY8	1,905177484	0,110285716	Putative chaperonin TCP20
Q70GE8	1,894287481	0,067285715	Thiol-dependent reductase 1

(cont. on next page)

Table 4.2. (cont.)

Entry Name	p-value	Difference	Protein Name
A0A5Q2WYC5	1,875420935	0,399142861	40S ribosomal protein S4
Q4Q937	1,867875959	0,088285714	Putative thimet oligopeptidase
Q4QBT5	1,828666561	0,114285714	Putative proteasome regulatory ATPase subunit 5
Q4QG76	1,815117882	0,059857143	Protein kinase domain-containing protein
E9AFD1	1,794009431	0,035571428	Uncharacterized protein
E9AFY0	1,793831476	0,132571429	Uncharacterized protein
Q95Z92	1,792736561	0,033	Putative cAMP-specific phosphodiesterase
E9AE82	1,770615169	0,037714287	Putative GTP-binding protein
Q4Q7T4	1,767516706	0,019285715	Putative ubiquitin hydrolase
Q4Q3D9	1,767386248	0,018285714	Uncharacterized protein
E9AEB9	1,763626877	0,050285714	Putative serine/threonine-protein kinase
E9AF02	1,762668539	0,049857143	Trypanin-like protein
Q4QII4	1,749500923	0,194714291	Peptidyl-prolyl cis-trans isomerase
Q4Q5L5	1,707988773	0,019857143	Putative OSM3-like kinesin
E9AF31	1,683961641	0,023428571	Putative calcium motive P-type ATPase
C6KJE4	1,577951438	0,139	Actin
Q4QI38	1,567318737	0,152714284	Dimethylargininase
Q4Q9X6	1,564833281	0,111	ATP synthase subunit beta
Q4Q2S5	1,501552684	0,113714284	RRM domain-containing protein
Q4QJ88	1,491262772	0,085857142	V-type proton ATPase subunit
E9ADW8	1,458664857	0,081428573	Ankyrin_rpt-contain_dom domain-containing protein
E9AD28	1,398648063	0,007571429	Putative calpain-like cysteine peptidase
Q4QJJ3	1,377815856	0,067857143	Serine/threonine-protein phosphatase
E9ADQ2	1,348070713	0,208	ADF/Cofilin

Table 4.3. Differentially Abundant Proteins in VL

Entry Name	p-value	Difference	Protein Name
Q4QBF5	4,219338905	-0,833285696	Putative endoribonuclease L-PSP (Pb5)
Q4Q6F0	3,93161304	-0,113428572	Putative N-acyl-L-amino acid amidohydrolase
Q4QH22	3,359594543	-0,333142857	Putative cytochrome b5
P84155	2,524126117	-0,109857144	Oxygen-dependent coproporphyrinogen-III oxidase
Q4Q9N8	2,41927191	-0,151000002	Putative 2,4-dihydroxyhept-2-ene-1,7-dioic acid aldolase
Q4Q7A3	2,408400006	-0,104142857	Succinyl-CoA:3-ketoacid-coenzyme A transferase
Q4Q9R8	2,052655307	-0,130285709	Pyruvate dehydrogenase E1 component subunit beta
Q4QEL8	2,042663737	-0,043857143	Putative kinesin
E9AD65	2,031954238	-0,06042857	Oxoglutarate dehydrogenase (succinyl-transferring)
Q4Q0Q2	2,029108739	-0,041000001	Uncharacterized protein
Q4QFJ7	1,904173291	-0,040285715	Putative tyrosyl-tRNA synthetase
Q4Q4I6	1,883023884	-0,390714279	Heat shock protein 83-1
Q07DU5	1,854668398	-1,398714287	Peroxidoxin 2

(cont. on next page)

Table 4.2. (cont.)

Entry Name	p-value	Difference	Protein Name
Q4Q735	1,734432428	-0,064571431	Formyltetrahydrofolate synthetase
Q4Q7T9	1,656732986	-0,120285715	Putative 2-hydroxy-3-oxopropionate reductase
Q4QH21	1,646479059	-0,06757143	Putative 3-methylcrotonoyl-CoA carboxylase beta subunit
Q4Q812	1,633440168	-0,070142857	Putative acyl-CoA dehydrogenase
Q4Q939	1,614333076	-0,061714285	Trifunctional enzyme alpha subunit, mitochondrial-like protein
Q4QI59	1,5779671	-0,088428571	Uncharacterized protein
Q95Z84	1,535135557	-0,205142856	Spermidine synthase
E9AEW4	1,524458929	-0,082857143	Threonyl-tRNA synthetase
Q4QDQ1	1,508641616	-0,138857141	Putative pyruvate dehydrogenase E1 component alpha subunit
Q4QAB9	1,4948162	-0,109428576	HMG_CoA_synt_N domain-containing protein
E9AE81	1,493889697	-0,021428571	Uncharacterized protein
Q4QBJ3	1,405898947	-0,059	Alanine--tRNA ligase
Q4QFI3	1,387181214	-0,521714291	Histone H4
Q4Q8A8	1,362736107	-0,085285714	Putative hydrolase, alpha/beta fold family
A0A7S5YR77	1,353135251	-0,338571421	Leishmanolysin (Fragment)
E9AFS3	1,321058176	-0,429714288	Sm protein F

The identified proteins that are statistically significant between the designated two groups were categorized according to their molecular functions with Gene Ontology (GO) classification using UniProt database as binding, catalytic activity, ATP-dependent activity, structural constituent of ribosome, antioxidant activity, transmembrane transporter activity, cytoskeletal motor activity, translation factor activity, RNA binding, iron chaperone activity, molecular adaptor activity, and microtubule motor activity (Figure 4.5.). It is observed that the differentially abundant proteins in both visceral and cutaneous groups are mainly involved in binding and catalytic activity as a molecular function.

Binding and catalytic activities are detailed in Figure 4.6. for cutaneous isolates and Figure 4.7. for visceral isolates. Cutaneous isolates have proteins involved in catalytic activities acting on RNA and acting on a protein, which are different from visceral samples. Fibrillarin (Q4Q1B2) shows catalytic activity acting on RNA. Putative thimet oligopeptidase (Q4Q937), serine/threonine-protein phosphatase (Q4QJJ3), protein kinase domain-containing protein (Q4QG76), putative 26S proteasome regulatory subunit (Q4Q5P6), peptidyl-prolyl cis-trans isomerase (Q4QII4), tryparedoxin (E9ADX3), proteasome subunit beta (Q4Q8Q9), fibrillarin (Q4Q1B2), putative serine/threonine-protein kinase (E9AEB9), and thiol-dependent reductase 1 (Q70GE8) proteins are

involved in catalytic activity, acting on a protein. Moreover, ferroxidase (Q4Q9Y8) protein is involved in 2 iron, 2 sulfur cluster binding function, which is also not expressed in visceral isolates.

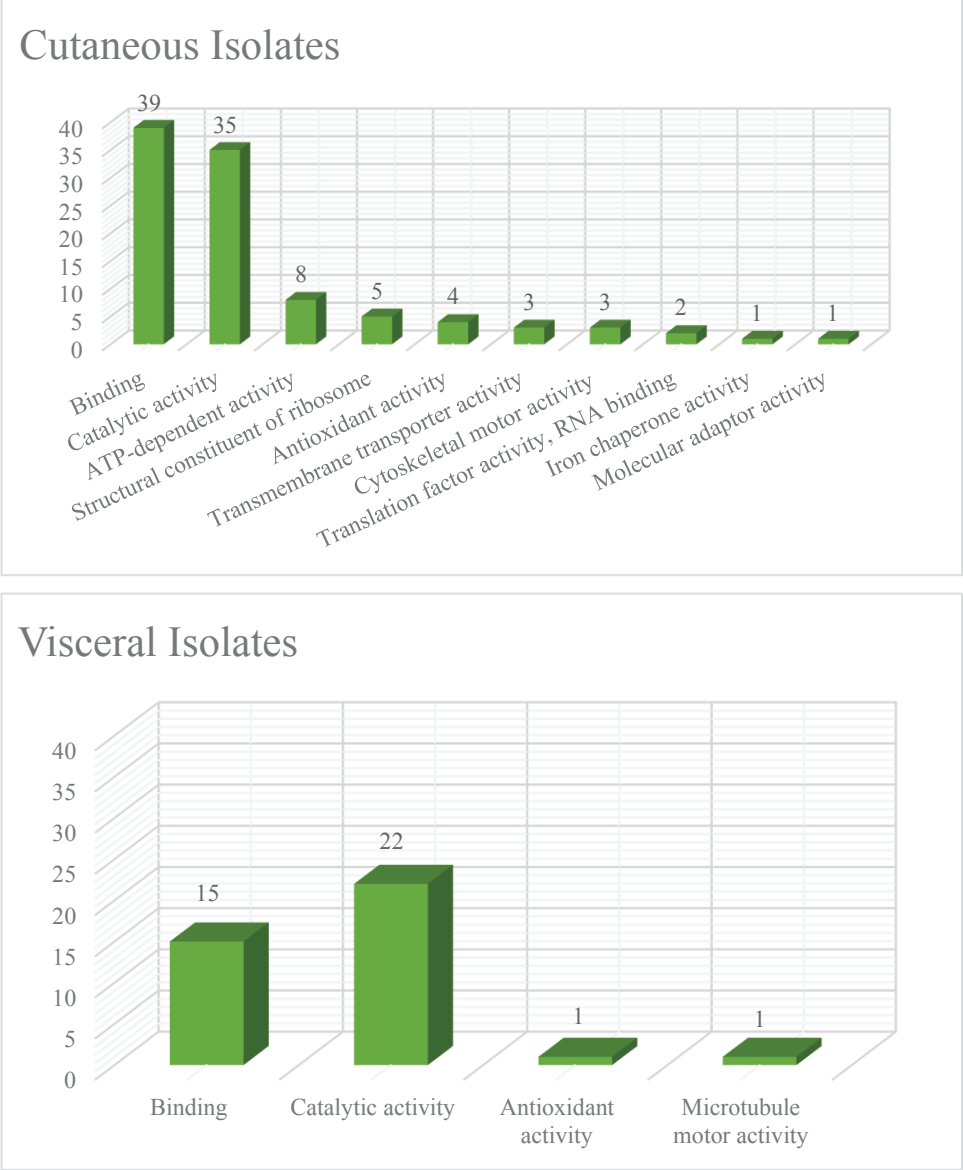

Figure 4.5. Molecular Function Classification of Differentially Abundant Proteins of *L. tropica*

It is observed that proteins related to phosphorylation, cysteine-related proteins, proteasomes, ribosomal proteins, and chaperone-containing t-complex proteins have accumulated in cutaneous samples. However, these proteins are not expressed with same the intensity in visceral isolates.

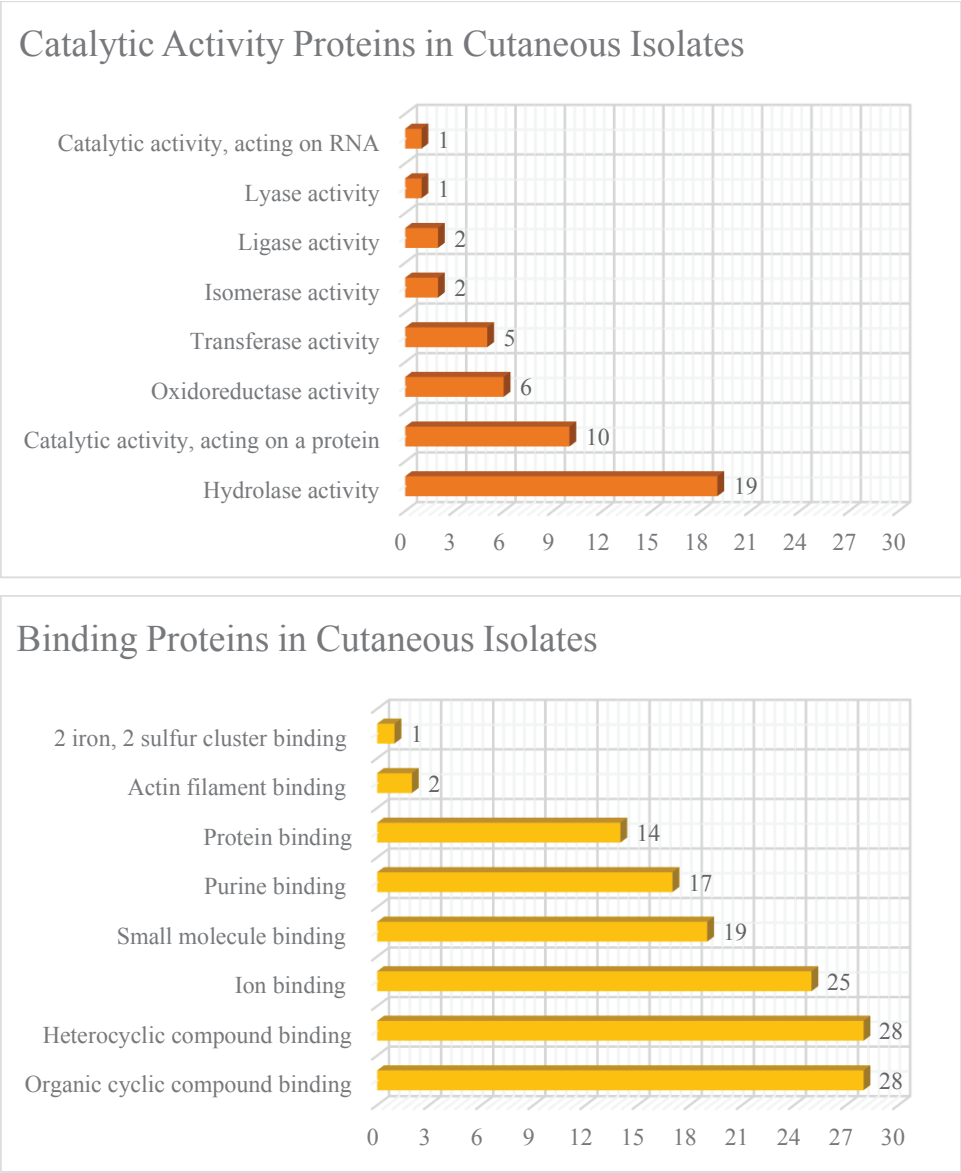

Figure 4.6. Catalytic Activity and Binding Proteins for Cutaneous Isolates

Instead, visceral samples expressed proteins involved in catalytic activity, acting on a tRNA: putative tyrosyl-tRNA synthetase (Q4QFJ7), alanine-tRNA ligase (Q4QBJ3), and threonyl-tRNA synthetase (E9AEW4). Also, oxoglutarate dehydrogenase (E9AD65) protein involving thiamine pyrophosphate binding is differentially expressed in visceral isolates.

In visceral *L. tropica* samples, the proteins involved in the amide biosynthetic process and pyruvate metabolic process have accumulated differently from cutaneous samples.

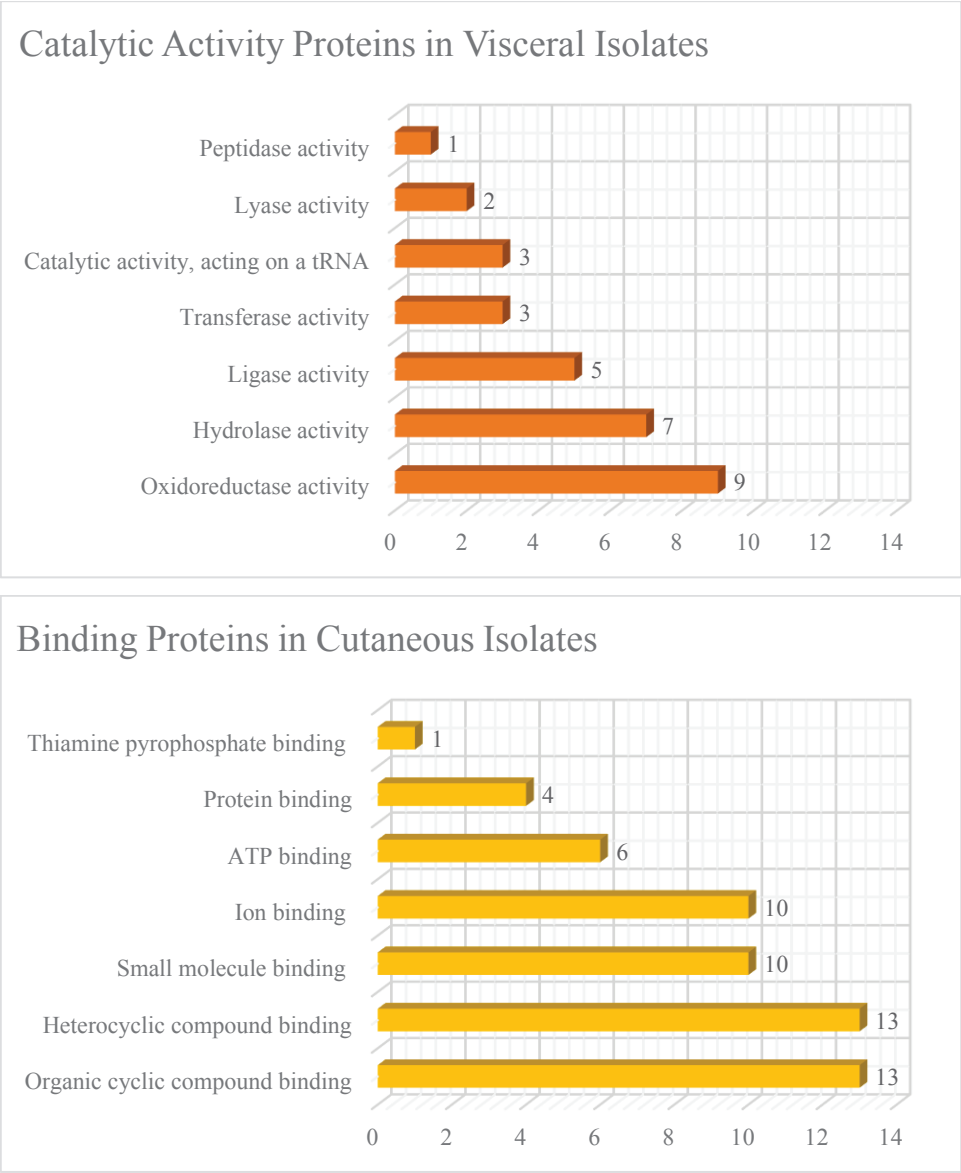

Figure 4.7. Catalytic Activity and Binding Proteins for Visceral Isolates

These differentially abundant proteins between cutaneous and visceral isolates are investigated detailly to understand the reason behind viscerotropism in *L. tropica*. One of the protein groups that seems to have an effect on this situation is paraflagellar rod proteins. Paraflagellar rod (PFR) is a major part of the flagellum of kinetoplastids and is involved in various functions, including cell motility, chemotaxis, cell signaling, and host cell invasion [47]. Studies showed that PRF proteins are found in both promastigote and amastigote forms of the Leishmania, but down-regulated in the amastigote stage, since amastigotes do not possess a flagellum [48–51]. Some of the paraflagellar rod proteins are differentially abundant in cutaneous isolates, which are paraflagellar rod protein 2C (Q4QEM2), myosin XXI (Q4Q4N5), fibrillarin (Q4Q1B2), actin (C6KJE4), and

ADF/cofilin (E9ADQ2). Actin is a ubiquitous cytoskeletal protein that has a crucial role in cell motility in all eukaryotic cells. ADF/cofilin is an actin dynamics-regulating protein and is an essential component of the assembly and motility of the eukaryotic flagellum [51,52]. The study of Tammana et. al. indicates that in the lack of ADF/cofilin, Leishmania cells are immotile, have a shorter cell body and flagellar, and limited cell growth [47]. According to the study of Katta et. al., myosin XXI also has a function in actin dynamics during the formation of the kinetoplastid flagellum and can contribute to flagellum assembly and motility function [50].

Additionally, several studies state that PFR proteins are immunogenic [49,53,54]. Saravia et. al. studied the immune response against *L. mexicana* and *L. panamensis* depending on the inoculation strategy and the sex of the hamsters [53]. The results showed that the PFR-2 DNA vaccine is able to delay the formation of cutaneous lesions caused by *L. mexicana* in male hamsters and cause lesion reduction. However, it was not effective in female hamsters. Although it is unclear how the PFR proteins can generate an immune response, some theories exist. It has been proposed that during the transformation of Leishmania promastigotes to amastigotes inside the host macrophages, degradation of the flagellum can cause the components of the paraflagellar rod to become available for immune recognition [49,53,54]. The results indicate that the paraflagellar rod proteins have significantly higher expression levels in cutaneous isolates, which could mean that the flagellar of the parasite might be longer and more developed, and the cells might have higher motility compared to visceral promastigotes. Thus, the parasite can avoid the recognition of the immune system by down-regulating the paraflagellar rod proteins in the visceral form.

Another protein decreasing in abundance in visceral form is elongation factor 1 alpha (EF-1alpha) (Q4QEI9). EF-1alpha is a highly conserved protein with the molecular function of GTP-binding and controlling the rate of polypeptide elongation throughout the translation. It may also affect the structure of actin-based polymers in cells. It regulates the actin cytoskeleton and assembles the actin filaments, adjusting cell motility. An increase in EF-1alpha expression may cause an increase in cell motility [55]. However, some studies determined that EF-1alpha plays a role in disease pathogenesis. Nandan et. al. have identified EF-1alpha as a potential virulence factor. This protein has the ability to enter the cytosol of infected macrophages and cause macrophage deactivation by activating SHP-1 [56]. EF-1alpha might minimize the revealing of immune response by diminution of expression in visceral form. Additionally, since it has a function in protein

synthesis and assembly, reducing the expression level in visceral form might provide a limitation of immune system stimulation [57].

One of the proteins expressed at a higher level in visceral form is N-acyl-L-amino acid amidohydrolase, and it has aminoacylase and hydrolase activity according to UniProt. Amidohydrolases are a type of hydrolases that break down amide bonds. Other than peptide bonds, this enzyme operates on carbon-nitrogen bonds, specifically linear amides. According to the Student's t-test results, putative N-acyl-L-amino acid amidohydrolase (Q4Q6F0) is the second most differentially abundant protein in the visceral isolates. However, this protein is represented by five accession codes throughout all data: Q4Q6F0, Q4Q7G6, Q4QCM4, Q4QCM5, and Q4QCM6. The findings show that all the samples in both groups have putative N-acyl-L-amino acid amidohydrolase with distinct codes.

The attachment of the parasite to host macrophages and invasion of them is a crucial stage in the host-parasite interaction. It is known that the Leishmania parasite uses receptor-mediated phagocytosis for invasion, whether in the promastigote or amastigote stage. Promastigote surface antigen (PSA) is a membrane-bound protein existing in various Leishmania species and plays a role in parasite attachment and invasion of macrophages [58]. Numerous studies are showing that PSA-2 is immunogenic. Kemp et. al. determined that Th1 cells of humans who previously had self-healing cutaneous lesions can recognize PSA and display an immune response [59]. Also, in another study, it is found that *L. amazonensis*-specific PSA protein (LaPSA-38S) increases the expression of a particular cytokine to stimulate the macrophages in humans who have immunity to *L. major* and *L. infantum*, suggesting that PSA might be linked to protective immunity [60]. Again, the study of Handman et. al. determined that the infection with *L. major* may be protected by vaccination with the recombinant PSA-2 [61]. Surface antigen-like protein (Q9XZX9) is significantly up-regulated in cutaneous isolates compared to visceral samples. It is possible that visceral promastigotes may be hiding from macrophages by expressing surface antigens in a lesser amount.

Furthermore, proteins that have peroxidoxin function can be another factor for pathogenicity of Leishmania parasite. Among these 91 differentially expressed proteins, there are four that have peroxidoxin function: peroxidoxin 2 (Q07DU5), thiol-specific antioxidant (A0A173DUZ9), tryparedoxin (E9ADX3), and superoxide dismutase (A0A1Z1LZQ6). Essentially, peroxidoxins eliminate the free radicals produced within the cells as an immune response and are toxic to the biological systems of the parasite.

Leishmania parasites are transmitted to mammalian host macrophages in the promastigote stage from the vector's gut, where they transform into amastigotes and proliferate. The macrophages produce nitric oxide, peroxynitrite, hydroxyl radicals, hydrogen peroxide, hydroperoxide, and superoxide radicals to destroy the parasites as a defense mechanism. These reactive nitrogen species (RNS) and oxygen species (ROS) react with proteins, DNA, and lipids, and they have a part in many cell functions, including pathogen infection defense [62]. Several reports state that Leishmania parasites are able to ROS and RNS-mediated killing [63–66]. Peroxidoxins assist electron transfer in order to detoxify hydroperoxides and provide antioxidant defense by decomposing ROS and RNS [57]. The increasing level of peroxidoxin in Leishmania enhances resistance to oxidative stress induced by macrophages and contributes to the parasite survival in macrophages.

Both cutaneous isolates and visceral isolates have these antioxidant proteins, but the two most notable are thiol-specific antioxidants and peroxidoxin 2. Although they are 98% identical, thiol-specific antioxidant protein is up-regulated in cutaneous isolates, while peroxidoxin 2 is differentially abundant in visceral samples. Out of 199 amino acids, only three are different between these two proteins, and these are not placed on the active site of the proteins. According to the Mascot database search, all three peptides of thiol-specific antioxidant protein, different from the peptides of peroxidoxin 2, have deficient peptide match scores in visceral isolates. Furthermore, 2 of the differential peptides in peroxidoxin 2 have high scores in visceral isolates. It is possible that these two proteins may have undergone single nucleotide mutation. The amino acid difference between these two proteins can be meaningful, and remained to be investigated.

Putative cytochrome b5 (Q4QH22) is a notable protein since it is expressed in the six visceral samples out of 7 and is not present in any cutaneous samples. Cytochrome b5 (CB5) family proteins are involved in several biotic and abiotic stress mechanisms and play a vital role in numerous redox reactions in cells as electron donor [67]. Mukherjee et. al. determined that NAD(P)H cytochrome b5 oxidoreductase deficiency caused increased oxidative stress and apoptosis in *L. major* [68]. Additionally, decreased expression level of cytochrome-b depending on the depletion of universal minicircle sequence binding protein (UMSBP) results in ROS generation, increased oxidative stress, slower multiplication of cells, and eventually apoptosis in *L. donovani* [69]. Cytochrome b5 protein might also improve the resistance to oxidative stress generated by macrophages and aid parasite survival.

Aside from all the proteins that is designated as statistically significant according to the Student's t-test, the most differentially abundant protein in the visceral samples is putative endoribonuclease L-PSP (Pb5) (Q4QBF5). This protein is involved in intracellular survival and proteolysis [57]. It is active on single-stranded mRNA, and its primary function is inhibition of protein synthesis by cleavage of mRNA [70]. It is also suggested that it has a role in purine biosynthesis regulation. The up-regulation of proteolysis proteins in visceral isolates might protect the parasite against the accumulation of damaged proteins by ROS or any other sources of stress.

Besides, there are differentially expressed uncharacterized proteins consistent with literature studies. One of the uncharacterized proteins with unknown function in the CL group with entry name E9AFY0 is 98.8% identical to Q25299 coded hypothetical protein in a comparative study by Dinc et. al. [71]. Both proteins are up-regulated in the cutaneous isolates. The molecular function and role of this protein in viscerotropism require further investigations.

Finally, in comparison with the reference sample, it can be seen that 55 of these 91 significant proteins were also obtained in the reference sample, which are listed on APPENDIX B by p-value. Among these 55 proteins, the significant ones can be listed as paraflagellar rod protein 2C (Q4QEM2), tryparedoxin (E9ADX3), fibrillarin (Q4Q1B2), putative endoribonuclease L-PSP (Q4QBF5), and peroxidoxin 2 (Q07DU5). In contrast, the proteins obtained in the samples but not in the reference are surface antigen-like protein (Q9XZX9), superoxide dismutase (A0A1Z1LZQ6), thiol-specific antioxidant (A0A173DUZ9), elongation factor 1-alpha (Q4QEI9), myosin XXI (Q4Q4N5), actin (C6KJE4), ADF/cofilin (E9ADQ2), uncharacterized protein (E9AFYO), putative N-acyl-L-amino acid amidohydrolase (Q4Q6F0), and putative cytochrome b5 (Q4QH22). The parasite can activate or synthesize these proteins either to hide against certain situations such as oxidative stress or to increase the pathogenesis in the mammalian host.

However, the most striking point here is that despite the 98% similarity between them, peroxidoxin 2 protein is synthesized in the reference sample, but thiol-specific antioxidant is not present. The reference sample is essentially cutaneous since it is the earliest form of *L. tropica* and is not visceralized. In other words, the fact that the thiol-specific antioxidant is not in the reference promastigote sample and any visceral samples but only in the cutaneous isolates highlights the importance of those three amino acids which are different from peroxidoxin 2 protein. It can be suggested that this amino acid

difference between these two proteins might play a significant role in viscerotropism, and this situation will be investigated in more detail in future studies.

To summarize all given information, these findings suggest that down-regulation of paraflagellar rod proteins, elongation factor 1-alpha protein, and surface antigen proteins is significant for avoiding immune recognition. Also, proteins with peroxidoxin function, cytochrome b5, and endoribonuclease play essential roles in *L. tropica* survival in macrophages.

CHAPTER 5

CONCLUSION

To this day, the most prevalent clinical forms of Leishmaniasis disease in Turkey are Cutaneous Leishmaniasis (CL) and Visceral Leishmaniasis (VL). While CL causes cutaneous skin lesions, VL causes weight loss, fever, diarrhea, lymph nodes, and spleen or liver enlargement. *L. tropica* strain is one of the causative agents for CL. However, numerous literature studies determined that *L. tropica* can now cause visceral symptoms such as fever, weight loss, and liver and spleen enlargement. This study aims to clarify the causes of viscerotropism and unveil the virulence factors of *L. tropica*. Hence, the mass spectrometric shotgun approach is used to analyze *L. tropica* isolates from CL and VL patients.

All samples have been pre-separated by off-line HPLC with high pH reverse phase column to improve the proteome coverage. Next, LC-MS/MS analyses are done with low pH reverse phase column and electrospray ionization. According to the results, 2102 Leishmania proteins have been identified with Mascot database search. Among them, 91 proteins are designated as statistically significant according to Student's t-test done by Perseus software, 62 of which are differentially abundant in cutaneous isolates, and 29 are up-regulated in visceral isolates. The difference between these numbers may be caused by the hiding of visceral isolates from immune system recognition.

It can be said that most of the differentially abundant proteins have catalytic activity and binding as molecular functions. Also, there are many paraflagellar rod proteins among them. These PFR proteins play a significant role in the flagellum length, size, development, and cell motility. In comparison to visceral promastigotes, the flagellar of the parasite might be longer and more developed, and the cells may have higher motility. Besides, several literature studies showed that some of these PFR proteins are immunogenic, which means they affect the pathogenicity of the parasite. There are other proteins that are known as immunogenic in our results, such as surface antigen proteins. And all of them are down-regulated in visceral isolates so as can avoid immune recognition. It may be the best way for visceral isolates to prevent the stimulation of

macrophages and the recognition of the interference by the immune system to reduce the synthesis of immunogenic proteins.

Meanwhile, statistical tests determined that numerous oxidative stress proteins are differentially expressed between two groups. When the macrophages are exposed to the Leishmania parasite, they produce reactive oxygen species as a defense mechanism. ROS are toxic to the parasite, so *L. tropica* increases the expression level of oxidative stress proteins. Literature also supports this survival mechanism in *L. tropica* and other leishmania strains. However, the most notable proteins among these oxidative stress proteins are thiol-specific antioxidant and peroxidoxin 2. Despite the 98% similarity, they are differentially expressed in different groups. Also, thiol-specific antioxidant is not expressed in the reference sample, so the slight difference between the amino acid sequences of these two proteins might have a significant impact on viscerotropism. These two proteins, as well as uncharacterized proteins with unknown functions determined to be significant between cutaneous and visceral isolates, need to be investigated in further studies.

REFERENCES

(1) Cholewiński, M.; Derda, M.; Hadaś, E. Parasitic Diseases in Humans Transmitted by Vectors. *Ann. Parasitol.* **2015**, *61* (3), 137–157. https://doi.org/10.17420/ap6103.01.

(2) Arenas, R.; Torres-Guerrero, E.; Quintanilla-Cedillo, M. R.; Ruiz-Esmenjaud, J. Leishmaniasis A Review. *F1000Research* **2017**, *6* (May), 1–15. https://doi.org/10.12688/f1000research.11120.1.

(3) Bruschi, F.; Gradoni, L. *The Leishmaniases-Old Neglected Tropical Diseases*; 2018. https://doi.org/10.1007/978-3-319-72386-0.

(4) Donelson, J. E.; Gardner, M. J.; El-sayed, N. M. More Surprises from Kinetoplastida. **1999**, *96* (March), 2579–2581.

(5) Submitted, T. Proteomic Studies and Its Application to Biological Samples Using Mass Spectrometry. **2017**, No. May.

(6) Tez, S.; Dan, T.; Ate, E. C. Leishmaniasise Karşı Tanı Amaçlı Kağıt Tabanlı Mikroakışkan Analitik Tanı Kiti Tasarımı. **2021**.

(7) Submitted, T. Mass Spectrometry-Based Proteome Analysis of Leishmania Major Parasite in Two Clinical Isolates Which Exhibit Different Impact on Virulence. **2018**, No. December.

(8) Menderes, A. A.; Programi, S.; Top, N. C.; Tez, S.; Do, M. A. N.; Bakirci, S. Muğla Yöresi Köpeklerinde Leishmania Türlerinin Moleküler ve Serolojik Olarak Belirlenmesi. **2020**.

(9) Leifso, K.; Cohen-Freue, G.; Dogra, N.; Murray, A.; McMaster, W. R. Genomic and Proteomic Expression Analysis of Leishmania Promastigote and Amastigote Life Stages The Leishmania Genome Is Constitutively Expressed. *Mol. Biochem. Parasitol.* **2007**, *152* (1), 35–46. https://doi.org/10.1016/j.molbiopara.2006.11.009.

(10) World Health Organization. Control of the Leishmaniases. *World Health Organ. Tech. Rep. Ser.* **2010**, No. 949, 22–26.

(11) Alvar, J.; Vélez, I. D.; Bern, C.; Herrero, M.; Desjeux, P.; Cano, J.; Jannin, J.; de Boer, M. Leishmaniasis Worldwide and Global Estimates of Its Incidence. *PLoS One* **2012**, *7* (5). https://doi.org/10.1371/journal.pone.0035671.

(12) Ok, Ü. Z.; Balcioğlu, I. C.; Taylan Özkan, A.; Özensoy, S.; Özbel, Y. Leishmaniasis in Turkey. *Acta Trop.* **2002**, *84* (1), 43–48. https://doi.org/10.1016/S0001-706X(02)00134-1.

(13) Hayani, K.; Dandashli, A.; Weisshaar, E. Cutaneous Leishmaniasis in Syria: Clinical Features, Current Status and the Effects of War. *Acta Derm. Venereol.* **2015**, *95* (1), 62–66. https://doi.org/10.2340/00015555-1988.

(14) Şen, Ö. L. A Holistic View of Climate Change and Its Impacts in Turkey. **2013**.

(15) Tayanç, M.; İm, U.; Doğruel, M.; Karaca, M. Climate Change in Turkey for the Last Half Century. *Clim. Change* **2009**, *94* (3–4), 483–502. https://doi.org/10.1007/s10584-008-9511-0.

(16) Zeyrek, F. Y. ıldı.; Gürses, G.; Uluca, N.; Yentür Doni, N.; Toprak, Ş.; Yeşilova, Y.; Çulha, G. Is the Agent of Cutaneous Leishmaniasis in Sanliurfa Changing First Cases of Leishmania Major. *Turkiye Parazitol. Derg.* **2014**, *38* (4), 270–274. https://doi.org/10.5152/tpd.2014.3820.

(17) Culha, G.; Akyar, I.; Yildiz Zeyrek, F.; Kurt, Ö.; Gündüz, C.; Özensoy Töz, S.; Östan, I.; Cavus, I.; Gülkan, B.; Kocagöz, T.; Özbel, Y.; Özbilgin, A. Leishmaniasis in Turkey Determination of Leishmania Species by Matrix-Assisted Laser Desorption Ionization Time-Of-Flight Mass Spectrometry (MALDI-TOF MS). *Iran. J. Parasitol.* **2014**, *9* (2), 239–248.

(18) Smoluch, M.; Silberring, J. A Brief History of Mass Spectrometry. *Mass Spectrom. An Appl. Approach* **2019**, 5–8. https://doi.org/10.1002/9781119377368.ch2.

(19) Ivanova, N.; Gugleva, V.; Dobreva, M.; Pehlivanov, I.; Stefanov, S.; Andonova, V. A Short Overview of the Components in Mass Spectrometry Instrumentation for Proteomics Analyses. *Intech* **2016**, *i* (tourism), 13.

(20) El-Aneed, A.; Cohen, A.; Banoub, J. Mass Spectrometry, Review of the Basics Electrospray, MALDI, and Commonly Used Mass Analyzers. *Appl. Spectrosc. Rev.* **2009**, *44* (3), 210–230. https://doi.org/10.1080/05704920902717872.

(21) Cannella, D. *Mass Spectrometry Principles and Applications*; 2018; Vol. 1796. https://doi.org/10.1007/978-1-4939-7877-9_17.

(22) STAFFORD, G. Ion Trap Mass Spectrometry A Personal Perspective. *Am. Soc. Mass Spectrom.* **2002**, *13* (02), 589–596.

(23) Bartlett, J. &. *Introducing Proteomics from Concepts to Sample Separation, Mass Spectrometry and Data Analysis*; 2013; Vol. 53.

(24) Choi, J.; Malakowsky, C. A.; Talent, J. M.; Conrad, C. C.; Gracy, R. W. Identification of Oxidized Plasma Proteins in Alzheimer's Disease. *Biochem. Biophys. Res. Commun.* **2002**, *293* (5), 1566–1570. https://doi.org/10.1016/S0006-291X(02)00420-5.

(25) Greber, S.; Lubec, G.; Cairns, N.; Fountoulakis, M. Decreased Levels of Synaptosomal Associated Protein 25 in the Brain of Patients with Down Syndrome and Alzheimer's Disease. *From Genome to Proteome Adv. Pract. Appl. Proteomics* **2007**, 348–354. https://doi.org/10.1002/9783527613489.ch45.

(26) Lehrer, S.; Roboz, J.; Ding, H.; Zhao, S.; Diamond, E. J.; Holland, J. F.; Stone, N. N.; Droller, M. J.; Stock, R. G. Putative Protein Markers in the Sera of Men with Prostatic Neoplasms. *BJU Int.* **2003**, *92* (3), 223–225. https://doi.org/10.1046/j.1464-410X.2003.04341.x.

(27) Graves, P. R.; Haystead, T. A. J. Molecular Biologist's Guide to Proteomics. *Microbiol. Mol. Biol. Rev.* **2002**, *66* (1), 39–63. https://doi.org/10.1128/mmbr.66.1.39-63.2002.

(28) Fournier, M. L.; Gilmore, J. M.; Martin-brown, S. A.; Washburn, M. P.

Multidimensional Separations-Based Shotgun Proteomics. **2007**, No. 816, 3654–3686.

(29) Berkelman, T.; Stenstedt, T. 2-D Electrophoresis Using Immobilized PH Gradients: Principles and Methods. *Electrophoresis* **2001**, 100.

(30) Baggerman, G.; Vierstraete, E.; Loof, A. De; Schoofs, L. Gel-Based Versus Gel-Free Proteomics : A Review. **2005**, 669–677.

(31) Wang, Y.; Yang, F.; Gritsenko, M. A.; Wang, Y.; Clauss, T.; Liu, T.; Shen, Y.; Monroe, M. E.; Lopez-ferrer, D.; Reno, T.; Moore, J.; Klemke, R. L.; Ii, D. G. C.; Smith, R. D. Reversed-Phase Chromatography with Multiple Fraction Concatenation Strategy for Proteome Profiling of Human MCF10A Cells. **2019**, *11* (10), 2019–2026. https://doi.org/10.1002/pmic.201000722.Reversed-phase.

(32) Shi, Y.; Xiang, R.; Horváth, C.; Wilkins, J. A. The Role of Liquid Chromatography in Proteomics. *J. Chromatogr. A* **2004**, *1053* (1-2 SPEC. ISS.), 27–36. https://doi.org/10.1016/j.chroma.2004.07.044.

(33) Chait, B. T. Mass Spectrometry: Bottom-up or Top-Down? *Science (80-.).* **2006**, *314* (5796), 65–66. https://doi.org/10.1126/science.1133987.

(34) Armirotti, A.; Damonte, G. Achievements and Perspectives of Top-Down Proteomics. *Proteomics* **2010**, *10* (20), 3566–3576. https://doi.org/10.1002/pmic.201000245.

(35) Rogers, J. C.; Bomgarden, R. D. Sample Preparation for Mass Spectrometry-Based Proteomics; from Proteomes to Peptides. *Adv. Exp. Med. Biol.* **2016**, *919*, 43–62. https://doi.org/10.1007/978-3-319-41448-5_3.

(36) Switzar, L.; Giera, M.; Niessen, W. M. A. Protein Digestion: An Overview of the Available Techniques and Recent Developments. *J. Proteome Res.* **2013**, *12* (3), 1067–1077. https://doi.org/10.1021/pr301201x.

(37) Jonathan Posner and Bradley S. Peterson, J. A. R. Mass Spectromerty for Proteomics. *Bone* **2008**, *23* (1), 1–7. https://doi.org/10.1016/j.cbpa.2008.07.024.Mass.

(38) McDonald, W. H.; Yates, J. R. Shotgun Proteomics and Biomarker Discovery. *Dis. Markers* **2002**, *18* (2), 99–105. https://doi.org/10.1155/2002/505397.

(39) Yang, F.; Shen, Y.; Camp, D. G.; Smith, R. D. High PH Reversed-Phase Chromatography with Fraction Concatenation as an Alternative to Strong-Cation Exchange Chromatography for Two-Dimensional Proteomic Analysis. *Expert Rev. Proteomics* **2012**, *9* (2), 129–134. https://doi.org/10.1586/epr.12.15.

(40) Zhu, W.; Smith, J. W.; Huang, C. M. Mass Spectrometry-Based Label-Free Quantitative Proteomics. *J. Biomed. Biotechnol.* **2010**, *2010*. https://doi.org/10.1155/2010/840518.

(41) Vogel, K. E. Spectral Counting Label-Free Proteomics. *LR Lloyd's Regist.* **2000**, *100* (July), 1–35. https://doi.org/10.1007/978-1-4939-0685-7.

(42) Chu, I. K.; Siu, C. K.; Lau, J. K. C.; Tang, W. K.; Mu, X.; Lai, C. K.; Guo, X.; Wang, X.; Li, N.; Xia, Y.; Kong, X.; Oh, H. Bin; Ryzhov, V.; Tureček, F.; Hopkinson, A. C.; Siu, K. W. M. Proposed Nomenclature for Peptide Ion

Fragmentation. *Int. J. Mass Spectrom.* **2015**, *390*, 24–27. https://doi.org/10.1016/j.ijms.2015.07.021.

(43) Alborzi, A.; Rasouli, M.; Shamsizadeh, A. Leishmania Tropica Isolated Patient with Visceral Leishmaniasis in Southern Iran. *Am. J. Trop. Med. Hyg.* **2006**, *74* (2), 306–307. https://doi.org/10.4269/ajtmh.2006.74.306.

(44) Promega Corporation (Madison), Doyle, K and Miles, J. Acetone Precipitation of Proteins. *Protoc. Appl. Guid.* **1996**, 7–8.

(45) Ishihama, Y.; Oda, Y.; Tabata, T.; Sato, T.; Nagasu, T.; Rappsilber, J.; Mann, M. Exponentially Modified Protein Abundance Index (EmPAI) for Estimation of Absolute Protein Amount in Proteomics by the Number of Sequenced Peptides per Protein. *Mol. Cell. Proteomics* **2005**, *4* (9), 1265–1272. https://doi.org/10.1074/mcp.M500061-MCP200.

(46) Tyanova, S.; Temu, T.; Sinitcyn, P.; Carlson, A.; Hein, M. Y.; Geiger, T.; Mann, M.; Cox, J. The Perseus Computational Platform for Comprehensive Analysis of (Prote)Omics Data. *Nat. Methods* **2016**, *13* (9), 731–740. https://doi.org/10.1038/nmeth.3901.

(47) Tammana, T. V. S.; Sahasrabuddhe, A. A.; Mitra, K.; Bajpai, V. K.; Gupta, C. M. Actin-Depolymerizing Factor, ADF/Cofilin, Is Essentially Required in Assembly of Leishmania Flagellum. *Mol. Microbiol.* **2008**, *70* (4), 837–852. https://doi.org/10.1111/j.1365-2958.2008.06448.x.

(48) Moore, L. L.; Santrich, C.; LeBowitz, J. H. Stage-Specific Expression of the Leishmania Mexicana Paraflagellar Rod Protein PFR-2. *Mol. Biochem. Parasitol.* **1996**, *80* (2), 125–135. https://doi.org/10.1016/0166-6851(96)02688-6.

(49) Portman, N.; Gull, K. The Paraflagellar Rod of Kinetoplastid Parasites: From Structure to Components and Function. *Int. J. Parasitol.* **2010**, *40* (2), 135–148. https://doi.org/10.1016/j.ijpara.2009.10.005.

(50) Katta, S. S.; Sahasrabuddhe, A. A.; Gupta, C. M. Flagellar Localization of a Novel Isoform of Myosin, Myosin XXI, in Leishmania. *Mol. Biochem. Parasitol.* **2009**, *164* (2), 105–110. https://doi.org/10.1016/j.molbiopara.2008.12.002.

(51) Ashrafmansouri, M.; Amiri-Dashatan, N.; Ahmadi, N.; Rezaei-Tavirani, M.; SeyyedTabaei, S.; Haghighi, A. Quantitative Proteomic Analysis to Determine Differentially Expressed Proteins in Axenic Amastigotes of Leishmania Tropica and Leishmania Major. *IUBMB Life* **2020**, *72* (8), 1715–1724. https://doi.org/10.1002/iub.2300.

(52) Skupiński, W.; Mikosz, J.; Malinowski, S. ESR Investigation of the MgO-VCl4 System. *React. Kinet. Catal. Lett.* **1980**, *14* (3), 363–366. https://doi.org/10.1007/BF02073506.

(53) Saravia, N. G.; Hazbón, M. H.; Osorio, Y.; Valderrama, L.; Walker, J.; Santrich, C.; Cortázar, T.; LeBowitz, J. H.; Travi, B. L. Protective Immunogenicity of the Paraflagellar Rod Protein 2 of Leishmania Mexicana. *Vaccine* **2005**, *23* (8), 984–995. https://doi.org/10.1016/j.vaccine.2004.07.044.

(54) Maharana, B. R.; Tewari, A. K.; Singh, V. An Overview on Kinetoplastid Paraflagellar Rod. *Journal of Parasitic Diseases*. 2015.

https://doi.org/10.1007/s12639-014-0422-x.

(55) Condeelis, J. Elongation Factor 1α, Translation and the Cytoskeleton. *Trends Biochem. Sci.* **1995**, *20* (5), 169–170. https://doi.org/10.1016/S0968-0004(00)88998-7.

(56) Nandan, D.; Yi, T.; Lopez, M.; Lai, C.; Reiner, N. E. Leishmania EF-1α Activates the Src Homology 2 Domain Containing Tyrosine Phosphatase SHP-1 Leading to Macrophage Deactivation. *J. Biol. Chem.* **2002**, *277* (51), 50190–50197. https://doi.org/10.1074/jbc.M209210200.

(57) Hajjaran, H.; Mousavi, P.; Burchmore, R.; Mohebali, M.; Mohammadi Bazargani, M.; Hosseini Salekdeh, G.; Kazemi-Rad, E.; Khoramizadeh, M. R. Comparative Proteomic Profiling of Leishmania Tropica: Investigation of a Case Infected with Simultaneous Cutaneous and Viscerotropic Leishmaniasis by 2-Dimentional Electrophoresis and Mass Spectrometry. *Iran. J. Parasitol.* **2015**, *10* (3), 366–380.

(58) Kedzierski, L.; Montgomery, J.; Bullen, D.; Curtis, J.; Gardiner, E.; Jimenez-Ruiz, A.; Handman, E. A Leucine-Rich Repeat Motif of Leishmania Parasite Surface Antigen 2 Binds to Macrophages through the Complement Receptor 3 . *J. Immunol.* **2004**, *172* (8), 4902–4906. https://doi.org/10.4049/jimmunol.172.8.4902.

(59) Kemp, M.; Handman, E.; Kemp, K.; Ismail, A.; Mustafa, M. D.; Kordofani, A. Y.; Bendtzen, K.; Kharazmi, A.; Theander, T. G. The Leishmania Promastigote Surface Antigen-2 (PSA-2) Is Specifically Recognised by Th1 Cells in Humans with Naturally Acquired Immunity to L. Major. *FEMS Immunol. Med. Microbiol.* **1998**, *20* (3), 209–218. https://doi.org/10.1016/S0928-8244(98)00015-7.

(60) Chamakh-Ayari, R.; Bras-Gonçalves, R.; Bahi-Jaber, N.; Petitdidier, E.; Markikou-Ouni, W.; Aoun, K.; Moreno, J.; Carrillo, E.; Salotra, P.; Kaushal, H.; Negi, N. S.; Arevalo, J.; Falconi-Agapito, F.; Privat, A.; Cruz, M.; Pagniez, J.; Papierok, G. M.; Rhouma, F. B. H.; Torres, P.; Lemesre, J. L.; Chenik, M.; Meddeb-Garnaoui, A. In Vitro Evaluation of a Soluble Leishmania Promastigote Surface Antigen as a Potential Vaccine Candidate against Human Leishmaniasis. *PLoS One* **2014**, *9* (5). https://doi.org/10.1371/journal.pone.0092708.

(61) Handman, E.; Symons, F. M.; Baldwin, T. M.; Curtis, J. M.; Scheerlinck, J. P. Y. Protective Vaccination with Promastigote Surface Antigen 2 from Leishmania Major Is Mediated by a TH1 Type of Immune Response. *Infect. Immun.* **1995**, *63* (11), 4261–4267. https://doi.org/10.1128/iai.63.11.4261-4267.1995.

(62) Barr, S. D.; Gedamu, L. Role of Peroxidoxins in Leishmania Chagasi Survival. Evidence of an Enzymatic Defense against Nitrosative Stress. *J. Biol. Chem.* **2003**, *278* (12), 10816–10823. https://doi.org/10.1074/jbc.M212990200.

(63) Zarley, J. H.; Britigan, B. E.; Wilson, M. E. Hydrogen Peroxide-Mediated Toxicity for Leishmania Donovani Chagasi Promastigotes: Role of Hydroxyl Radical and Protection by Heat Shock. *J. Clin. Invest.* **1991**, *88* (5), 1511–1521. https://doi.org/10.1172/JCI115461.

(64) Wilson, M. E.; Andersen, K. A.; Britigan, B. E. Response of Leishmania Chagasi Promastigotes to Oxidant Stress. *Infect. Immun.* **1994**, *62* (11), 5133–5141.

https://doi.org/10.1128/iai.62.11.5133-5141.1994.

(65) Mauel, J.; Ransijn, A.; Buchmuller-Rouiller, Y. Killing of Leishmania Parasites in Activated Murine Macrophages Is Based on an L-Arginine-Dependent Process That Produces Nitrogen Derivatives. *J. Leukoc. Biol.* **1991**, *49* (1), 73–82. https://doi.org/10.1002/jlb.49.1.73.

(66) Murray, B. H. W.; Nathan, C. F. Macrophage Microbicidal Mechanisms In Vivo : Reactive. *Differences* **1999**, *189* (4), 741–746.

(67) Zheng, H.; Li, X.; Shi, L.; Jing, Y.; Song, Q.; Chen, Y.; He, L.; Wang, F.; Gao, J.; Bi, Y. Genome-Wide Identification and Analysis of the Cytochrome B5 Protein Family in Chinese Cabbage (Brassica Rapa L. Ssp. Pekinensis). *Int. J. Genomics* **2019**, *2019*. https://doi.org/10.1155/2019/2102317.

(68) Mukherjee, S.; Santara, S. Sen; Das, S.; Bose, M.; Roy, J.; Adak, S. NAD(P)H Cytochrome B5 Oxidoreductase Deficiency in Leishmania Major Results in Impaired Linoleate Synthesis Followed by Increased Oxidative Stress and Cell Death. *J. Biol. Chem.* **2012**, *287* (42), 34992–35003. https://doi.org/10.1074/jbc.M112.389338.

(69) Singh, R.; Purkait, B.; Abhishek, K.; Saini, S.; Das, S.; Verma, S.; Mandal, A.; Ghosh, A. K.; Ansari, Y.; Kumar, A.; Sardar, A. H.; Kumar, A.; Parrack, P.; Das, P. Universal Minicircle Sequence Binding Protein of Leishmania Donovani Regulates Pathogenicity by Controlling Expression of Cytochrome-B. *Cell Biosci.* **2016**, *6* (1), 1–17. https://doi.org/10.1186/s13578-016-0072-z.

(70) Maxwell, M. J.; Chan, S. K.; Robinson, D. P.; Dwyer, D. M.; Nandan, D.; Foster, L. J.; Reiner, N. E. Proteomic Analysis of the Secretome of Leishmania Donovani. *Genome Biol.* **2008**, *9* (2). https://doi.org/10.1186/gb-2008-9-2-r35.

(71) Dinç, M.; Yalçln, T.; Çavuş, İ.; Özbilgin, A. Comparative Proteomic Analysis of Leishmania Parasites Isolated from Visceral and Cutaneous Leishmaniasis Patients. *Parasitology* **2022**, *149* (3), 298–305. https://doi.org/10.1017/S0031182021001967.

APPENDIX A

emPAI DATA FOR PROTEINS FOUND IN AT LEAST FOUR SAMPLES

Table A.1. emPAI Data for Proteins Found in at Least Four Samples

Entry Name	A0A089FQZ7	A0A089GSF5	A0A0R6XZU5	A0A0R6Y3Z1	A0A0R6YB19	A0A142C7A6	A0A142C7A7
C1	0,432	0,432	0,000	0,000	0,000	0,959	0,000
C2	1,461	0,000	0,226	0,000	0,226	0,979	0,000
C3	0,637	0,000	0,000	0,000	0,089	1,415	0,000
C4	0,708	0,000	0,000	0,561	0,148	0,639	0,787
C5	0,000	0,637	0,000	0,000	0,000	1,413	0,000
C6	0,172	0,000	0,172	0,000	0,000	1,275	0,000
C7	0,000	0,614	0,184	0,307	0,086	0,799	0,418
Ref.	0,297	0,000	0,144	0,000	0,000	1,639	0,000
V1	0,508	0,508	0,000	0,580	0,071	1,129	0,000
V2	0,000	0,861	0,000	0,000	0,120	1,119	1,377
V3	0,738	0,000	0,000	0,000	0,000	1,639	0,502
V4	0,000	0,522	0,000	0,000	0,252	1,868	1,346
V5	0,000	1,022	0,000	0,000	0,099	1,576	0,000
V6	0,000	0,778	0,000	0,000	0,000	2,784	0,000
V7	0,205	0,000	0,000	0,341	0,096	0,887	0,000

(cont. on next page)

Table A.1. (cont.)

A0A5B8YY69	A0A482KHF1	A0A3G4YQ88	A0A3G4YQ87	A0A1Z1LZU1	A0A1Z1LZQ6	A0A1B1FKZ0	A0A173DUZ9	A0A145YEQ2	**Entry Name**
0,216	1,287	1,650	0,449	0,000	0,328	0,199	1,348	0,000	**C1**
0,844	0,000	0,000	0,226	0,000	0,271	0,226	1,792	0,151	**C2**
0,000	0,000	1,567	0,408	0,000	0,484	0,191	1,109	0,000	**C3**
0,000	0,826	1,878	0,983	0,354	0,374	0,069	0,856	0,000	**C4**
0,000	1,069	0,000	0,662	0,000	0,802	0,293	0,000	0,000	**C5**
0,287	0,414	0,816	0,597	0,000	0,724	0,080	2,873	0,000	**C6**
0,307	1,032	3,441	0,909	0,000	0,774	0,283	1,917	0,000	**C7**
0,000	0,345	1,179	0,709	0,345	0,000	0,144	0,000	0,326	**Ref.**
0,397	0,854	0,000	1,668	0,000	0,000	0,000	0,000	0,000	**V1**
0,430	0,620	1,222	2,238	0,000	0,310	0,120	0,000	0,172	**V2**
0,369	0,532	0,000	0,768	0,000	0,000	0,103	0,000	0,148	**V3**
0,000	0,606	0,000	0,538	0,269	0,000	0,000	0,000	0,000	**V4**
0,000	0,511	1,746	1,050	0,000	0,000	0,000	0,000	0,000	**V5**
0,000	0,000	0,778	0,376	0,000	0,000	0,000	0,000	0,000	**V6**
0,164	1,147	0,969	1,010	0,218	0,000	0,314	0,000	0,000	**V7**

(cont. on next page)

Table A.1. (cont.)

E9ABZ4	E3VNP2	D2EAU7	CISY	C6KJE4	A2CIQ8	A2CIC8	A0A7S5YR77	A0A5Q2WYE3	A0A5Q2WYC5	A0A5B8YYQ3	**Entry Name**
0,000	0,052	0,000	0,268	0,251	0,000	0,000	0,000	0,095	0,674	1,374	**C1**
0,000	0,196	0,000	0,226	0,136	0,090	0,121	0,000	0,000	0,618	1,567	**C2**
0,064	0,166	0,000	0,191	0,370	0,076	0,102	0,000	0,000	0,522	2,026	**C3**
0,049	0,059	0,000	0,069	0,000	0,000	0,334	0,000	0,000	0,403	1,023	**C4**
0,064	0,076	0,000	0,089	0,115	0,153	0,204	0,000	0,000	0,993	1,324	**C5**
0,000	0,069	0,000	0,000	0,000	0,138	0,000	0,000	0,000	0,896	1,195	**C6**
0,000	0,074	0,946	0,381	0,234	0,000	0,098	0,000	0,000	0,725	1,278	**C7**
0,000	0,000	0,000	0,000	0,000	0,058	0,153	0,000	0,498	0,393	3,048	**Ref.**
0,000	0,061	0,000	0,417	0,000	0,061	0,000	0,000	0,000	0,264	0,000	**V1**
0,000	0,000	0,000	0,000	0,000	0,000	0,000	0,000	0,000	0,000	1,050	**V2**
0,000	0,000	0,000	0,221	0,133	0,000	0,000	0,413	0,162	0,871	0,000	**V3**
0,084	0,000	0,000	0,252	0,000	0,101	0,000	0,471	0,000	0,437	1,750	**V4**
0,000	0,000	0,923	0,440	0,000	0,000	0,114	0,000	0,156	0,000	2,257	**V5**
0,000	0,000	1,329	0,000	0,000	0,000	0,201	1,104	0,000	0,301	1,530	**V6**
0,000	0,082	1,051	0,096	0,000	0,000	0,109	0,382	0,150	0,164	0,000	**V7**

(cont. on next page)

Table A.1. (cont.)

E9ACZ6	E9ACT7	E9ACL4	E9ACJ9	E9ACJ7	E9ACI8	E9ACG7	E9ACE8	E9ACE5	E9ACB2	E9ACA6	E9AC56	E9AC38	E9AC29	E9AC22	**Entry Name**
0,130	0,000	0,009	0,069	0,000	0,726	0,052	0,086	0,035	0,052	0,043	0,000	0,000	0,000	0,095	**C1**
0,000	0,000	0,000	0,121	0,000	0,542	0,090	0,000	0,000	0,090	0,075	0,105	0,000	0,000	0,166	**C2**
0,000	0,000	0,000	0,102	0,051	0,459	0,153	0,127	0,051	0,076	0,064	0,089	0,000	0,115	0,000	**C3**
0,305	0,000	0,010	0,000	0,039	0,354	0,059	0,000	0,039	0,059	0,049	0,000	0,049	0,000	0,000	**C4**
0,000	0,000	0,000	0,102	0,051	0,458	0,076	0,127	0,000	0,000	0,064	0,089	0,000	0,000	0,000	**C5**
0,000	0,000	0,034	0,000	0,000	0,000	0,000	0,057	0,000	0,069	0,057	0,000	0,000	0,103	0,000	**C6**
0,000	0,172	0,012	0,098	0,000	0,000	0,074	0,061	0,049	0,000	0,061	0,000	0,000	0,049	0,135	**C7**
0,000	0,000	0,058	0,077	0,038	0,000	0,058	0,096	0,000	0,000	0,048	0,067	0,048	0,000	0,000	**Ref.**
0,153	0,000	0,000	0,000	0,000	0,000	0,061	0,153	0,000	0,061	0,051	0,000	0,051	0,000	0,000	**V1**
0,000	0,241	0,000	0,000	0,000	0,000	0,207	0,086	0,069	0,000	0,086	0,120	0,000	0,155	0,000	**V2**
0,221	0,000	0,000	0,118	0,000	0,000	0,000	0,074	0,059	0,000	0,000	0,103	0,074	0,000	0,000	**V3**
0,000	0,236	0,000	0,000	0,000	0,606	0,101	0,084	0,000	0,101	0,084	0,000	0,084	0,151	0,000	**V4**
0,000	0,000	0,000	0,000	0,057	0,000	0,170	0,142	0,000	0,085	0,071	0,000	0,000	0,057	0,000	**V5**
0,000	0,000	0,000	0,000	0,000	0,903	0,150	0,376	0,000	0,150	0,000	0,000	0,000	0,000	0,276	**V6**
0,000	0,191	0,000	0,000	0,055	0,000	0,000	0,068	0,000	0,000	0,068	0,000	0,000	0,000	0,000	**V7**

(cont. on next page)

Table A.1. (cont.)

E9ADF2	E9ADF0	E9ADB9	E9ADB2	E9ADB1	E9ADA4	E9ADA3	E9AD91	E9AD89	E9AD65	E9AD53	E9AD28	E9AD27	E9AD01	E9ACZ8	**Entry Name**
0,000	0,086	0,095	0,130	0,112	0,311	0,095	0,035	0,000	0,026	0,518	0,017	0,147	0,000	0,104	**C1**
0,000	0,000	0,000	0,151	0,090	0,196	0,166	0,060	0,000	0,045	0,557	0,015	0,136	0,075	0,181	**C2**
0,000	0,127	0,000	0,331	0,000	0,076	0,140	0,000	0,000	0,089	1,121	0,000	0,166	0,000	0,153	**C3**
0,010	0,098	0,108	0,197	0,000	0,128	0,216	0,000	0,138	0,069	0,590	0,010	0,157	0,000	0,118	**C4**
0,000	0,127	0,000	0,255	0,076	0,165	0,140	0,000	0,000	0,000	0,471	0,013	0,127	0,000	0,000	**C5**
0,000	0,241	0,264	0,230	0,069	0,149	0,126	0,046	0,161	0,000	1,011	0,000	0,115	0,057	0,000	**C6**
0,000	0,000	0,000	0,123	0,000	0,160	0,270	0,000	0,000	0,086	1,081	0,012	0,135	0,000	0,000	**C7**
0,010	0,096	0,000	0,192	0,058	0,125	0,105	0,000	0,000	0,096	0,844	0,000	0,048	0,096	0,000	**Ref.**
0,000	0,000	0,112	0,051	0,061	0,132	0,000	0,000	0,142	0,102	0,895	0,000	0,061	0,000	0,122	**V1**
0,000	0,000	0,189	0,086	0,000	0,224	0,000	0,069	0,241	0,120	0,637	0,000	0,052	0,086	0,000	**V2**
0,000	0,000	0,000	0,148	0,089	0,000	0,000	0,000	0,000	0,044	0,886	0,000	0,074	0,000	0,000	**V3**
0,000	0,000	0,000	0,168	0,101	0,000	0,185	0,000	0,000	0,118	1,481	0,000	0,050	0,000	0,202	**V4**
0,014	0,142	0,000	0,213	0,000	0,185	0,000	0,000	0,000	0,142	0,241	0,000	0,043	0,000	0,000	**V5**
0,000	0,000	0,000	0,251	0,000	0,000	0,000	0,000	0,000	0,075	0,000	0,000	0,125	0,000	0,000	**V6**
0,014	0,000	0,000	0,068	0,000	0,082	0,000	0,000	0,000	0,137	0,505	0,014	0,055	0,068	0,000	**V7**

(cont. on next page)

Table A.1. (cont.)

E9ADX5	E9ADX4	E9ADX3	E9ADW8	E9ADV5	E9ADU3	E9ADT8	E9ADT0	E9ADQ2	E9ADL4	E9ADI3	E9ADI2	E9ADH0	E9ADF9	E9ADF8	**Entry Name**
0,078	0,199	0,199	0,000	0,000	0,000	0,000	0,052	0,216	0,138	0,233	0,121	0,207	0,052	0,000	**C1**
0,136	0,346	0,000	0,136	0,000	0,105	0,166	0,166	0,000	0,121	0,121	0,000	0,362	0,196	0,000	**C2**
0,115	0,293	0,637	0,242	0,000	0,000	0,140	0,140	0,000	0,051	0,102	0,000	0,000	0,000	0,000	**C3**
0,089	0,511	0,226	0,089	0,000	0,000	0,108	0,108	0,246	0,039	0,177	0,069	0,236	0,000	0,128	**C4**
0,115	0,293	0,637	0,000	0,000	0,089	0,140	0,076	0,318	0,051	0,102	0,000	0,675	0,000	0,076	**C5**
0,103	0,264	0,575	0,103	0,000	0,080	0,000	0,000	0,000	0,046	0,092	0,080	0,000	0,000	0,000	**C6**
0,000	0,283	0,283	0,000	0,025	0,000	0,135	0,135	0,676	0,135	0,098	0,086	0,000	0,000	0,074	**C7**
0,000	0,000	0,220	0,000	0,000	0,134	0,105	0,058	0,000	0,105	0,173	0,067	0,000	0,058	0,000	**Ref.**
0,000	0,234	0,000	0,000	0,000	0,071	0,112	0,112	0,000	0,081	0,275	0,305	0,244	0,000	0,132	**V1**
0,155	0,396	0,000	0,000	0,000	0,120	0,189	0,103	0,000	0,138	0,310	0,120	0,000	0,000	0,103	**V2**
0,133	0,340	0,000	0,000	0,000	0,000	0,000	0,089	0,000	0,118	0,000	0,103	0,354	0,089	0,000	**V3**
0,151	0,387	0,000	0,000	0,034	0,118	0,185	0,000	0,000	0,067	0,135	0,118	0,404	0,000	0,000	**V4**
0,000	0,326	0,000	0,000	0,000	0,000	0,000	0,085	0,000	0,057	0,000	0,199	0,341	0,185	0,000	**V5**
0,226	0,000	0,000	0,000	0,050	0,000	0,000	0,000	0,000	0,000	0,451	0,000	0,000	0,000	0,000	**V6**
0,123	0,314	0,000	0,000	0,027	0,096	0,150	0,000	0,000	0,055	0,109	0,096	0,000	0,000	0,000	**V7**

(cont. on next page)

Table A.1. (cont.)

E9AEE2	E9AEC7	E9AEB9	E9AEB3	E9AEA9	E9AEA8	E9AE86	E9AE82	E9AE81	E9AE78	E9AE37	E9AE36	E9AE33	E9ADY9	E9ADY5	**Entry Name**
0,086	0,000	0,000	0,060	0,130	0,000	0,000	0,043	0,017	0,060	0,924	0,000	0,242	0,043	0,035	**C1**
0,000	0,000	0,105	0,000	0,000	0,226	0,000	0,000	0,000	0,000	0,000	1,024	0,422	0,075	0,121	**C2**
0,127	0,038	0,089	0,178	0,000	0,191	0,000	0,064	0,000	0,089	0,663	0,000	0,000	0,064	0,051	**C3**
0,000	0,030	0,069	0,069	0,000	0,148	0,000	0,049	0,000	0,069	0,590	0,000	0,275	0,049	0,079	**C4**
0,127	0,038	0,089	0,089	0,000	0,000	0,051	0,064	0,025	0,000	0,000	0,980	0,000	0,064	0,000	**C5**
0,000	0,000	0,000	0,080	0,000	0,000	0,000	0,057	0,000	0,000	1,000	0,000	0,322	0,126	0,000	**C6**
0,000	0,000	0,000	0,086	0,000	0,184	0,049	0,061	0,000	0,086	0,836	0,000	0,344	0,061	0,000	**C7**
0,000	0,000	0,000	0,134	0,000	0,144	0,038	0,048	0,000	0,067	0,288	0,000	0,268	0,163	0,077	**Ref.**
0,000	0,000	0,000	0,071	0,000	0,000	0,000	0,000	0,051	0,071	0,000	0,783	0,000	0,112	0,041	**V1**
0,000	0,000	0,000	0,120	0,258	0,000	0,000	0,000	0,000	0,000	0,293	0,000	0,000	0,086	0,000	**V2**
0,000	0,044	0,000	0,103	0,221	0,000	0,000	0,074	0,030	0,000	0,768	0,000	0,000	0,074	0,000	**V3**
0,000	0,000	0,000	0,118	0,000	0,252	0,000	0,000	0,034	0,000	0,387	0,000	0,000	0,000	0,000	**V4**
0,000	0,000	0,000	0,000	0,213	0,000	0,000	0,000	0,000	0,000	0,000	0,426	0,000	0,071	0,000	**V5**
0,000	0,000	0,000	0,176	0,000	0,000	0,000	0,000	0,050	0,000	0,752	0,000	0,000	0,000	0,000	**V6**
0,137	0,000	0,000	0,096	0,000	0,205	0,109	0,000	0,027	0,000	0,232	0,000	0,000	0,000	0,000	**V7**

(cont. on next page)

Table A.1. (cont.)

E9AF13	E9AF02	E9AEZ6	E9AEY3	E9AEX6	E9AEX1	E9AEW4	E9AEW1	E9AEU5	E9AEU4	E9AES2	E9AES1	E9AER5	E9AEQ0	E9AEI0	**Entry Name**
0,000	0,000	0,000	0,000	0,095	0,000	0,035	0,121	0,000	0,130	0,164	0,000	0,121	0,138	0,190	**C1**
0,000	0,105	0,000	0,060	0,346	0,000	0,121	0,000	0,482	0,226	0,286	0,060	0,000	0,241	0,211	**C2**
0,421	0,000	0,370	0,051	0,140	0,127	0,000	0,089	0,408	0,000	0,000	0,051	0,178	0,204	0,280	**C3**
0,325	0,069	0,000	0,000	0,108	0,098	0,000	0,138	0,148	0,148	0,000	0,000	0,138	0,157	0,216	**C4**
0,000	0,089	0,369	0,000	0,000	0,000	0,051	0,000	0,191	0,191	0,115	0,000	0,000	0,204	0,178	**C5**
0,000	0,000	0,000	0,000	0,126	0,000	0,000	0,080	0,172	0,172	0,000	0,000	0,000	0,184	0,161	**C6**
0,000	0,086	0,000	0,000	0,000	0,000	0,000	0,000	0,000	0,000	0,234	0,111	0,172	0,197	0,086	**C7**
0,316	0,000	0,278	0,067	0,000	0,000	0,038	0,000	0,307	0,000	0,278	0,038	0,000	0,000	0,211	**Ref.**
0,336	0,000	0,295	0,041	0,112	0,000	0,081	0,000	0,000	0,153	0,193	0,000	0,142	0,000	0,142	**V1**
0,000	0,000	0,499	0,000	0,189	0,000	0,138	0,000	0,258	0,000	0,000	0,000	0,241	0,585	0,241	**V2**
0,000	0,000	0,428	0,000	0,162	0,000	0,192	0,000	0,472	0,221	0,133	0,059	0,207	0,000	0,103	**V3**
0,000	0,000	0,488	0,067	0,387	0,168	0,219	0,000	0,000	0,555	0,320	0,067	0,000	0,269	0,118	**V4**
0,000	0,000	0,000	0,057	0,000	0,000	0,057	0,000	0,213	0,000	0,000	0,057	0,000	0,000	0,000	**V5**
0,000	0,000	0,000	0,100	0,577	0,251	0,100	0,000	0,376	0,376	0,000	0,100	0,351	0,401	0,176	**V6**
0,000	0,000	0,000	0,055	0,314	0,000	0,000	0,096	0,205	0,451	0,000	0,055	0,191	0,218	0,191	**V7**

(cont. on next page)

Table A.1. (cont.)

E9AFX7	E9AFW1	E9AFS3	E9AFP0	E9AFM5	E9AFL3	E9AFL0	E9AFK8	E9AFK3	E9AFI6	E9AFE7	E9AFD4	E9AFD1	E9AF31	E9AF23	**Entry Name**
0,052	0,000	0,415	0,052	0,017	0,216	0,052	0,121	0,225	0,000	0,328	0,251	0,069	0,052	0,112	**C1**
0,000	0,000	0,000	0,000	0,030	0,377	0,090	0,000	0,392	0,000	0,256	0,301	0,060	0,000	0,437	**C2**
0,000	0,000	0,612	0,076	0,064	0,000	0,153	0,000	0,331	0,000	0,217	0,089	0,051	0,038	0,370	**C3**
0,000	0,000	0,000	0,177	0,000	0,000	0,059	0,138	0,256	0,216	0,266	0,197	0,039	0,030	0,285	**C4**
0,076	0,000	0,000	0,000	0,000	0,000	0,076	0,178	0,331	0,000	0,344	0,369	0,051	0,038	0,165	**C5**
0,000	0,000	0,000	0,138	0,023	0,287	0,000	0,000	0,299	0,000	0,195	0,230	0,046	0,000	0,333	**C6**
0,074	0,123	0,000	0,000	0,025	0,307	0,147	0,172	0,000	0,000	0,209	0,197	0,000	0,037	0,160	**C7**
0,058	0,000	0,460	0,115	0,019	0,000	0,182	0,278	0,556	0,211	0,364	0,105	0,038	0,029	0,278	**Ref.**
0,061	0,102	0,488	0,061	0,051	0,000	0,061	0,000	0,264	0,000	0,173	0,203	0,000	0,031	0,132	**V1**
0,103	0,000	0,826	0,000	0,034	0,430	0,000	0,000	0,448	0,000	0,138	0,413	0,000	0,000	0,224	**V2**
0,089	0,000	0,709	0,000	0,030	0,827	0,000	0,000	0,384	0,000	0,251	0,354	0,000	0,000	0,428	**V3**
0,202	0,168	0,808	0,101	0,000	0,000	0,000	0,000	0,000	0,000	0,286	0,185	0,067	0,000	0,488	**V4**
0,085	0,000	0,000	0,085	0,000	0,000	0,000	0,000	0,000	0,312	0,241	0,057	0,000	0,000	0,185	**V5**
0,000	0,000	1,204	0,000	0,000	0,000	0,000	0,000	0,000	0,000	0,201	0,100	0,000	0,000	0,727	**V6**
0,000	0,137	0,000	0,000	0,000	0,341	0,000	0,191	0,000	0,300	0,232	0,096	0,000	0,000	0,000	**V7**

(cont. on next page)

Table A.1. (cont.)

PURA	PGFS	O97220	O97213	O97204	O02614	MVP	IF4A	HEM6	GP63	GMPR	FUM2	FUM1	E9AG04	E9AFY0	**Entry Name**
0,043	0,000	0,086	0,285	0,000	0,173	0,069	0,000	0,000	0,095	0,060	0,225	0,112	0,078	0,000	**C1**
0,075	0,000	0,151	0,226	0,000	0,000	0,060	0,121	0,000	0,000	0,105	0,000	0,000	0,136	0,000	**C2**
0,064	0,000	0,127	0,421	0,000	0,255	0,000	0,000	0,000	0,140	0,089	0,000	0,076	0,115	0,255	**C3**
0,049	0,118	0,098	0,148	0,020	0,197	0,079	0,079	0,000	0,216	0,000	0,187	0,059	0,089	0,197	**C4**
0,064	0,000	0,127	0,191	0,000	0,000	0,051	0,102	0,000	0,000	0,000	0,000	0,165	0,000	0,000	**C5**
0,057	0,000	0,115	0,172	0,023	1,252	0,000	0,195	0,000	0,184	0,080	0,000	0,218	0,103	0,230	**C6**
0,061	0,000	0,123	0,184	0,000	0,541	0,000	0,000	0,000	0,135	0,086	0,000	0,074	0,111	0,246	**C7**
0,048	0,000	0,096	0,144	0,000	1,045	0,000	0,470	0,000	0,000	0,067	0,000	0,125	0,000	0,000	**Ref.**
0,051	0,122	0,102	0,336	0,000	0,752	0,041	0,173	0,112	0,163	0,000	0,000	0,061	0,092	0,000	**V1**
0,000	0,207	0,172	0,568	0,086	0,000	0,000	0,138	0,189	0,275	0,000	0,000	0,103	0,155	0,000	**V2**
0,074	0,177	0,148	0,221	0,000	0,650	0,000	0,118	0,162	0,000	0,000	0,000	0,000	0,000	0,000	**V3**
0,084	0,202	0,168	0,252	0,000	0,337	0,000	0,000	0,000	0,185	0,000	0,000	0,000	0,151	0,000	**V4**
0,000	0,000	0,142	0,213	0,000	1,050	0,000	0,114	0,156	0,071	0,000	0,085	0,085	0,000	0,000	**V5**
0,000	0,000	0,000	0,376	0,050	1,104	0,000	0,000	0,000	0,000	0,000	0,150	0,000	0,000	0,000	**V6**
0,000	0,000	0,137	0,205	0,000	0,273	0,055	0,000	0,150	0,000	0,000	0,000	0,082	0,000	0,000	**V7**

(cont. on next page)

Table A.1. (cont.)

Q4Q0M6	Q4Q0M2	Q4Q0L9	Q4Q0J9	Q4Q0E9	Q4Q0C1	Q4Q092	Q4Q090	Q4Q080	Q4Q079	Q4Q063	Q2PD62	Q2PD27	Q27687	Q07DU5	**Entry Name**
0,104	0,078	0,095	0,052	0,173	0,052	0,155	0,164	0,000	0,000	0,173	0,000	0,000	0,086	0,000	**C1**
0,181	0,000	0,166	0,136	0,301	0,000	0,000	0,286	0,000	0,000	0,090	0,000	0,000	0,151	1,792	**C2**
0,000	0,115	0,306	0,076	0,000	0,076	0,000	0,344	0,000	0,166	0,166	0,000	0,127	0,268	1,109	**C3**
0,000	0,000	0,108	0,089	0,000	0,000	0,177	0,334	0,049	0,128	0,059	0,079	0,000	0,098	0,856	**C4**
0,153	0,255	0,000	0,076	0,000	0,000	0,000	0,165	0,000	0,165	0,165	0,102	0,000	0,127	0,764	**C5**
0,000	0,103	0,000	0,034	0,000	0,000	0,207	0,310	0,057	0,000	0,230	0,000	0,000	0,115	0,000	**C6**
0,000	0,111	0,000	0,074	0,000	0,074	0,000	0,234	0,061	0,000	0,074	0,000	0,000	0,123	0,000	**C7**
0,115	0,000	0,000	0,058	0,000	0,058	0,173	0,259	0,000	0,125	0,518	0,000	0,000	0,000	1,495	**Ref.**
0,000	0,092	0,112	0,031	0,203	0,000	0,000	0,193	0,051	0,132	0,061	0,173	0,000	0,102	0,885	**V1**
0,000	0,000	0,413	0,052	0,000	0,000	0,000	0,103	0,086	0,000	0,103	0,000	0,172	0,172	4,303	**V2**
0,000	0,133	0,000	0,133	0,295	0,000	0,000	0,089	0,000	0,000	0,089	0,118	0,325	0,000	2,303	**V3**
0,000	0,000	0,000	0,050	0,000	0,000	0,303	0,219	0,000	0,000	0,219	0,000	0,000	0,353	2,002	**V4**
0,000	0,128	0,000	0,043	0,000	0,000	0,000	0,270	0,071	0,000	0,284	0,000	0,142	0,142	1,689	**V5**
0,000	0,000	0,276	0,000	0,000	0,000	0,451	0,326	0,000	0,000	0,150	0,000	0,000	0,251	1,505	**V6**
0,164	0,123	0,000	0,082	0,273	0,000	0,000	0,082	0,068	0,000	0,273	0,232	0,000	0,000	1,625	**V7**

(cont. on next page)

Table A.1. (cont.)

Q4Q1B2	Q4Q1A9	Q4Q198	Q4Q171	Q4Q159	Q4Q156	Q4Q140	Q4Q131	Q4Q124	Q4Q0Z3	Q4Q0Z1	Q4Q0X8	Q4Q0W9	Q4Q0S1	Q4Q0Q2	**Entry Name**
0,130	0,276	0,233	0,026	0,190	1,183	0,346	0,043	0,138	0,000	0,026	0,069	0,000	0,000	0,026	**C1**
0,000	0,000	0,196	0,000	0,527	1,175	0,603	0,000	0,000	0,000	0,000	0,121	0,000	0,136	0,000	**C2**
0,000	0,000	0,166	0,000	0,446	0,994	0,510	0,064	0,000	0,000	0,000	0,102	0,064	0,000	0,038	**C3**
0,148	0,148	0,128	0,000	0,344	1,347	0,000	0,108	0,157	0,000	0,030	0,167	0,049	0,000	0,030	**C4**
0,191	0,191	0,165	0,089	0,446	1,744	0,509	0,140	0,446	0,000	0,000	0,000	0,064	0,115	0,000	**C5**
0,172	0,368	0,310	0,000	0,402	1,574	0,460	0,000	0,643	0,000	0,034	0,000	0,057	0,000	0,000	**C6**
0,381	0,000	0,332	0,000	0,270	1,684	0,492	0,061	0,553	0,037	0,000	0,209	0,061	0,111	0,000	**C7**
0,144	0,000	0,125	0,029	0,211	0,000	0,383	0,163	0,336	0,000	0,000	0,163	0,048	0,000	0,029	**Ref.**
0,000	0,153	0,437	0,031	0,000	0,336	0,407	0,000	0,254	0,031	0,031	0,000	0,051	0,000	0,071	**V1**
0,000	0,000	0,000	0,052	0,189	0,568	0,688	0,086	0,275	0,000	0,052	0,000	0,000	0,000	0,052	**V2**
0,000	0,221	0,192	0,044	0,000	1,152	0,591	0,074	0,369	0,044	0,000	0,000	0,074	0,133	0,044	**V3**
0,000	0,000	0,219	0,000	0,185	1,312	0,673	0,000	0,269	0,000	0,000	0,000	0,084	0,000	0,000	**V4**
0,000	0,000	0,383	0,099	0,156	0,468	0,568	0,071	0,355	0,043	0,000	0,000	0,000	0,000	0,043	**V5**
0,000	0,000	0,677	0,000	0,276	0,000	1,003	0,276	0,401	0,000	0,000	0,000	0,125	0,226	0,075	**V6**
0,000	0,000	0,177	0,000	0,150	0,451	0,546	0,068	0,218	0,000	0,000	0,000	0,000	0,123	0,096	**V7**

(cont. on next page)

Table A.1. (cont.)

Q4Q1W6	Q4Q1V0	Q4Q1T9	Q4Q1T2	Q4Q1S5	Q4Q1S4	Q4Q1R2	Q4Q1M7	Q4Q1M1	Q4Q1M0	Q4Q1J6	Q4Q1I2	Q4Q1F5	Q4Q1D2	Q4Q1C4	**Entry Name**
0,000	0,596	0,155	0,000	0,173	0,060	0,138	0,112	0,112	0,302	0,078	0,164	0,138	0,216	0,328	**C1**
0,000	0,136	0,422	0,000	0,301	0,105	0,090	0,000	0,196	0,527	0,136	0,000	0,121	0,377	0,407	**C2**
0,000	0,382	0,433	0,000	0,000	0,089	0,127	0,000	0,255	0,446	0,242	0,115	0,000	0,319	0,484	**C3**
0,266	0,187	0,226	0,000	0,000	0,069	0,118	0,128	0,266	0,266	0,187	0,089	0,079	0,246	0,747	**C4**
0,344	0,115	0,165	0,013	0,255	0,000	0,204	0,369	0,344	0,560	0,115	0,115	0,204	0,318	0,344	**C5**
0,000	0,103	0,149	0,011	0,000	0,000	0,069	0,149	0,310	0,230	0,218	0,345	0,184	0,000	0,575	**C6**
0,332	0,000	0,160	0,012	0,000	0,086	0,049	0,160	0,332	0,332	0,234	0,111	0,000	0,307	0,332	**C7**
0,259	0,288	0,431	0,000	0,000	0,067	0,077	0,125	0,585	1,275	0,086	0,000	0,000	0,240	0,729	**Ref.**
0,000	0,702	0,132	0,000	0,203	0,000	0,061	0,132	0,203	0,203	0,092	0,427	0,163	0,254	0,275	**V1**
0,000	0,155	0,155	0,000	0,000	0,000	0,069	0,224	0,224	0,465	0,155	0,000	0,138	0,430	0,138	**V2**
0,000	0,443	0,192	0,000	0,295	0,192	0,207	0,192	0,192	0,295	0,281	0,133	0,236	0,369	0,000	**V3**
0,000	0,925	0,303	0,017	0,000	0,000	0,000	0,000	0,101	0,219	0,320	0,151	0,269	0,000	0,454	**V4**
0,000	0,426	0,185	0,000	0,284	0,000	0,085	0,185	0,284	0,383	0,000	0,000	0,000	0,355	0,000	**V5**
0,000	0,477	0,326	0,000	0,000	0,000	0,000	0,000	0,150	0,502	0,000	0,226	0,000	0,000	0,201	**V6**
0,000	0,259	0,055	0,000	0,000	0,096	0,000	0,000	0,177	0,369	0,123	0,123	0,109	0,000	0,232	**V7**

(cont. on next page)

Table A.1. (cont.)

Q4Q2T4	Q4Q2S5	Q4Q2R6	Q4Q2R2	Q4Q2M2	Q4Q2J4	Q4Q2H9	Q4Q2H7	Q4Q2D5	Q4Q2C5	Q4Q286	Q4Q259	Q4Q242	Q4Q230	Q4Q1Z5	**Entry Name**
0,060	0,112	0,000	0,000	0,026	0,000	0,181	0,095	0,035	0,000	0,000	0,665	0,000	0,121	0,000	**C1**
0,000	0,196	0,000	0,000	0,000	0,105	0,000	0,000	0,000	0,015	0,136	0,708	0,196	0,000	0,000	**C2**
0,000	0,166	0,255	0,000	0,000	0,000	0,268	0,064	0,000	0,013	0,000	0,599	0,166	0,178	0,089	**C3**
0,000	0,000	0,197	0,049	0,000	0,000	0,207	0,167	0,039	0,010	0,089	0,511	0,128	0,138	0,000	**C4**
0,000	0,000	0,000	0,064	0,000	0,089	0,267	0,064	0,000	0,000	0,000	0,815	0,000	0,178	0,000	**C5**
0,080	0,322	0,000	0,057	0,000	0,000	0,540	0,057	0,000	0,000	0,103	0,540	0,000	0,161	0,000	**C6**
0,086	0,000	0,000	0,061	0,037	0,086	0,258	0,061	0,000	0,000	0,000	0,946	0,000	0,381	0,086	**C7**
0,067	0,000	0,192	0,000	0,000	0,067	0,201	0,163	0,038	0,000	0,000	0,613	0,000	0,297	0,000	**Ref.**
0,071	0,000	0,000	0,051	0,000	0,071	0,214	0,051	0,041	0,000	0,000	0,478	0,132	0,315	0,071	**V1**
0,120	0,000	0,344	0,000	0,000	0,120	0,361	0,189	0,000	0,000	0,155	1,325	0,224	0,241	0,000	**V2**
0,000	0,000	0,000	0,000	0,044	0,221	0,310	0,074	0,103	0,000	0,000	0,694	0,192	0,458	0,000	**V3**
0,118	0,000	0,337	0,000	0,000	0,000	0,353	0,084	0,067	0,017	0,000	0,976	0,219	0,236	0,000	**V4**
0,000	0,000	0,000	0,000	0,043	0,000	0,298	0,071	0,000	0,000	0,000	0,738	0,000	0,199	0,000	**V5**
0,000	0,000	0,000	0,000	0,000	0,000	0,527	0,000	0,000	0,025	0,000	0,778	0,000	0,000	0,176	**V6**
0,000	0,000	0,000	0,000	0,000	0,000	0,287	0,068	0,000	0,014	0,000	0,874	0,177	0,191	0,000	**V7**

(cont. on next page)

Table A.1. (cont.)

Q4Q3V0	Q4Q3U8	Q4Q3T3	Q4Q3T0	Q4Q3M1	Q4Q3K2	Q4Q3J4	Q4Q3I5	Q4Q3G7	Q4Q3D9	Q4Q3C1	Q4Q361	Q4Q350	Q4Q2X6	Q4Q2T7	**Entry Name**
0,052	0,043	0,181	0,121	0,000	0,095	0,000	0,043	0,138	0,026	0,130	0,086	1,132	0,026	0,147	**C1**
0,090	0,075	0,196	0,211	0,000	0,166	0,000	0,075	0,241	0,000	0,482	0,316	0,783	0,000	0,000	**C2**
0,076	0,064	0,076	0,178	0,000	0,000	0,000	0,064	0,102	0,038	0,408	0,268	0,663	0,000	0,217	**C3**
0,059	0,108	0,128	0,138	0,000	0,108	0,000	0,049	0,157	0,030	0,000	0,325	0,856	0,000	0,000	**C4**
0,000	0,000	0,267	0,178	0,000	0,293	0,140	0,064	0,102	0,000	0,407	0,000	1,108	0,000	0,216	**C5**
0,000	0,057	0,149	0,000	0,563	0,126	0,437	0,000	0,000	0,034	0,172	0,115	0,597	0,000	0,000	**C6**
0,000	0,061	0,258	0,086	0,270	0,000	0,000	0,061	0,197	0,000	0,184	0,123	1,069	0,000	0,000	**C7**
0,000	0,153	0,058	0,067	0,000	0,000	0,230	0,048	0,000	0,000	0,489	0,096	0,498	0,029	0,000	**Ref.**
0,061	0,051	0,376	0,071	0,224	0,112	0,244	0,000	0,000	0,000	0,153	0,000	0,000	0,031	0,376	**V1**
0,103	0,000	0,103	0,241	0,000	0,189	0,413	0,000	0,138	0,000	0,258	0,000	0,000	0,000	0,637	**V2**
0,089	0,074	0,310	0,103	0,000	0,000	0,000	0,000	0,118	0,000	0,221	0,148	0,340	0,000	0,000	**V3**
0,101	0,185	0,219	0,236	0,000	0,000	0,000	0,000	0,135	0,000	0,538	0,000	0,000	0,050	0,000	**V4**
0,085	0,156	0,185	0,099	0,696	0,156	0,156	0,000	0,000	0,000	0,454	0,000	0,000	0,000	0,241	**V5**
0,000	0,000	0,527	0,351	0,000	0,000	0,276	0,000	0,201	0,000	0,803	0,251	0,000	0,000	0,426	**V6**
0,082	0,000	0,628	0,096	0,000	0,000	0,000	0,068	0,000	0,000	0,000	0,000	0,000	0,041	0,232	**V7**

(cont. on next page)

Table A.1. (cont.)

Q4Q4I8	Q4Q4I6	Q4Q4G0	Q4Q4F3	Q4Q4E4	Q4Q4C4	Q4Q4A0	Q4Q495	Q4Q475	Q4Q449	Q4Q424	Q4Q416	Q4Q3Y1	Q4Q3W0	Q4Q3V3	**Entry Name**
0,000	0,484	0,000	0,017	0,000	0,207	0,130	0,000	0,000	0,000	0,000	0,043	0,000	0,000	0,199	**C1**
0,075	0,648	0,045	0,030	0,271	0,105	0,226	0,000	0,000	0,000	0,000	0,000	0,000	0,090	0,226	**C2**
0,000	0,319	0,038	0,025	0,229	0,000	0,191	0,102	0,051	0,102	0,000	0,064	0,000	0,000	0,191	**C3**
0,000	0,492	0,000	0,020	0,177	0,069	0,148	0,000	0,039	0,079	0,157	0,000	0,000	0,059	0,226	**C4**
0,000	0,000	0,000	0,025	0,000	0,191	0,191	0,102	0,000	0,000	0,000	0,064	0,000	0,000	0,191	**C5**
0,000	0,735	0,034	0,023	0,207	0,000	0,172	0,000	0,000	0,000	0,000	0,000	0,333	0,149	0,356	**C6**
0,000	0,688	0,037	0,025	0,221	0,086	0,184	0,000	0,000	0,000	0,000	0,000	0,000	0,000	0,381	**C7**
0,048	0,479	0,000	0,000	0,000	0,067	0,316	0,077	0,038	0,000	0,153	0,000	0,000	0,058	0,144	**Ref.**
0,000	0,885	0,061	0,020	0,183	0,153	0,153	0,081	0,041	0,264	0,000	0,000	0,295	0,061	0,407	**V1**
0,000	0,964	0,052	0,034	0,000	0,000	0,258	0,000	0,069	0,000	0,275	0,000	0,000	0,103	0,120	**V2**
0,074	0,738	0,044	0,030	0,000	0,221	0,221	0,000	0,000	0,384	0,000	0,074	0,428	0,192	0,340	**V3**
0,000	0,841	0,050	0,034	0,000	0,252	0,252	0,000	0,067	0,286	0,269	0,084	0,488	0,101	0,118	**V4**
0,071	1,363	0,000	0,000	0,256	0,000	0,213	0,000	0,000	0,000	0,000	0,000	0,000	0,000	0,326	**V5**
0,000	0,627	0,000	0,000	0,000	0,000	0,376	0,201	0,000	0,652	0,401	0,000	0,000	0,000	0,176	**V6**
0,000	0,683	0,041	0,041	0,000	0,000	0,205	0,000	0,000	0,000	0,218	0,068	0,396	0,000	0,314	**V7**

(cont. on next page)

Table A.1. (cont.)

Q4Q5M0	Q4Q5L5	Q4Q5K7	Q4Q5J8	Q4Q5I7	Q4Q5I2	Q4Q5H6	Q4Q5D1	Q4Q5C3	Q4Q527	Q4Q513	Q4Q4W8	Q4Q4U5	Q4Q4U1	Q4Q4N5	**Entry Name**
0,155	0,026	0,130	0,112	0,035	0,052	0,000	0,130	0,000	0,898	0,000	0,095	0,173	0,207	0,052	**C1**
0,000	0,045	0,000	0,090	0,000	0,090	0,000	0,151	0,121	0,919	0,000	0,000	0,301	0,226	0,000	**C2**
0,000	0,038	0,000	0,000	0,000	0,000	0,064	0,064	0,102	0,344	0,000	0,140	0,166	0,089	0,076	**C3**
0,000	0,030	0,000	0,128	0,069	0,128	0,000	0,000	0,000	0,000	0,000	0,108	0,128	0,148	0,098	**C4**
0,229	0,000	0,000	0,000	0,051	0,000	0,000	0,064	0,000	0,777	0,000	0,140	0,165	0,089	0,038	**C5**
0,000	0,000	0,000	0,149	0,000	0,000	0,057	0,000	0,195	0,310	0,000	0,126	0,310	0,172	0,000	**C6**
0,000	0,000	0,184	0,074	0,000	0,074	0,000	0,000	0,000	0,750	0,123	0,135	0,160	0,086	0,037	**C7**
0,000	0,029	0,144	0,000	0,038	0,058	0,048	0,096	0,000	0,259	0,000	0,000	0,192	0,144	0,000	**Ref.**
0,000	0,000	0,153	0,000	0,041	0,000	0,000	0,051	0,081	1,058	0,000	0,112	0,203	0,153	0,000	**V1**
0,000	0,000	0,000	0,000	0,000	0,103	0,086	0,000	0,138	1,790	0,172	0,189	0,224	0,120	0,000	**V2**
0,000	0,000	0,221	0,000	0,000	0,000	0,000	0,074	0,118	0,901	0,148	0,000	0,000	0,000	0,000	**V3**
0,303	0,000	0,000	0,000	0,000	0,000	0,000	0,000	0,286	0,000	0,000	0,000	0,337	0,118	0,000	**V4**
0,000	0,000	0,213	0,000	0,000	0,085	0,000	0,000	0,000	0,866	0,000	0,000	0,085	0,341	0,000	**V5**
0,000	0,000	0,000	0,000	0,000	0,000	0,000	0,000	0,201	0,000	0,000	0,000	0,000	0,176	0,000	**V6**
0,246	0,000	0,000	0,000	0,000	0,000	0,000	0,000	0,000	0,000	0,137	0,000	0,177	0,096	0,000	**V7**

(cont. on next page)

Table A.1. (cont.)

Q4Q6L9	Q4Q6F6	Q4Q6F0	Q4Q6E2	Q4Q6E1	Q4Q6A0	Q4Q636	Q4Q5Y0	Q4Q5W1	Q4Q5U3	Q4Q5R2	Q4Q5P6	Q4Q5P5	Q4Q5P0	Q4Q5N9	**Entry Name**
0,043	0,000	0,000	0,000	0,207	0,173	0,078	0,354	0,017	0,043	0,320	0,078	0,147	0,242	0,104	**C1**
0,075	0,196	0,000	0,000	0,136	0,301	0,136	0,000	0,000	0,000	0,000	0,136	0,090	0,422	0,000	**C2**
0,000	0,357	0,102	0,000	0,306	0,255	0,115	0,000	0,025	0,000	0,000	0,000	0,395	0,357	0,000	**C3**
0,049	0,128	0,000	0,010	0,187	0,197	0,000	0,187	0,030	0,000	0,000	0,000	0,305	0,128	0,000	**C4**
0,000	0,165	0,000	0,013	0,178	0,000	0,115	0,000	0,038	0,064	0,000	0,115	0,395	0,165	0,153	**C5**
0,057	0,149	0,000	0,000	0,218	0,000	0,103	0,000	0,000	0,000	0,425	0,103	0,276	0,000	0,138	**C6**
0,000	0,160	0,000	0,000	0,000	0,000	0,111	0,234	0,025	0,000	0,455	0,111	0,295	0,160	0,147	**C7**
0,000	0,268	0,077	0,010	0,038	0,000	0,086	0,393	0,019	0,048	0,000	0,000	0,364	0,268	0,000	**Ref.**
0,092	0,285	0,081	0,010	0,041	0,000	0,092	0,000	0,020	0,051	0,376	0,000	0,244	0,132	0,122	**V1**
0,086	0,775	0,138	0,017	0,069	0,000	0,155	0,000	0,000	0,000	0,637	0,000	0,293	0,000	0,000	**V2**
0,074	0,192	0,118	0,000	0,207	0,295	0,000	0,281	0,000	0,074	0,000	0,000	0,251	0,000	0,177	**V3**
0,000	0,219	0,135	0,000	0,067	0,337	0,000	0,000	0,034	0,084	0,000	0,000	0,185	0,000	0,000	**V4**
0,000	0,397	0,114	0,000	0,128	0,284	0,128	0,000	0,000	0,000	0,000	0,000	0,241	0,000	0,000	**V5**
0,000	0,326	0,201	0,000	0,000	0,000	0,000	0,477	0,000	0,000	0,000	0,000	0,150	0,326	0,000	**V6**
0,000	0,177	0,109	0,000	0,191	0,273	0,000	0,000	0,027	0,068	0,000	0,000	0,150	0,000	0,164	**V7**

(cont. on next page)

Table A.1. (cont.)

Q4Q6Z5	Q4Q6Y5	Q4Q6X7	Q4Q6X0	Q4Q6W5	Q4Q6V9	Q4Q6V5	Q4Q6V3	Q4Q6V0	Q4Q6U6	Q4Q6S3	Q4Q6R5	Q4Q6R3	Q4Q6Q9	Q4Q6M4	**Entry Name**
0,086	0,000	0,026	0,259	0,147	0,078	0,000	0,078	0,026	0,035	0,285	0,000	0,078	0,130	0,000	**C1**
0,000	0,000	0,045	0,000	0,166	0,000	0,000	0,075	0,045	0,060	0,241	1,069	0,060	0,000	0,000	**C2**
0,000	0,000	0,089	0,892	0,140	0,000	0,000	0,178	0,038	0,051	0,204	0,000	0,051	0,000	0,051	**C3**
0,098	0,000	0,030	0,295	0,108	0,000	0,177	0,089	0,030	0,039	0,157	0,000	0,039	0,148	0,039	**C4**
0,255	0,025	0,089	0,891	0,216	0,115	0,229	0,064	0,000	0,051	0,204	2,432	0,000	0,000	0,051	**C5**
0,115	0,000	0,000	0,804	0,195	0,103	0,000	0,057	0,000	0,046	0,184	0,000	0,103	0,172	0,000	**C6**
0,123	0,000	0,037	0,000	0,000	0,000	0,221	0,061	0,000	0,049	0,197	0,000	0,111	0,000	0,049	**C7**
0,000	0,000	0,067	0,288	0,048	0,086	0,364	0,000	0,029	0,000	0,316	0,000	0,125	0,000	0,000	**Ref.**
0,000	0,020	0,071	0,712	0,244	0,000	0,183	0,000	0,031	0,000	0,163	0,722	0,183	0,153	0,041	**V1**
0,000	0,034	0,052	0,516	0,189	0,000	0,000	0,086	0,052	0,000	0,275	0,000	0,155	0,258	0,000	**V2**
0,148	0,030	0,044	0,443	0,162	0,000	0,000	0,074	0,044	0,059	0,236	1,048	0,000	0,000	0,000	**V3**
0,000	0,000	0,118	0,505	0,000	0,000	0,000	0,000	0,050	0,000	0,269	1,195	0,000	0,000	0,000	**V4**
0,000	0,000	0,000	0,994	0,156	0,000	0,256	0,071	0,000	0,000	0,227	0,000	0,057	0,000	0,000	**V5**
0,000	0,000	0,075	0,752	0,426	0,000	0,000	0,000	0,075	0,100	0,000	0,000	0,000	0,376	0,100	**V6**
0,137	0,000	0,000	0,410	0,000	0,000	0,000	0,068	0,041	0,000	0,218	0,000	0,055	0,000	0,055	**V7**

(cont. on next page)

Table A.1. (cont.)

Q4Q7X6	Q4Q7X1	Q4Q7U0	Q4Q7T9	Q4Q7T4	Q4Q7N4	Q4Q7H9	Q4Q7G6	Q4Q7A3	Q4Q7A2	Q4Q772	Q4Q744	Q4Q735	Q4Q707	Q4Q702	**Entry Name**
0,095	0,000	0,000	0,000	0,026	0,000	0,095	0,000	0,121	0,121	0,009	0,138	0,000	0,259	0,052	**C1**
0,166	0,000	0,075	0,000	0,000	0,000	0,000	0,000	0,000	0,105	0,015	0,000	0,000	0,000	0,090	**C2**
0,140	0,102	0,000	0,000	0,038	0,000	0,000	0,140	0,000	0,089	0,000	0,000	0,000	0,000	0,000	**C3**
0,108	0,000	0,000	0,000	0,000	0,344	0,000	0,108	0,000	0,138	0,000	0,049	0,000	0,000	0,059	**C4**
0,140	0,204	0,064	0,000	0,000	0,204	0,000	0,000	0,000	0,089	0,000	0,064	0,076	0,000	0,000	**C5**
0,126	0,276	0,000	0,000	0,034	0,000	0,000	0,000	0,000	0,161	0,000	0,126	0,000	0,345	0,000	**C6**
0,135	0,098	0,000	0,000	0,037	0,000	0,000	0,000	0,000	0,172	0,012	0,000	0,000	1,438	0,000	**C7**
0,000	0,077	0,000	0,000	0,029	0,153	0,000	0,000	0,000	0,067	0,000	0,000	0,000	0,288	0,058	**Ref.**
0,112	0,000	0,000	0,000	0,000	0,163	0,000	0,112	0,142	0,000	0,010	0,224	0,000	0,000	0,122	**V1**
0,189	0,000	0,000	0,207	0,000	0,000	0,000	0,000	0,120	0,000	0,000	0,275	0,103	0,000	0,103	**V2**
0,162	0,118	0,074	0,000	0,000	0,517	0,162	0,000	0,103	0,000	0,015	0,000	0,089	0,000	0,089	**V3**
0,185	0,135	0,084	0,000	0,000	0,000	0,185	0,185	0,118	0,000	0,000	0,000	0,101	0,000	0,000	**V4**
0,000	0,000	0,000	0,170	0,000	0,000	0,156	0,000	0,000	0,000	0,000	0,227	0,085	0,000	0,000	**V5**
0,000	0,000	0,000	0,301	0,000	0,401	0,000	0,000	0,176	0,000	0,000	0,000	0,000	0,000	0,000	**V6**
0,150	0,000	0,000	0,164	0,000	0,000	0,519	0,000	0,191	0,000	0,000	0,396	0,150	0,000	0,000	**V7**

(cont. on next page)

Table A.1. (cont.)

Q4Q8H1	Q4Q8G4	Q4Q8F2	Q4Q8E6	Q4Q8A8	Q4Q893	Q4Q884	Q4Q871	Q4Q848	Q4Q833	Q4Q822	Q4Q821	Q4Q812	Q4Q800	Q4Q7Y4	**Entry Name**
0,216	0,000	0,095	0,138	0,000	0,026	0,000	0,000	0,043	0,069	0,078	0,121	0,043	0,035	0,639	**C1**
0,000	0,000	0,000	0,075	0,000	0,045	0,105	0,151	0,000	0,256	0,000	0,572	0,000	0,000	0,527	**C2**
0,000	0,000	0,140	0,280	0,127	0,000	0,000	0,064	0,064	0,217	0,000	0,370	0,064	0,153	0,535	**C3**
0,000	0,295	0,000	0,285	0,098	0,030	0,226	0,098	0,157	0,079	0,000	0,138	0,049	0,039	0,285	**C4**
0,000	0,000	0,140	0,204	0,000	0,089	0,000	0,064	0,064	0,000	0,000	0,000	0,064	0,000	0,827	**C5**
0,287	0,345	0,126	0,253	0,000	0,034	0,000	0,000	0,000	0,195	0,000	0,080	0,000	0,046	0,000	**C6**
0,307	0,000	0,000	0,135	0,000	0,037	0,000	0,061	0,061	0,000	0,000	0,086	0,000	0,000	0,000	**C7**
0,000	0,000	0,000	0,211	0,096	0,029	0,067	0,048	0,153	0,000	0,086	0,278	0,048	0,038	0,709	**Ref.**
0,000	0,305	0,112	0,163	0,203	0,031	0,153	0,102	0,051	0,173	0,092	0,142	0,173	0,041	0,580	**V1**
0,000	0,516	0,000	0,189	0,172	0,000	0,000	0,172	0,086	0,000	0,000	0,120	0,086	0,069	0,000	**V2**
0,000	0,000	0,000	0,162	0,000	0,044	0,103	0,074	0,162	0,118	0,000	0,310	0,074	0,059	0,325	**V3**
0,000	0,000	0,000	0,185	0,168	0,050	0,000	0,168	0,084	0,135	0,000	0,488	0,185	0,067	0,589	**V4**
0,355	0,000	0,341	0,227	0,142	0,043	0,099	0,000	0,000	0,114	0,128	0,000	0,000	0,000	0,596	**V5**
0,000	0,000	0,000	0,401	0,000	0,000	0,000	0,125	0,125	0,000	0,000	0,176	0,125	0,000	0,878	**V6**
0,000	0,942	0,150	0,068	0,137	0,041	0,096	0,068	0,150	0,232	0,123	0,287	0,068	0,055	0,000	**V7**

(cont. on next page)

Table A.1. (cont.)

Q4Q9N7	Q4Q9H8	Q4Q9D0	Q4Q983	Q4Q970	Q4Q956	Q4Q939	Q4Q937	Q4Q931	Q4Q922	Q4Q8Z7	Q4Q8Q9	Q4Q8K1	Q4Q8I6	Q4Q8H8	**Entry Name**
0,095	0,000	1,382	0,009	0,043	0,147	0,043	0,130	0,354	0,147	0,000	0,147	0,199	0,225	0,000	**C1**
0,166	0,000	1,341	0,000	0,000	0,000	0,075	0,000	0,618	0,000	0,015	0,256	0,166	0,392	0,000	**C2**
0,000	0,000	1,134	0,000	0,064	0,000	0,064	0,064	0,522	0,000	0,013	0,217	0,000	0,331	0,000	**C3**
0,108	0,138	0,000	0,000	0,108	0,000	0,049	0,049	0,403	0,167	0,000	0,167	0,108	0,256	0,000	**C4**
0,000	0,000	1,133	0,013	0,000	0,000	0,064	0,191	0,000	0,000	0,013	0,216	0,140	0,000	0,000	**C5**
0,000	0,000	1,023	0,011	0,057	0,000	0,000	0,000	1,149	0,195	0,011	0,195	0,000	0,299	0,046	**C6**
0,135	0,172	1,966	0,000	0,000	0,209	0,000	0,184	0,504	0,000	0,000	0,209	0,000	0,320	0,000	**C7**
0,105	0,134	1,534	0,000	0,000	0,163	0,144	0,096	0,393	0,000	0,000	0,163	0,105	0,556	0,000	**Ref.**
0,000	0,142	0,386	0,000	0,000	0,000	0,092	0,000	0,417	0,376	0,010	0,000	0,000	0,264	0,173	**V1**
0,000	0,241	0,000	0,000	0,000	0,293	0,155	0,000	0,000	0,293	0,000	0,000	0,000	0,000	0,000	**V2**
0,000	0,000	0,000	0,000	0,000	0,000	0,133	0,000	0,605	0,000	0,000	0,000	0,000	0,000	0,000	**V3**
0,185	0,236	0,000	0,017	0,000	0,000	0,151	0,000	1,683	0,000	0,000	0,000	0,000	0,000	0,135	**V4**
0,000	0,000	0,539	0,000	0,000	0,000	0,128	0,000	0,582	0,000	0,000	0,000	0,000	0,000	0,057	**V5**
0,000	0,000	0,000	0,000	0,000	0,000	0,000	0,000	2,508	0,000	0,000	0,000	0,000	0,000	0,100	**V6**
0,000	0,000	0,519	0,000	0,150	0,000	0,068	0,000	1,365	0,232	0,014	0,000	0,150	0,000	0,000	**V7**

(cont. on next page)

Table A.1. (cont.)

Q4QA83	Q4QA70	Q4QA53	Q4QA42	Q4QA41	Q4QA28	Q4QA19	Q4QA12	Q4Q9Z6	Q4Q9Y8	Q4Q9X6	Q4Q9T0	Q4Q9R8	Q4Q9P4	Q4Q9N8	**Entry Name**
0,000	0,000	0,000	0,000	0,000	0,000	0,233	0,501	0,009	0,000	0,181	0,086	0,086	0,026	0,000	**C1**
0,000	0,000	0,000	0,000	0,000	0,090	0,000	0,874	0,000	0,286	0,211	0,151	0,000	0,045	0,000	**C2**
0,064	0,484	0,025	0,000	0,153	0,076	0,000	0,331	0,013	0,242	0,178	0,127	0,127	0,038	0,000	**C3**
0,049	0,374	0,020	0,000	0,246	0,118	0,079	0,256	0,000	0,187	0,000	0,000	0,000	0,030	0,000	**C4**
0,000	0,000	0,025	0,000	0,000	0,076	0,216	0,331	0,000	0,242	0,178	0,127	0,000	0,038	0,000	**C5**
0,000	0,437	0,023	0,057	0,000	0,000	0,310	0,299	0,000	0,218	0,333	0,115	0,000	0,034	0,000	**C6**
0,000	0,000	0,000	0,000	0,000	0,000	0,000	0,320	0,000	0,234	0,086	0,000	0,000	0,037	0,000	**C7**
0,000	0,000	0,000	0,000	0,115	0,058	0,077	0,000	0,010	0,000	0,134	0,000	0,000	0,000	0,115	**Ref.**
0,051	0,386	0,020	0,051	0,000	0,000	0,000	0,264	0,010	0,000	0,071	0,102	0,102	0,000	0,000	**V1**
0,000	0,000	0,034	0,086	0,000	0,000	0,138	0,000	0,017	0,000	0,120	0,000	0,172	0,000	0,207	**V2**
0,074	0,000	0,030	0,000	0,000	0,000	0,118	0,856	0,015	0,000	0,103	0,000	0,295	0,000	0,177	**V3**
0,000	0,639	0,034	0,084	0,000	0,101	0,000	0,437	0,000	0,000	0,000	0,000	0,168	0,000	0,202	**V4**
0,000	0,000	0,028	0,000	0,000	0,000	0,000	0,823	0,000	0,000	0,000	0,000	0,000	0,000	0,170	**V5**
0,000	0,000	0,000	0,000	0,000	0,150	0,000	2,483	0,000	0,000	0,000	0,000	0,251	0,000	0,301	**V6**
0,068	0,000	0,000	0,000	0,341	0,082	0,369	0,000	0,000	0,000	0,096	0,137	0,137	0,000	0,000	**V7**

(cont. on next page)

Table A.1. (cont.)

Q4QBD1	Q4QBC6	Q4QBC0	Q4QBB8	Q4QB62	Q4QB32	Q4QAZ0	Q4QAY0	Q4QAW2	Q4QAT9	Q4QAP8	Q4QAC4	Q4QAB9	Q4QAA9	Q4QA84	**Entry Name**
0,069	0,017	0,000	0,035	0,000	0,164	0,121	0,199	0,035	0,199	0,259	0,138	0,060	0,190	0,112	**C1**
0,000	0,030	0,000	0,060	0,000	0,196	0,000	0,000	0,000	0,166	0,000	0,075	0,211	0,000	0,422	**C2**
0,000	0,025	0,064	0,000	0,000	0,166	0,178	0,293	0,051	0,140	0,382	0,140	0,000	0,000	0,357	**C3**
0,079	0,020	0,049	0,079	0,000	0,000	0,138	0,000	0,039	0,108	0,295	0,108	0,069	0,216	0,275	**C4**
0,000	0,025	0,064	0,051	0,000	0,165	0,000	0,000	0,000	0,140	0,178	0,140	0,178	0,280	0,356	**C5**
0,000	0,023	0,000	0,000	0,000	0,149	0,161	0,000	0,000	0,126	0,161	0,126	0,080	0,253	0,322	**C6**
0,000	0,025	0,000	0,049	0,000	0,074	0,369	0,000	0,000	0,000	0,172	0,061	0,086	0,000	0,344	**C7**
0,000	0,000	0,000	0,000	0,029	0,182	0,288	0,220	0,000	0,105	0,288	0,105	0,134	0,211	0,000	**Ref.**
0,000	0,051	0,000	0,000	0,000	0,132	0,305	0,234	0,000	0,112	0,142	0,163	0,142	0,224	0,285	**V1**
0,000	0,034	0,172	0,000	0,000	0,000	0,000	0,000	0,000	0,189	0,516	0,189	0,120	0,000	0,224	**V2**
0,118	0,030	0,000	0,059	0,000	0,089	0,207	0,340	0,059	0,162	0,443	0,074	0,207	0,000	0,413	**V3**
0,000	0,034	0,000	0,000	0,050	0,000	0,000	0,387	0,000	0,185	0,505	0,185	0,236	0,000	0,219	**V4**
0,114	0,028	0,000	0,000	0,043	0,000	0,000	0,000	0,057	0,000	0,426	0,071	0,298	0,000	0,397	**V5**
0,000	0,000	0,000	0,100	0,000	0,000	0,351	0,000	0,000	0,276	0,000	0,125	0,351	0,000	0,326	**V6**
0,109	0,000	0,000	0,000	0,041	0,000	0,410	0,000	0,000	0,150	0,410	0,068	0,096	0,000	0,177	**V7**

(cont. on next page)

Table A.1. (cont.)

Q4QC00	Q4QBY1	Q4QBV0	Q4QBU0	Q4QBT5	Q4QBR9	Q4QBL1	Q4QBL0	Q4QBK6	Q4QBJ3	Q4QBJ1	Q4QBI4	Q4QBF5	Q4QBD8	Q4QBD6	**Entry Name**
0,259	0,112	0,190	0,207	0,294	0,216	0,078	0,052	0,000	0,026	0,164	0,086	0,199	0,000	0,000	**C1**
1,054	0,090	0,331	0,000	0,121	0,000	0,000	0,090	0,798	0,045	0,000	0,151	0,000	0,000	0,000	**C2**
0,382	0,076	0,280	0,000	0,204	0,000	0,115	0,076	1,134	0,038	0,242	0,000	0,293	0,127	0,038	**C3**
0,482	0,197	0,216	0,157	0,079	0,000	0,089	0,059	0,521	0,030	0,187	0,000	0,226	0,000	0,000	**C4**
0,624	0,000	0,280	0,102	0,102	0,153	0,115	0,000	0,306	0,089	0,242	0,000	0,000	0,127	0,038	**C5**
0,804	0,000	0,253	0,000	0,000	0,287	0,000	0,000	0,276	0,034	0,218	0,115	0,264	0,115	0,000	**C6**
0,369	0,074	0,270	0,098	0,000	0,147	0,111	0,074	0,000	0,000	0,234	0,000	0,283	0,123	0,000	**C7**
0,470	0,000	0,211	0,000	0,230	0,115	0,000	0,058	0,230	0,000	0,182	0,096	0,479	0,096	0,000	**Ref.**
0,712	0,061	0,224	0,163	0,000	0,122	0,092	0,000	1,363	0,071	0,193	0,000	0,854	0,102	0,000	**V1**
1,205	0,000	0,379	0,000	0,000	0,000	0,327	0,000	0,413	0,052	0,327	0,000	1,446	0,000	0,000	**V2**
0,443	0,000	0,325	0,236	0,000	0,177	0,281	0,000	1,314	0,162	0,281	0,000	0,738	0,000	0,044	**V3**
1,178	0,101	0,370	0,000	0,000	0,000	0,151	0,101	0,404	0,118	0,320	0,168	1,413	0,168	0,050	**V4**
0,696	0,000	0,312	0,000	0,000	0,000	0,128	0,000	1,263	0,000	0,000	0,000	0,710	0,142	0,000	**V5**
1,229	0,150	0,552	0,000	0,000	0,000	0,000	0,000	1,329	0,176	0,000	0,251	1,254	0,000	0,000	**V6**
0,410	0,000	0,300	0,000	0,000	0,000	0,259	0,082	0,328	0,096	0,259	0,137	0,683	0,000	0,000	**V7**

(cont. on next page)

Table A.1. (cont.)

Q4QCG8	Q4QCG1	Q4QCE4	Q4QCD8	Q4QCD3	Q4QCD2	Q4QCD1	Q4QCC9	Q4QC98	Q4QC89	Q4QC87	Q4QC71	Q4QC61	Q4QC38	Q4QC12	**Entry Name**
0,026	0,086	0,043	0,000	0,026	0,121	0,017	0,009	0,017	0,207	0,052	0,112	0,121	0,069	0,173	**C1**
0,045	0,151	0,075	0,075	0,045	0,000	0,030	0,030	0,000	0,000	0,090	0,196	0,000	0,000	0,301	**C2**
0,000	0,000	0,000	0,064	0,038	0,051	0,025	0,025	0,025	0,306	0,000	0,166	0,000	0,306	0,255	**C3**
0,000	0,098	0,049	0,049	0,010	0,039	0,000	0,030	0,000	0,000	0,059	0,266	0,069	0,236	0,197	**C4**
0,000	0,127	0,064	0,000	0,038	0,000	0,000	0,013	0,025	0,687	0,076	0,165	0,089	0,306	0,255	**C5**
0,000	0,115	0,000	0,000	0,011	0,103	0,000	0,000	0,000	0,000	0,069	0,000	0,080	0,092	0,230	**C6**
0,000	0,123	0,061	0,000	0,000	0,049	0,061	0,000	0,000	0,000	0,000	0,516	0,000	0,418	0,246	**C7**
0,029	0,096	0,000	0,000	0,038	0,038	0,048	0,019	0,000	0,000	0,058	0,259	0,000	0,422	0,192	**Ref.**
0,071	0,102	0,000	0,000	0,000	0,041	0,000	0,020	0,000	0,244	0,000	0,132	0,142	0,081	0,203	**V1**
0,000	0,172	0,000	0,000	0,000	0,000	0,034	0,017	0,000	0,000	0,000	0,224	0,120	0,000	0,344	**V2**
0,044	0,148	0,000	0,000	0,000	0,000	0,000	0,030	0,000	0,354	0,000	0,192	0,207	0,118	0,295	**V3**
0,000	0,000	0,084	0,000	0,000	0,067	0,000	0,017	0,000	0,000	0,000	0,000	0,118	0,269	0,337	**V4**
0,000	0,142	0,000	0,071	0,000	0,000	0,000	0,014	0,000	0,341	0,000	0,000	0,099	0,000	0,000	**V5**
0,000	0,251	0,000	0,000	0,000	0,000	0,000	0,000	0,000	0,000	0,000	0,000	0,000	0,000	0,502	**V6**
0,041	0,137	0,000	0,068	0,000	0,000	0,000	0,000	0,027	0,000	0,000	0,000	0,000	0,109	0,273	**V7**

(cont. on next page)

Table A.1. (cont.)

Q4QD56	Q4QD53	Q4QD52	Q4QD36	Q4QD34	Q4QD30	Q4QCX5	Q4QCW5	Q4QCS8	Q4QCS7	Q4QCR7	Q4QCR1	Q4QCM4	Q4QCJ0	Q4QCH1	**Entry Name**
0,138	0,060	0,000	0,000	0,276	0,026	0,052	0,121	0,069	0,043	0,216	0,026	0,069	0,130	0,000	**C1**
0,121	0,000	0,000	0,075	0,226	0,000	0,000	0,136	0,060	0,000	0,181	0,000	0,000	0,105	0,000	**C2**
0,102	0,178	0,000	0,000	0,293	0,038	0,000	0,178	0,051	0,000	0,153	0,038	0,102	0,000	0,153	**C3**
0,157	0,000	0,000	0,000	0,069	0,030	0,059	0,049	0,000	0,049	0,118	0,030	0,000	0,000	0,000	**C4**
0,204	0,000	0,165	0,064	0,191	0,038	0,076	0,115	0,000	0,064	0,000	0,000	0,102	0,089	0,000	**C5**
0,092	0,080	0,000	0,000	0,080	0,000	0,069	0,057	0,046	0,000	0,000	0,034	0,092	0,172	0,000	**C6**
0,197	0,000	0,000	0,061	0,000	0,037	0,000	0,111	0,098	0,000	0,307	0,037	0,209	0,086	0,000	**C7**
0,153	0,134	0,125	0,000	0,144	0,000	0,115	0,134	0,077	0,000	0,115	0,029	0,077	0,307	0,000	**Ref.**
0,081	0,071	0,132	0,000	0,234	0,000	0,000	0,000	0,041	0,051	0,122	0,031	0,000	0,071	0,122	**V1**
0,138	0,000	0,000	0,000	0,120	0,000	0,000	0,000	0,000	0,086	0,207	0,000	0,000	0,000	0,207	**V2**
0,236	0,103	0,192	0,000	0,103	0,000	0,089	0,133	0,000	0,000	0,000	0,044	0,000	0,000	0,000	**V3**
0,135	0,118	0,219	0,000	0,000	0,000	0,000	0,151	0,000	0,000	0,202	0,000	0,000	0,000	0,000	**V4**
0,227	0,000	0,000	0,000	0,000	0,043	0,000	0,071	0,114	0,000	0,170	0,000	0,114	0,099	0,000	**V5**
0,201	0,000	0,000	0,000	0,000	0,000	0,000	0,000	0,000	0,000	0,301	0,000	0,201	0,000	0,000	**V6**
0,109	0,000	0,000	0,068	0,000	0,041	0,000	0,000	0,000	0,000	0,000	0,000	0,000	0,000	0,164	**V7**

(cont. on next page)

Table A.1. (cont.)

Q4QDW8	Q4QDU1	Q4QDS1	Q4QDQ2	Q4QDQ1	Q4QDL6	Q4QDK6	Q4QDK5	Q4QDJ5	Q4QDI9	Q4QDI8	Q4QDG7	Q4QDB7	Q4QDB6	Q4QDB5	**Entry Name**
0,060	0,276	0,035	0,069	0,000	0,000	0,104	0,078	0,035	0,043	0,000	0,000	0,155	0,000	0,000	**C1**
0,226	0,000	0,060	0,060	0,000	0,000	0,000	0,136	0,000	0,000	0,090	0,000	0,000	0,000	0,000	**C2**
0,000	0,408	0,000	0,102	0,000	0,000	0,000	0,115	0,102	0,000	0,076	0,000	0,000	0,229	0,076	**C3**
0,000	0,315	0,039	0,079	0,089	0,000	0,118	0,089	0,079	0,000	0,059	0,167	0,000	0,177	0,059	**C4**
0,089	0,407	0,051	0,102	0,000	0,993	0,000	0,115	0,102	0,000	0,076	0,102	0,000	0,000	0,000	**C5**
0,000	0,000	0,000	0,138	0,000	0,000	0,000	0,000	0,000	0,000	0,069	0,000	0,000	0,000	0,069	**C6**
0,000	0,393	0,000	0,098	0,111	0,000	0,000	0,000	0,049	0,000	0,074	0,209	0,000	0,221	0,000	**C7**
0,144	0,307	0,038	0,211	0,000	0,000	0,115	0,086	0,077	0,000	0,000	0,000	0,000	0,173	0,000	**Ref.**
0,153	0,000	0,092	0,173	0,285	0,793	0,122	0,000	0,041	0,051	0,061	0,000	0,112	0,000	0,000	**V1**
0,258	0,551	0,155	0,069	0,000	0,000	0,000	0,000	0,000	0,086	0,000	0,138	0,000	0,000	0,000	**V2**
0,103	0,472	0,000	0,118	0,000	0,000	0,000	0,000	0,000	0,074	0,089	0,000	0,089	0,000	0,000	**V3**
0,118	0,000	0,000	0,000	0,151	1,312	0,000	0,000	0,067	0,000	0,101	0,135	0,000	0,202	0,000	**V4**
0,000	0,000	0,000	0,241	0,128	0,000	0,000	0,000	0,057	0,071	0,000	0,000	0,085	0,000	0,000	**V5**
0,376	0,000	0,226	0,100	0,226	0,828	0,000	0,226	0,000	0,000	0,000	0,201	0,000	0,000	0,150	**V6**
0,000	0,437	0,055	0,000	0,382	0,000	0,000	0,123	0,055	0,000	0,000	0,000	0,000	0,082	0,000	**V7**

(cont. on next page)

Table A.1. (cont.)

Q4QEM2	Q4QEL8	Q4QEL2	Q4QEK5	Q4QEK4	Q4QEJ8	Q4QEI9	Q4QEI8	Q4QEE6	Q4QED4	Q4QE62	Q4QE40	Q4QE27	Q4QDZ1	Q4QDX5	**Entry Name**
0,674	0,035	0,000	0,043	0,000	0,035	0,000	0,207	0,000	0,000	0,043	0,078	0,060	0,138	0,000	**C1**
0,452	0,000	0,000	0,075	0,181	0,060	0,362	0,000	0,000	0,045	0,000	0,136	0,211	0,060	0,000	**C2**
0,293	0,000	0,000	0,000	0,000	0,051	0,204	0,000	0,000	0,038	0,000	0,000	0,089	0,153	0,000	**C3**
0,511	0,000	0,000	0,049	0,118	0,128	0,000	0,157	0,059	0,000	0,000	0,000	0,069	0,157	0,098	**C4**
0,764	0,051	0,000	0,140	0,000	0,000	0,204	0,000	0,000	0,000	0,115	0,000	0,089	0,153	0,064	**C5**
0,597	0,000	0,092	0,000	0,000	0,046	0,276	0,000	0,069	0,034	0,000	0,000	0,080	0,138	0,000	**C6**
0,541	0,000	0,000	0,000	0,000	0,049	0,418	0,000	0,000	0,000	0,061	0,111	0,086	0,147	0,123	**C7**
0,105	0,077	0,000	0,048	0,000	0,086	0,000	0,527	0,000	0,000	0,086	0,173	0,067	0,240	0,048	**Ref.**
0,112	0,041	0,163	0,000	0,000	0,000	0,000	0,081	0,000	0,031	0,051	0,000	0,071	0,122	0,102	**V1**
0,086	0,069	0,000	0,000	0,000	0,000	0,000	0,000	0,000	0,000	0,000	0,000	0,241	0,138	0,000	**V2**
0,162	0,059	0,118	0,074	0,000	0,059	0,000	0,000	0,089	0,103	0,074	0,133	0,103	0,236	0,148	**V3**
0,185	0,067	0,135	0,000	0,202	0,000	0,000	0,135	0,101	0,050	0,151	0,000	0,118	0,202	0,000	**V4**
0,156	0,057	0,000	0,071	0,000	0,000	0,000	0,000	0,000	0,000	0,000	0,000	0,099	0,057	0,000	**V5**
0,125	0,100	0,000	0,000	0,000	0,100	0,000	0,000	0,000	0,000	0,000	0,000	0,176	0,000	0,000	**V6**
0,068	0,000	0,000	0,000	0,164	0,000	0,000	0,000	0,000	0,000	0,000	0,000	0,096	0,055	0,000	**V7**

(cont. on next page)

Table A.1. (cont.)

Q4QF62	Q4QF49	Q4QF42	Q4QF35	Q4QF32	Q4QF31	Q4QF06	Q4QF03	Q4QEZ4	Q4QEW5	Q4QEW0	Q4QEU3	Q4QES5	Q4QER1	Q4QEQ4	**Entry Name**
1,304	0,000	0,095	0,207	0,000	0,035	0,000	0,009	0,000	0,060	0,035	0,285	0,130	0,112	0,605	**C1**
0,542	0,000	0,166	0,000	0,437	0,105	0,000	0,000	0,000	0,000	0,030	0,708	0,105	0,000	0,000	**C2**
1,083	0,102	0,140	0,153	0,370	0,089	0,268	0,000	0,000	0,000	0,000	0,599	0,191	0,166	0,242	**C3**
0,836	0,079	0,177	0,118	0,000	0,000	0,207	0,000	0,000	0,069	0,000	0,462	0,148	0,000	0,187	**C4**
1,082	0,000	0,140	0,153	0,369	0,051	0,267	0,000	0,089	0,089	0,025	0,420	0,000	0,165	0,000	**C5**
0,977	0,092	0,000	0,276	0,000	0,080	0,000	0,000	0,080	0,000	0,023	0,115	0,000	0,000	0,218	**C6**
1,045	0,000	0,135	0,000	0,000	0,049	0,258	0,000	0,086	0,086	0,025	0,258	0,283	0,160	0,234	**C7**
0,815	0,000	0,105	0,000	0,278	0,000	0,201	0,019	0,067	0,067	0,000	0,201	0,067	0,125	0,000	**Ref.**
0,864	0,000	0,061	0,244	0,000	0,041	0,214	0,010	0,000	0,071	0,020	0,336	0,000	0,000	0,427	**V1**
1,463	0,000	0,310	0,000	0,499	0,069	0,000	0,017	0,000	0,000	0,000	0,568	0,000	0,224	0,327	**V2**
1,255	0,118	0,089	0,354	0,000	0,059	0,000	0,000	0,000	0,103	0,030	0,310	0,103	0,192	0,620	**V3**
1,430	0,000	0,000	0,404	0,000	0,118	0,000	0,000	0,000	0,000	0,000	0,168	0,252	0,219	0,000	**V4**
0,511	0,000	0,000	0,000	0,412	0,000	0,000	0,000	0,000	0,000	0,000	0,298	0,099	0,000	0,000	**V5**
0,903	0,000	0,000	0,301	0,000	0,000	0,527	0,000	0,000	0,000	0,000	0,527	0,000	0,326	0,000	**V6**
1,161	0,000	0,082	0,328	0,000	0,055	0,287	0,000	0,000	0,000	0,027	0,137	0,205	0,177	0,000	**V7**

(cont. on next page)

Table A.1. (cont.)

Q4QFZ6	Q4QFY9	Q4QFY8	Q4QFX2	Q4QFT9	Q4QFP8	Q4QFP2	Q4QFL8	Q4QFL2	Q4QFJ7	Q4QFI3	Q4QFH9	Q4QFH5	Q4QFF7	Q4QF83	**Entry Name**
0,207	0,035	0,242	0,078	0,000	0,259	0,000	1,676	0,000	0,043	0,700	0,000	0,302	0,052	0,000	**C1**
0,000	0,000	0,090	0,000	0,000	0,452	0,060	3,660	0,000	0,000	0,000	0,000	0,241	0,000	0,045	**C2**
0,306	0,013	0,166	0,000	0,127	0,892	0,000	2,472	0,051	0,064	0,000	0,000	0,204	0,000	0,038	**C3**
0,000	0,010	0,128	0,000	0,098	1,859	0,000	1,908	0,000	0,049	0,797	0,000	0,157	0,059	0,098	**C4**
0,000	0,000	0,165	0,000	0,000	2,406	0,000	2,190	0,000	0,064	0,433	0,153	0,102	0,000	0,076	**C5**
0,276	0,023	0,000	0,000	0,115	0,804	0,000	2,229	0,000	0,057	0,391	0,138	0,092	0,000	0,034	**C6**
0,000	0,000	0,246	0,000	0,123	1,499	0,000	2,667	0,000	0,000	0,418	0,000	0,307	0,074	0,000	**C7**
0,230	0,000	0,268	0,192	0,000	0,671	0,038	1,860	0,000	0,096	1,371	0,000	0,000	0,000	0,058	**Ref.**
0,000	0,010	0,061	0,092	0,102	1,241	0,081	1,180	0,041	0,051	0,824	0,122	0,163	0,112	0,000	**V1**
0,000	0,017	0,103	0,000	0,172	0,516	0,000	1,222	0,069	0,086	1,394	0,000	0,000	0,000	0,103	**V2**
0,000	0,015	0,000	0,000	0,148	1,801	0,059	2,244	0,000	0,074	1,196	0,000	0,118	0,089	0,000	**V3**
0,404	0,000	0,101	0,151	0,000	2,053	0,000	2,894	0,067	0,084	1,363	0,000	0,000	0,101	0,000	**V4**
0,341	0,000	0,000	0,000	0,298	0,994	0,000	2,754	0,000	0,071	1,150	0,000	0,000	0,000	0,241	**V5**
0,000	0,000	0,000	0,000	0,251	0,752	0,000	1,781	0,100	0,125	0,000	0,301	0,401	0,000	0,075	**V6**
0,000	0,014	0,000	0,000	0,137	0,956	0,000	2,075	0,000	0,068	0,464	0,000	0,109	0,000	0,082	**V7**

(cont. on next page)

Table A.1. (cont.)

Q4QGR8	Q4QGN9	Q4QGN0	Q4QGM6	Q4QGG2	Q4QGE5	Q4QGD8	Q4QGC5	Q4QGA9	Q4QGA2	Q4QG97	Q4QG76	Q4QG66	Q4QG45	Q4QG44	**Entry Name**
0,035	0,000	0,000	0,078	0,078	0,320	0,060	0,371	0,579	0,104	0,803	0,052	0,130	0,380	0,026	**C1**
0,060	0,000	0,105	0,000	0,136	0,316	0,105	0,362	0,000	0,181	0,828	0,090	0,151	0,241	0,045	**C2**
0,051	0,140	0,089	0,255	0,000	0,268	0,089	0,421	0,370	0,153	0,319	0,076	0,064	0,433	0,076	**C3**
0,128	0,059	0,069	0,089	0,089	0,207	0,138	0,148	0,285	0,118	0,915	0,059	0,049	0,079	0,059	**C4**
0,000	0,076	0,000	0,000	0,115	0,369	0,000	0,191	0,369	0,153	0,318	0,153	0,064	0,204	0,076	**C5**
0,046	0,126	0,000	0,506	0,000	0,529	0,161	0,172	0,333	0,138	0,632	0,000	0,057	0,000	0,034	**C6**
0,049	0,074	0,000	0,000	0,111	0,258	0,172	0,295	0,356	0,000	0,307	0,074	0,061	0,197	0,000	**C7**
0,077	0,230	0,000	0,086	0,086	0,278	0,067	0,230	0,642	0,000	0,891	0,115	0,096	0,153	0,000	**Ref.**
0,041	0,000	0,071	0,315	0,092	0,468	0,142	0,153	0,295	0,122	0,254	0,000	0,153	0,081	0,031	**V1**
0,069	0,000	0,000	0,000	0,155	0,792	0,120	0,120	0,000	0,207	0,000	0,000	0,172	0,000	0,052	**V2**
0,059	0,089	0,000	0,133	0,133	0,089	0,103	0,221	0,000	0,000	0,000	0,000	0,148	0,118	0,044	**V3**
0,067	0,000	0,118	0,000	0,151	0,353	0,118	0,118	0,000	0,202	0,000	0,000	0,168	0,000	0,050	**V4**
0,000	0,000	0,000	0,128	0,000	0,298	0,099	0,099	0,951	0,000	0,355	0,085	0,071	0,000	0,000	**V5**
0,000	0,150	0,176	0,502	0,000	0,727	0,000	0,376	0,000	0,301	0,000	0,000	0,125	0,201	0,075	**V6**
0,000	0,000	0,000	0,000	0,123	0,396	0,096	0,328	0,396	0,164	0,341	0,000	0,068	0,218	0,082	**V7**

(cont. on next page)

Table A.1. (cont.)

Q4QH88	Q4QH84	Q4QH73	Q4QH56	Q4QH45	Q4QH22	Q4QH21	Q4QH17	Q4QH01	Q4QGX9	Q4QGX0	Q4QGW6	Q4QGW5	Q4QGW3	Q4QGS2	**Entry Name**
0,000	0,000	0,017	0,121	0,536	0,000	0,000	0,000	0,432	0,035	0,060	0,052	0,035	0,225	0,069	**C1**
0,000	0,000	0,030	0,211	0,663	0,000	0,000	0,000	0,000	0,060	0,105	0,000	0,000	0,392	0,256	**C2**
0,127	0,000	0,000	0,000	0,561	0,000	0,000	0,000	0,000	0,000	0,089	0,000	0,051	0,752	0,217	**C3**
0,098	0,000	0,000	0,138	0,266	0,000	0,059	0,000	0,492	0,069	0,069	0,059	0,000	0,256	0,079	**C4**
0,000	0,000	0,000	0,000	0,165	0,000	0,000	0,000	0,000	0,089	0,089	0,038	0,051	0,751	0,102	**C5**
0,000	0,115	0,023	0,000	0,712	0,000	0,000	0,069	0,977	0,046	0,080	0,000	0,000	0,678	0,092	**C6**
0,000	0,000	0,000	0,172	0,541	0,000	0,000	0,000	0,000	0,049	0,086	0,037	0,000	0,725	0,098	**C7**
0,096	0,000	0,019	0,134	0,259	0,000	0,000	0,058	0,000	0,038	0,067	0,058	0,038	0,000	0,077	**Ref.**
0,102	0,102	0,000	0,142	0,447	0,244	0,061	0,000	0,234	0,071	0,071	0,061	0,041	0,264	0,173	**V1**
0,000	0,000	0,034	0,000	0,465	0,413	0,103	0,000	0,000	0,120	0,120	0,000	0,000	0,448	0,138	**V2**
0,000	0,148	0,030	0,207	0,399	0,000	0,000	0,000	0,340	0,103	0,103	0,000	0,059	0,871	0,118	**V3**
0,168	0,000	0,084	0,236	0,454	0,404	0,101	0,000	0,000	0,067	0,118	0,000	0,000	0,000	0,286	**V4**
0,142	0,142	0,000	0,000	0,185	0,341	0,185	0,085	0,326	0,057	0,099	0,000	0,000	0,837	0,114	**V5**
0,000	0,000	0,125	0,351	0,000	0,602	0,000	0,000	1,254	0,000	0,000	0,000	0,100	0,000	0,201	**V6**
0,000	0,000	0,027	0,191	0,601	0,328	0,082	0,082	0,000	0,055	0,096	0,082	0,000	1,379	0,000	**V7**

(cont. on next page)

Table A.1. (cont.)

Q4QIE0	Q4QIC2	Q4QIC1	Q4QI80	Q4QI59	Q4QI38	Q4QI25	Q4QHT2	Q4QHS3	Q4QHP1	Q4QHM6	Q4QHJ7	Q4QHG6	Q4QHD6	Q4QHC9	**Entry Name**
0,268	0,268	0,000	0,078	0,000	0,216	0,000	9,641	0,043	0,648	0,259	0,268	0,069	0,069	0,553	**C1**
0,000	0,467	0,181	0,000	0,136	0,181	0,000	10,574	0,000	1,130	0,000	0,346	0,121	0,000	0,422	**C2**
0,000	0,905	0,153	0,229	0,000	0,000	0,000	8,946	0,064	0,000	0,000	0,293	0,229	0,000	0,000	**C3**
0,000	0,000	0,118	0,089	0,000	0,384	0,059	10,976	0,049	0,315	0,295	0,226	0,079	0,000	0,275	**C4**
0,000	0,000	0,000	0,000	0,000	0,318	0,000	5,461	0,000	0,000	0,000	0,191	0,102	0,000	0,356	**C5**
0,000	0,356	0,000	0,000	0,000	0,000	0,138	10,203	0,000	0,368	0,000	0,080	0,092	0,000	0,322	**C6**
0,000	0,873	0,147	0,000	0,000	0,147	0,000	6,772	0,135	0,393	0,000	0,184	0,098	0,209	0,344	**C7**
0,000	0,681	0,115	0,173	0,000	0,115	0,000	5,282	0,000	0,719	0,000	0,220	0,000	0,077	0,268	**Ref.**
0,142	0,722	0,000	0,000	0,193	0,000	0,061	14,206	0,173	0,000	0,305	0,071	0,081	0,000	0,651	**V1**
0,000	0,000	0,000	0,000	0,155	0,000	0,103	12,083	0,086	0,551	0,000	0,258	0,138	0,000	0,000	**V2**
0,207	0,000	0,000	0,000	0,133	0,177	0,089	8,135	0,074	1,107	0,000	0,221	0,000	0,118	0,413	**V3**
0,236	0,000	0,202	0,000	0,151	0,000	0,101	2,187	0,000	0,000	0,000	0,118	0,135	0,000	0,471	**V4**
0,440	0,440	0,000	0,000	0,000	0,000	0,000	15,841	0,241	1,065	0,426	0,000	0,000	0,000	0,908	**V5**
0,000	0,000	0,000	0,000	0,000	0,000	0,150	10,760	0,276	0,000	0,000	0,000	0,000	0,000	0,702	**V6**
0,000	0,423	0,000	0,000	0,123	0,000	0,532	15,238	0,068	0,437	0,000	0,314	0,000	0,000	0,382	**V7**

(cont. on next page)

Table A.1. (cont.)

Q4QJ39	Q4QJ37	Q4QIY1	Q4QIW9	Q4QIW7	Q4QIV6	Q4QIR7	Q4QIQ9	Q4QIQ0	Q4QIP1	Q4QIN2	Q4QIM8	Q4QIK0	Q4QII4	Q4QIG6	**Entry Name**
0,104	0,000	0,000	0,104	0,052	0,000	0,000	0,000	0,432	0,000	0,052	0,078	0,078	0,268	0,294	**C1**
0,000	0,196	0,000	0,181	0,000	0,000	0,000	0,090	0,000	0,000	0,090	0,090	0,000	0,000	0,000	**C2**
0,153	0,000	0,000	0,153	0,000	0,000	0,115	0,076	0,000	0,000	0,000	0,038	0,115	0,395	0,204	**C3**
0,000	0,275	0,138	0,256	0,000	0,089	0,000	0,000	0,226	0,128	0,000	0,000	0,187	0,305	0,157	**C4**
0,153	0,000	0,000	0,331	0,000	0,000	0,115	0,076	0,293	0,344	0,076	0,000	0,000	0,395	0,687	**C5**
0,138	0,000	0,161	0,138	0,000	0,000	0,000	0,000	0,264	0,000	0,069	0,000	0,000	0,000	0,184	**C6**
0,000	0,344	0,172	0,000	0,074	0,000	0,000	0,000	0,283	0,160	0,000	0,037	0,000	0,000	0,197	**C7**
0,000	0,125	0,134	0,115	0,000	0,086	0,000	0,000	0,000	0,259	0,115	0,029	0,086	0,297	0,153	**Ref.**
0,000	0,000	0,142	0,122	0,000	0,000	0,000	0,000	0,000	0,000	0,000	0,000	0,092	0,000	0,163	**V1**
0,000	0,224	0,000	0,207	0,000	0,000	0,000	0,000	0,000	0,000	0,000	0,000	0,000	0,000	0,275	**V2**
0,000	0,192	0,207	0,177	0,000	0,133	0,000	0,089	0,000	0,000	0,000	0,044	0,000	0,000	0,236	**V3**
0,000	0,219	0,505	0,202	0,101	0,151	0,151	0,101	0,000	0,000	0,000	0,050	0,320	0,000	0,000	**V4**
0,170	0,000	0,000	0,000	0,085	0,000	0,000	0,000	0,000	0,000	0,170	0,000	0,128	0,000	0,000	**V5**
0,301	0,000	0,000	0,301	0,150	0,000	0,000	0,000	0,000	0,000	0,000	0,075	0,000	0,000	0,000	**V6**
0,000	0,177	0,000	0,164	0,082	0,000	0,123	0,000	0,000	0,000	0,000	0,000	0,123	0,000	0,000	**V7**

(cont. on next page)

Table A.1. (cont.)

Q6IMM3	Q66NE0	Q5SDH5	Q5EEK0	Q4QJK0	Q4QJJ3	Q4QJG7	Q4QJF7	Q4QJF1	Q4QJE8	Q4QJE7	Q4QJA6	Q4QJ88	Q4QJ81	Q4QJ67	**Entry Name**
0,354	0,069	0,225	0,000	0,155	0,095	0,060	0,000	0,052	0,242	0,086	0,181	0,251	0,000	0,855	**C1**
0,286	0,256	0,000	0,000	0,271	0,166	0,000	0,000	0,090	0,000	0,000	0,151	0,136	0,000	0,618	**C2**
0,242	0,102	1,262	0,089	0,229	0,064	0,000	0,217	0,076	0,357	0,127	0,064	0,000	0,000	0,242	**C3**
0,000	0,167	0,570	0,069	0,177	0,108	0,138	0,000	0,118	0,275	0,000	0,148	0,000	0,000	0,187	**C4**
0,000	0,102	0,738	0,000	0,229	0,000	0,000	0,216	0,076	0,000	0,127	0,064	0,000	0,102	0,242	**C5**
0,000	0,092	0,299	0,000	0,000	0,057	0,161	0,000	0,069	0,000	0,000	0,241	0,103	0,000	0,218	**C6**
0,234	0,209	0,000	0,000	0,000	0,135	0,000	0,209	0,000	0,000	0,000	0,123	0,111	0,098	0,836	**C7**
0,182	0,077	0,249	0,067	0,364	0,153	0,000	0,000	0,058	0,268	0,000	0,096	0,000	0,000	0,652	**Ref.**
0,193	0,081	0,590	0,071	0,183	0,000	0,000	0,000	0,061	0,285	0,000	0,275	0,000	0,000	0,691	**V1**
0,000	0,293	0,448	0,120	0,310	0,000	0,000	0,000	0,000	0,000	0,172	0,172	0,000	0,000	0,706	**V2**
0,281	0,384	0,856	0,000	0,000	0,000	0,000	0,000	0,089	0,413	0,000	0,074	0,000	0,118	1,004	**V3**
0,000	0,000	0,437	0,118	0,639	0,000	0,118	0,000	0,101	0,000	0,168	0,252	0,000	0,000	0,000	**V4**
0,000	0,241	1,405	0,000	0,000	0,000	0,000	0,000	0,085	0,000	0,000	0,071	0,000	0,000	0,270	**V5**
0,000	0,000	0,652	0,000	0,451	0,000	0,000	0,426	0,000	0,000	0,000	0,000	0,000	0,201	0,000	**V6**
0,259	0,000	0,355	0,000	0,246	0,150	0,000	0,000	0,082	0,382	0,000	0,000	0,000	0,000	0,000	**V7**

(cont. on next page)

Table A.1. (cont.)

Q9XZX9	Q9U1E5	Q9U1E4	Q9U1E1	Q9U0W1	Q9U0T9	Q9NGR0	Q9NF77	Q95Z92	Q95Z84	Q94594	Q868B1	Q711P7	Q70GE8	Q6XFB3	**Entry Name**
0,043	0,000	0,000	0,752	0,086	0,035	0,130	0,026	0,000	0,000	0,570	0,155	0,181	0,060	0,060	**C1**
0,075	0,000	0,000	0,783	0,151	0,121	0,226	0,000	0,000	0,000	0,000	0,271	0,075	0,105	0,105	**C2**
0,064	0,025	0,000	0,663	0,000	0,051	0,089	0,038	0,064	0,140	0,000	0,229	0,127	0,089	0,089	**C3**
0,049	0,000	0,000	0,511	0,000	0,000	0,226	0,000	0,049	0,000	0,216	0,384	0,098	0,069	0,069	**C4**
0,064	0,000	0,000	1,108	0,000	0,051	0,191	0,000	0,000	0,000	0,000	0,229	0,267	0,089	0,089	**C5**
0,057	0,023	0,000	1,494	0,057	0,000	0,000	0,000	0,057	0,126	0,666	0,448	0,241	0,172	0,080	**C6**
0,061	0,025	0,061	1,069	0,061	0,000	0,000	0,000	0,061	0,000	0,713	0,479	0,123	0,086	0,086	**C7**
0,000	0,019	0,000	0,834	0,192	0,038	0,067	0,000	0,000	0,000	0,556	0,374	0,096	0,144	0,067	**Ref.**
0,000	0,020	0,000	0,885	0,102	0,041	0,071	0,031	0,000	0,244	0,508	0,397	0,102	0,000	0,071	**V1**
0,000	0,034	0,086	0,396	0,000	0,000	0,396	0,052	0,000	0,413	0,379	0,310	0,172	0,000	0,120	**V2**
0,000	0,000	0,074	1,285	0,074	0,059	0,221	0,000	0,000	0,561	0,000	0,266	0,236	0,103	0,103	**V3**
0,000	0,000	0,084	0,387	0,084	0,067	0,252	0,000	0,000	0,000	0,606	1,077	0,269	0,000	0,000	**V4**
0,000	0,000	0,000	1,845	0,142	0,000	0,099	0,000	0,000	0,156	0,000	0,554	0,142	0,000	0,000	**V5**
0,000	0,050	0,000	0,577	0,000	0,000	0,000	0,000	0,000	0,000	0,000	0,978	0,125	0,000	0,000	**V6**
0,000	0,000	0,000	1,775	0,000	0,000	0,000	0,041	0,000	0,328	0,000	0,000	0,137	0,096	0,000	**V7**

(cont. on next page)

Table A.1. (cont.)

RSSA	RS3A	RL40	RL18	**Entry Name**
0,121	0,233	0,510	0,147	**C1**
0,211	0,407	0,889	0,256	**C2**
0,178	0,535	0,752	0,217	**C3**
0,138	0,266	0,256	0,167	**C4**
0,178	0,344	0,331	0,216	**C5**
0,333	0,689	0,678	0,195	**C6**
0,356	0,516	0,320	0,209	**C7**
0,134	0,767	0,566	0,364	**Ref.**
0,000	0,132	0,600	0,000	**V1**
0,000	0,000	0,448	0,000	**V2**
0,207	0,192	0,384	0,000	**V3**
0,000	0,000	0,437	0,000	**V4**
0,000	0,185	1,419	0,000	**V5**
0,000	0,000	1,480	0,000	**V6**
0,191	0,177	1,365	0,000	**V7**

APPENDIX B

SIGNIFICANT PROTEINS IN REFERENCE *L. tropica* SAMPLE

Table B.1. Reference Proteins that are Differentially Abundant in CL

Entry name	p-values	Difference	Protein Name
Q4Q9D0	2,614448742	0,933571411	Putative 10 kDa heat shock protein
Q4Q350	5,818598152	0,838285714	Uncharacterized protein
Q4QG97	2,553688272	0,453142864	40S ribosomal protein S12
Q4QEM2	4,837533864	0,419714286	Paraflagellar rod protein 2C
A0A5Q2WYC5	1,875420935	0,399142861	40S ribosomal protein S4
E9ADX3	2,633132657	0,365285718	Tryparedoxin
RS3A	3,24112394	0,32914286	40S ribosomal protein S3a
Q4Q1C4	2,150588338	0,27385714	Succinate--CoA ligase [ADP-forming] subunit beta, mitochondrial
Q4Q159	2,826551114	0,23842858	Cysteine synthase
E9AE33	2,473171449	0,229285715	Histone H2A
Q4Q8I6	2,47992919	0,222714284	Putative RNA binding protein rbp16
Q4Q8Q9	8,365930214	0,201000001	Proteasome subunit beta
RL18	8,365930214	0,201000001	60S ribosomal protein L18
Q4QII4	1,749500923	0,194714291	Peptidyl-prolyl cis-trans isomerase
RSSA	2,07430654	0,159571429	40S ribosomal protein SA
Q4QI38	1,567318737	0,152714284	Dimethylargininase
Q4Q1B2	1,939797298	0,146000002	Fibrillarin
E9ADA3	2,740592587	0,138285716	Uncharacterized protein
Q4Q7A2	6,403654517	0,125	Succinyl-CoA:3-ketoacid-coenzyme A transferase
Q4QBT5	1,828666561	0,114285714	Putative proteasome regulatory ATPase subunit 5
Q4Q9X6	1,564833281	0,111	ATP synthase subunit beta
Q4QFY8	1,905177484	0,110285716	Putative chaperonin TCP20
Q4QB32	1,92847029	0,099000001	T-complex protein 1 subunit gamma
Q4Q0X8	2,107772619	0,095428571	Proteasome regulatory ATPase subunit
Q4Q937	1,867875959	0,088285714	Putative thimet oligopeptidase
E9AD27	4,204428951	0,074714288	Putative calpain-like cysteine peptidase
E9AFL0	2,213811416	0,073714286	CCT-eta
Q4QJJ3	1,377815856	0,067857143	Serine/threonine-protein phosphatase
Q70GE8	1,894287481	0,067285715	Thiol-dependent reductase 1
GMPR	2,504857599	0,06	GMP reductase (GMPR)
Q4QG76	1,815117882	0,059857143	Protein kinase domain-containing protein
Q4QC87	2,474725586	0,049428572	T-complex protein 1 subunit delta
Q4Q3I5	1,995735509	0,041142858	IFT81 CH domain-containing protein
E9AE82	1,770615169	0,037714287	Putative GTP-binding protein
E9AFD1	1,794009431	0,035571428	Uncharacterized protein
Q4QCD3	2,508738028	0,024	Uncharacterized protein
E9AF31	1,683961641	0,023428571	Putative calcium motive P-type ATPase
Q4Q5L5	1,707988773	0,019857143	Putative OSM3-like kinesin
Q4Q7T4	1,767516706	0,019285715	Putative ubiquitin hydrolase

Table B.2. Reference Proteins that are Differentially Abundant in VL

Entry name	p-values	Difference	Protein Name
Q4QFJ7	1,904173291	-0,040285715	Putative tyrosyl-tRNA synthetase
Q4Q0Q2	2,029108739	-0,041000001	Uncharacterized protein
Q4QEL8	2,042663737	-0,043857143	Putative kinesin
E9AD65	2,031954238	-0,06042857	Oxoglutarate dehydrogenase
Q4Q939	1,614333076	-0,061714285	Trifunctional enzyme alpha subunit, mitochondrial-like protein
Q4Q812	1,633440168	-0,070142857	Putative acyl-CoA dehydrogenase
E9AEW4	1,524458929	-0,082857143	Threonyl-tRNA synthetase
Q4Q8A8	1,362736107	-0,085285714	Putative hydrolase, alpha/beta fold family
Q4QAB9	1,4948162	-0,109428576	HMG_CoA_synt_N domain-containing protein
Q4Q6F0	3,93161304	-0,113428572	Putative N-acyl-L-amino acid amidohydrolase
Q4Q9N8	2,41927191	-0,151000002	Putative 2,4-dihydroxyhept-2-ene-1,7-dioic acid aldolase
Q4Q4I6	1,883023884	-0,390714279	Heat shock protein 83-1
E9AFS3	1,321058176	-0,429714288	Sm protein F
Q4QFI3	1,387181214	-0,521714291	Histone H4
Q4QBF5	4,219338905	-0,833285696	Putative endoribonuclease L-PSP (Pb5)
Q07DU5	1,854668398	-1,398714287	Peroxidoxin 2